

# Perspectives on NO<sub>x</sub> Emissions and Impacts from Ammonia Combustion Processes

Published as part of *Energy & Fuels special issue* "Celebrating Authors of Energy and Fuels Most-Impactful Articles (2021)".

Syed Mashruk,\* Hao Shi, Luca Mazzotta, Cihat Emre Ustun, B. Aravind, Roberto Meloni, Ali Alnasif, Elena Boulet, Radoslaw Jankowski, Chunkan Yu, Mohammad Alnajideen, Amin Paykani, Ulrich Maas, Rafal Slefarski, Domenico Borello, and Agustin Valera-Medina\*



Cite This: *Energy Fuels* 2024, 38, 19253–19292



Read Online

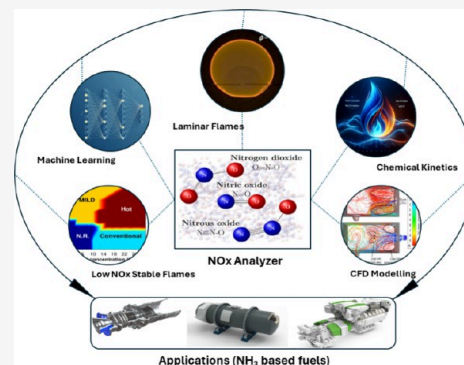
ACCESS |

Metrics & More

Article Recommendations

**ABSTRACT:** Climate change and global warming necessitate the shift toward low-emission, carbon-free fuels. Although hydrogen boasts zero carbon content and high performance, its utilization is impeded by the complexities and costs involved in liquefaction, preservation, and transportation. Ammonia has emerged as a viable alternative that offers potential as a renewable energy storage medium and supports the global economy's decarbonization. With its broader applicability in large power output applications, decentralized energy sources, and industrial locations off the grid, ammonia is increasingly regarded as an essential fuel for the future. Although ammonia provides a sustainable solution for future low-carbon energy fields, its wide-scale adoption is limited by NO<sub>x</sub> emissions and poor combustion performance under certain conditions. As research on ammonia combustion expands, recent findings reveal factors impacting the chemical reaction pathways of ammonia-based fuels, including the equivalence ratio, fuel mixture, pressure, and temperature.

Investigations into ammonia combustion and NO<sub>x</sub> emissions, at both laboratory and industrial scales, have identified NO<sub>x</sub> production peaks at equivalence ratios of 0.8–0.9 for ammonia/hydrogen blends. The latest studies about the NO<sub>x</sub> emissions of the ammonia flame at different conditions and their generating pathways are reviewed in this work. Effective reduction in NO<sub>x</sub> production from ammonia-based flames can be achieved with richer blends, which generate more NH<sub>i</sub> radicals. Other advanced NO<sub>x</sub> mitigation techniques such as plasma-assisted combustion have been also explored. Further research is required to address these challenges, reduce emissions, and improve efficiencies of ammonia-based fuel blends. Finally, the extinction limit of ammonia turbulent flame, its influential factors, and different strategies to promote the ammonia flame stability were discussed. The present review contributes to disseminating the latest advancements in the field of ammonia combustion and highlights the importance of refining reaction mechanisms, computational models, and understanding fundamental phenomena for practical implications.



## 1. INTRODUCTION

The global demand for energy is expected to increase significantly in the coming decades, with the International Energy Agency (IEA) predicting a 3-fold increase in the next 10 years and a 5-fold increase by the middle of the century.<sup>1</sup> This rise in energy demand, coupled with the escalating concentration of carbon dioxide in the atmosphere, presents a complex and critical challenge for humanity. Historically, the increase in energy requirements has led to a surge in emissions, resulting in climate changes and associated consequences.

According to the Intergovernmental Panel on Climate Change (IPCC), climate change is primarily caused by emissions such as carbon dioxide, which have already raised global temperatures by 0.8–1.2 °C. It is estimated that by 2050 the average increase will surpass 1.5 °C, and there are concerns

that it may reach 2.0 °C, a threshold beyond which the impacts on climate and the environment could become irreversible.<sup>2</sup> Therefore, the consequences of human activities and pollution will directly impact living standards and economic performance across regions.<sup>3</sup>

In response to these challenges, novel methods of energy generation have been conceived, such as wind, solar, and marine energies, which are being explored as sustainable

Received: July 13, 2024

Revised: September 13, 2024

Accepted: September 13, 2024

Published: October 2, 2024



alternatives. However, wind and solar energy systems face significant challenges. Their availability varies based on weather and seasonal conditions, making them intermittent energy sources. Moreover, large amounts of these energies are often stranded in remote locations that are economically impractical to connect directly to local grids. Marine energy, on the other hand, is hindered by high costs, challenging market environments, and the need for consistent energy production at reliable power outputs. These factors, along with political, social, and public perception considerations, can impede the widespread adoption of renewable energies that could reduce the dependence on fossil fuels and mitigate climate change emissions.

Among various methods of energy storage, chemical energy storage has been utilized for centuries, exemplified by our reliance on fossil fuels. Hence, the use of chemicals with low or no carbon content presents a unique solution for harnessing renewable, intermittent resources. Hydrogen storage is one such avenue, offering a chemical with zero carbon content and a high gravimetric energy density. However, hydrogen storage presents intrinsic challenges. Being the smallest molecule in the universe, hydrogen tends to permeate a wide range of materials, and its control in large-scale power generation systems, such as combustion-based systems, poses stability issues. Additionally, the explosive nature and fast-burning velocities of hydrogen make it difficult to handle compared with conventional sources. Moreover, the long-term storage costs of hydrogen can be economically unfeasible for many applications, as the molecule needs to be cooled to cryogenic conditions below 20 K ( $-253\text{ }^{\circ}\text{C}$ ).<sup>4</sup> These limitations have spurred the exploration of other molecules, supporting the concept of a “hydrogen economy”.

Ammonia, a molecule with a history spanning over 180 years, offers a unique platform for hydrogen storage and the delivery of renewable energy. Compared to hydrogen, ammonia ( $\text{NH}_3$ ) boasts a higher volumetric energy density (4325 vs 1305 Wh/L), higher liquefaction temperature (293.8 vs 20 K), and lower storage pressure (8 vs 700 bar), making it a promising alternative with high reliability and low cost.<sup>5</sup> Currently, the main method of ammonia production is the Haber–Bosch process, carried out in super-large-scale plants capable of producing between 2000 and 3000 tons/day, a capacity expected to increase substantially in the coming years.<sup>6</sup> Due to its feasibility in production, preservation, and distribution, ammonia is considered a sustainable option to meet the energy requirements of future low-carbon economies.

While ammonia has gained considerable acceptance in the industrial sector for power, heat, and propulsion generation through combustion systems, there are still unresolved questions that require further research and development. These include the reduction of emissions such as NO and  $\text{N}_2\text{O}$ , as well as unburned ammonia and carbon monoxide during cofiring processes. Therefore, gaining a better understanding of the mechanisms involved in the formation of  $\text{NO}_x$  products from ammonia is crucial for finding solutions to suppress these undesirable species.

This review addresses a critical gap in the existing literature by providing a comprehensive and timely analysis of  $\text{NO}_x$  emissions from ammonia combustion across various fuel blends and combustion applications, such as gas turbines, boilers, furnaces, and internal combustion engines (ICEs). While previous reviews, such as those by Tian et al.,<sup>7</sup> Elbaz et al.,<sup>8</sup> and Kobayashi et al.,<sup>9</sup> have explored the fundamentals and

specific aspects of ammonia combustion, this paper integrates the latest advancements in chemical kinetics mechanisms, reaction pathways of  $\text{NO}_x$  generation, and computational fluid dynamics (CFD) studies. This review also provides a holistic perspective on the challenges and potential solutions (e.g., MILD combustion) for reducing  $\text{NO}_x$  emissions in practical combustion systems.

Given the increasing interest in ammonia as a hydrogen carrier and its potential role in a hydrogen economy, understanding its combustion characteristics and environmental impacts is essential. This review fills a critical gap in the current literature by offering valuable insights for engineers and policymakers working on clean energy technologies. It identifies specific challenges and provides clear directions for future research, such as the need for improved chemical kinetics models and optimized combustion systems. By bridging the gap between fundamental combustion science and applied technology, this review contributes significantly to the advancement of the field.

## 2. $\text{NO}_x$ EMISSIONS IN AMMONIA COMBUSTION

To improve the design of combustion systems with the aim of minimizing the environmental impact of  $\text{NO}_x$  emissions, it is essential to understand the factors contributing to their increase. This requires a thorough investigation of the chemical kinetics behind  $\text{NO}_x$  emissions, which should be continually updated based on experimental data.  $\text{NO}_x$  refers to various forms of nitrogen oxides produced during combustion, primarily nitric oxide (NO), nitrogen dioxide ( $\text{NO}_2$ ), and nitrous oxide ( $\text{N}_2\text{O}$ ). NO is a colorless gas that acts as a precursor to  $\text{NO}_2$  and plays a significant role in photochemical reactions that lead to smog formation.<sup>10</sup>  $\text{NO}_2$  is particularly harmful as it can damage the respiratory system and, through reactions with water, oxygen, and other atmospheric chemicals, contribute to the formation of acid rain.<sup>11</sup> This rain adversely affects lakes and forests, degrading the ecosystem.  $\text{N}_2\text{O}$ , with its strong greenhouse effect, has a global warming potential 300 times greater than that of  $\text{CO}_2$ , thus presenting a severe threat to the environment.<sup>11,12</sup> Therefore, all forms of nitrogen oxides are major air pollutants that must be carefully managed in combustion processes, especially when  $\text{NH}_3$  (ammonia) is introduced as a fuel.

One of the main obstacles in the deployment of ammonia as a fuel is its proficiency in fuel  $\text{NO}_x$  production. Fuel  $\text{NO}_x$  is formed when nitrogen is chemically bonded to the fuel—which is the case for ammonia ( $\text{NH}_3$ )—through the production of intermediate products, such as CN, HCN, HNO, and  $\text{NH}_2$ , and further oxidation. Considerable amounts of thermal  $\text{NO}_x$  can also be generated with high enough flame temperatures.<sup>13</sup> Nitrogen oxides present a significant risk to both health and the environment. These emissions can affect drinking water distribution,<sup>14</sup> cause eutrophication,<sup>15</sup> and aggravate lung diseases if inhaled.<sup>16</sup> Nitrous oxide ( $\text{N}_2\text{O}$ ), another prospective product of ammonia combustion at certain operating conditions, has 273 times the 20-year global warming potential (GWP<sub>20</sub>) of  $\text{CO}_2$ .<sup>17</sup> Recent studies of ammonia/hydrogen blends have reported 240 ppm  $\text{N}_2\text{O}$  emissions to have a global warming impact approximately equal to that of  $\text{CO}_2$  emitted from pure methane flame operating at dry low  $\text{NO}_x$  (DLN) scenarios.<sup>18</sup>

**2.1. Initial Work.** The initial explorations of using ammonia as a potential candidate for combustion for power generation emerged in the 1960s. Newhall and Starkman<sup>19</sup>

pioneered a theoretical analysis of ammonia as a turbine fuel, considering the thermodynamic processes involved. They predicted that ammonia could yield a power output up to 10% greater than hydrocarbon fuels under the same conditions, with thermal efficiencies potentially 10% higher. However, they also noted that specific fuel consumption for ammonia would exceed that of hydrocarbons by 2.5–3 times due to the presence of inert nitrogen. Pratt<sup>20</sup> focused on the performance of ammonia-fired gas turbine combustors, both theoretically and experimentally. The authors confirmed that the chemical reaction between ammonia and air was relatively slow, necessitating adjustments in combustor design to accommodate for less efficient mixing at reduced air flow rates. Pratt suggested that smaller fuel nozzle orifices or multiple combustors in parallel could be potential solutions to improve the combustion efficiency. Verkamp et al.<sup>21</sup> conducted extensive experimental studies to determine the ignition energy, quenching distance, flame stability limits, and overall performance of ammonia–air mixtures in gas turbine burners. They found that ammonia required a minimum ignition energy of 8 mJ, significantly higher than propane's less than 0.5 mJ. The quenching distance for ammonia–air was also larger than that for propane–air, indicating a less stable combustion process. The study concluded that neat ammonia could not be directly used as a substitute for hydrocarbons in conventional gas turbines without modifications to the ignition system and combustion chamber design.

From 1964 to 1966, the U.S. Army in collaboration with the Solar Division of International Harvester Co., provided valuable insights into the characteristics of ammonia as a fuel and the engineering innovations required for its effective utilization in gas turbine engines.<sup>22</sup> The research involved a two-phase approach to address the complexities of ammonia combustion. Phase I focused on a broad range of tests and analytical studies to determine the feasibility of using ammonia in gas turbines. The phases included combustion system development, control and accessory adaptations, and material compatibility assessments. Phase II centered on modifying a 250 hp Solar T-350 gas turbine engine to operate on ammonia fuel with minimal changeover effort. The engine was equipped with two types of ammonia combustion systems: a vapor combustor and an oxidation-catalyst-aided combustor. Rigorous testing was conducted to ensure satisfactory engine performance and operation with both systems. The results indicated that while ammonia combustion is more challenging than hydrocarbon fuel combustion, it can be effectively managed with the right engineering solutions. The use of catalytic aids showed particular promise, offering an improved combustion efficiency and reduced combustor volume. The study concluded that ammonia can be a satisfactory substitute for hydrocarbon fuels in simple-cycle gas turbine engines. While the vapor combustor offered an adequate solution for certain applications, the catalytic combustion system showed potential for further development, particularly in enhancing response characteristics and reliability.

Moreover, the U.S. Army Aviation Materiel Laboratories assessed the feasibility of ammonia-fueled gas turbine engines for use in army aircraft,<sup>23</sup> considering the Nuclear Powered Energy Depot Concept. The research evaluated the design and characteristics of high- and low-pressure tanks for storing ammonia, considering its low boiling point and the need for pressurized or refrigerated storage. The use of refrigerated tanks for long-term storage and the potential for gelation of

ammonia to reduce the vapor pressure are also discussed. The study encompassed performance assessments in both rotary-wing (UH-1D helicopter) and fixed-wing (CV-7A aircraft) configurations and found that while ammonia could increase the maximum power output by approximately 15%, its lower heating value resulted in higher specific fuel consumption (SFC). The use of regeneration was considered crucial for improving the SFC of ammonia-fueled engines. This study also compared the mission radius, payload capacity, and productivity of these aircraft when using ammonia versus hydrocarbon fuels. It was concluded that ammonia-fueled aircraft exhibited significantly lower productivity and reduced mission radius capabilities. The researchers concluded that ammonia as a gas turbine fuel resulted in considerably lower aircraft productivity compared to hydrocarbon fuels. The specific fuel consumption for ammonia-fueled engines was found to be 2.20–2.6 times higher than that for hydrocarbon-fueled engines, while the maximum power output was only moderately higher. It was suggested that alternative technologies, such as variable compressor and turbine geometry, high-temperature turbines, and regeneration, should be explored to reduce hydrocarbon fuel logistics.

In the realm of aerospace, ammonia-based technology marked its foray into propulsion systems, exemplified by the development of the X-15 aircraft at the National Advisory Committee for Aeronautics (NACA) Langley Aeronautical Laboratory, which has since evolved into the NASA Langley Research Centre.<sup>24</sup> This vehicle was propelled by the XLR-99 engine, a throttleable powerhouse capable of generating up to 250 500 N of thrust. The engine's propulsion system was uniquely designed to utilize a combination of liquid ammonia and liquid oxygen (LOX), which together provided the necessary energy for its operation.

The selection of liquid ammonia as a fuel component was motivated by its stability and favorable volumetric energy density, which facilitated storage under the stringent conditions demanded by high-performance aerospace applications. Additionally, the cooling effects derived from the use of liquid propellants significantly enhanced the engine's operational efficiency. The X-15 was launched from a B-52 research aircraft, which itself was in flight at velocities approaching 800 km/h.

Despite these advancements, certain sources have<sup>25</sup> indicated that the program's discontinuation was precipitated by an incomplete appreciation for the ammonia system's potential and by the pursuit of fuels with higher gravimetric energy density. However, the X-15's legacy endures, as it achieved speeds of up to 6.7 times the speed of sound, a record that stood unmatched until the era of space shuttle travel.<sup>24</sup> The X-15's remarkable performance underscores the potential of ammonia as a fuel in aerospace applications, even as it highlights the challenges that must be surmounted to fully realize such technologies.

Recent advancements in ammonia combustion technology for power and propulsion have garnered significant attention. However, a primary challenge hindering its widespread adoption is the substantial NO<sub>x</sub> emissions associated with the combustion process. Factors such as operating load, ambient conditions, and fuel mixture composition significantly influence the NO<sub>x</sub> formation. To address this environmental concern, stringent regulations have been implemented, mandating a reduction in NO<sub>x</sub> emissions from 200 ppm to as low as 25 ppm or even 9 ppm.<sup>26</sup>



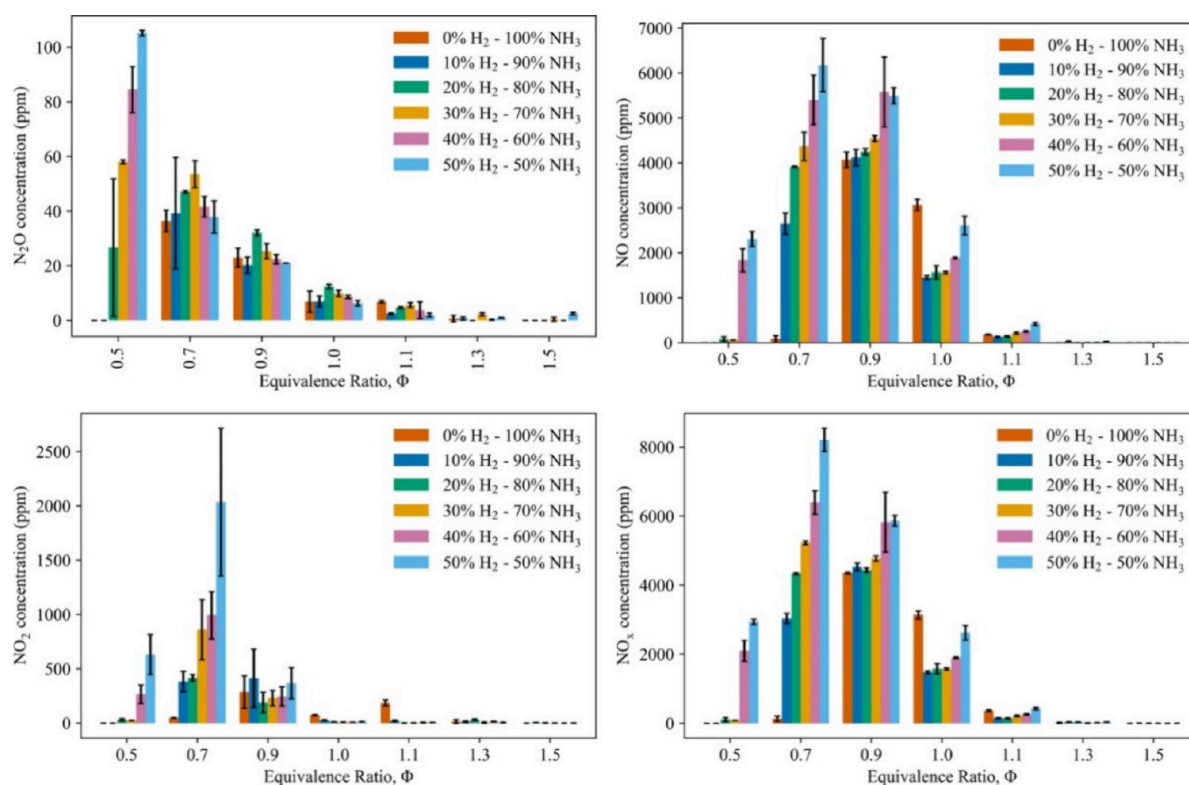


**Figure 1.** Recorded NO, NO<sub>2</sub>, N<sub>2</sub>O, and combined NO<sub>x</sub> emissions. Three trial averages and associated standard deviations for N<sub>2</sub>O, NO, NO<sub>2</sub>, and combined NO<sub>x</sub>, from left to right and from top to bottom, respectively. Reprinted with permission from ref 38. Copyright 2024 Elsevier.

While NO<sub>x</sub> emissions generally increase with engine power, reaching their peak at the rated output, technologies like SCO Duiker's have demonstrated the feasibility of combusting ammonia-rich streams (up to 100 vol %) in commercial applications, including furnaces and boilers in the processing and oil/gas extraction sectors. Mitsubishi Power's ongoing development of a 100% ammonia-fed boiler further underscores the potential for stable ammonia combustion and NO<sub>x</sub> suppression. It is imperative to note that, during ammonia combustion in conventional dry low NO<sub>x</sub> (DLN) combustion systems, nitrogen from the ammonia fuel is more prone to conversion into NO<sub>x</sub> compared to methane or hydrogen flames at similar temperatures. This can result in NO<sub>x</sub> emissions exceeding 1000 ppm, even with blends of ammonia and natural gas.<sup>27</sup> Consequently, extensive research is required to develop effective NO<sub>x</sub> suppression strategies for ammonia combustion across various operating conditions.

Beyond thermal NO<sub>x</sub> formation, the direct formation of N<sub>2</sub>O and NO<sub>x</sub> from ammonia fuel is another critical factor. While higher ammonia fuel fractions can lead to lower thermal NO<sub>x</sub> emissions, they may also increase direct NO and N<sub>2</sub>O formation. Pochet et al.<sup>28</sup> observed a temperature-dependent trade-off between NO and N<sub>2</sub>O, where conditions favoring the reduction of one species often promoted the formation of the other. Furthermore, fuel-rich operation can result in residual unburned hydrogen due to incomplete ammonia combustion. Hayakawa et al.<sup>29</sup> identified a crossover air–fuel ratio of approximately 1.05 where unburned ammonia, hydrogen, and residual NO were minimized. Fuel-richer operation tends to produce higher levels of NH<sub>3</sub> and H<sub>2</sub> in the exhaust, while stoichiometric or fuel-leaner conditions can lead to NO<sub>x</sub> emissions exceeding 1000 ppm. However, the potential for fuel-rich operation in ammonia engines, which is not feasible

with hydrocarbon fuels due to soot and CO formation, presents an opportunity for optimizing emissions. To fully understand the trade-offs between thermal- and fuel-borne NO<sub>x</sub> and N<sub>2</sub>O formation across a wide range of operating conditions, further research is essential. By addressing these challenges, the adoption of ammonia as a sustainable fuel source can be accelerated while minimizing its environmental impact.

**2.2. Ammonia Laminar Flames.** Ammonia, as a carbon-free fuel, holds promise for reducing greenhouse gas emissions in combustion processes. However, the formation of NO<sub>x</sub> during ammonia combustion poses a significant environmental challenge. Laminar flames, characterized by their stable and controlled nature, offer an ideal platform for dissecting the fundamental aspects of combustion and the intricate mechanisms of NO<sub>x</sub> formation. This section endeavors to synthesize recent findings on NO<sub>x</sub> emissions in ammonia laminar flames, focusing on the underlying chemical kinetics, the influence of various parameters on emission formation, and potential strategies for emission reduction.

The formation of NO<sub>x</sub> in ammonia flames is predominantly governed by two mechanisms: the thermal (Zeldovich) mechanism and the fuel nitrogen mechanism.<sup>30</sup> The thermal mechanism, which becomes dominant at temperatures exceeding 1800 K, involves the oxidation of atmospheric nitrogen to NO. Conversely, the fuel nitrogen mechanism is concerned with the conversion of nitrogen species bound within the fuel, such as NH<sub>3</sub>, to NO through a series of intermediate reactions. Lindstedt et al.<sup>31</sup> provided pioneering insights into the chemical kinetics of ammonia oxidation, elucidating the pivotal role of HNO as an intermediate in NO formation. The study underscored the dependency of HNO conversion pathways on flame conditions, highlighting the significance of the NH with

OH reaction in pure ammonia flames and the increasing importance of the Zeldovich mechanism in ammonia-doped hydrogen flames with increasing fuel concentrations. Sullivan et al.<sup>32</sup> further explored the conversion dynamics of  $\text{NH}_3$  to  $\text{NO}_x$ , finding that increased  $\text{NH}_3$  seeding leads to a higher conversion to  $\text{N}_2$  rather than  $\text{NO}$ , particularly in nonpremixed methane–air flames, emphasizing the complex interplay between fuel–nitrogen chemistry and  $\text{NO}_x$  formation.

The presence of hydrogen in ammonia flames introduces significant alteration in  $\text{NO}_x$  formation pathways, potentially enhancing  $\text{NO}$  production rates. Lee et al.<sup>33</sup> demonstrated that the presence of hydrogen in ammonia flames could lead to higher  $\text{NO}$  production rates, an effect moderated under fuel-rich conditions, suggesting an optimal operational window for emission minimization. Hayakawa et al.<sup>34</sup> further explored the product gas characteristics in ammonia/hydrogen/air premixed laminar flames, revealing a substantial increase in  $\text{NO}$  emissions at lean conditions, particularly when compared to pure ammonia/air flames. The study also identified a critical trade-off between  $\text{NO}$  and unburnt ammonia under slightly rich conditions and a rapid increase in  $\text{N}_2\text{O}$  mole fraction around an equivalence ratio of 0.6, underscoring the importance of equivalence ratio control in reducing  $\text{N}_2\text{O}$  emissions.

Wang et al.<sup>35</sup> studied the laminar burning velocities (LBVs) of  $\text{NH}_3/\text{H}_2$  blends at elevated pressures, and found that LBVs decrease with increasing ammonia mole fraction in the fuel mixture, while the addition of  $\text{H}_2$  significantly increases flame speed. The study concluded that ammonia blended with  $\text{H}_2$  can enhance combustion characteristics and promote  $\text{NO}$  formation by enriching the H and OH radical pools and increasing the flame temperature. Mei et al.<sup>36</sup> employed a partial fuel cracking strategy to decompose  $\text{NH}_3$  into  $\text{H}_2$  and  $\text{N}_2$ , leveraging the high reactivity of  $\text{H}_2$  to improve combustion characteristics. The LBVs of partially cracked  $\text{NH}_3$ /air mixtures increased with the cracking ratio and peaked at equivalence ratios of around 1.1. The highest LBV measured was 38.1 cm/s at 1 atm, which is close to that of methane/air mixtures at the same pressure, indicating the effectiveness of the cracking strategy. Zheng et al.<sup>37</sup> investigated the impact of radiation reabsorption on the laminar flame speed and  $\text{NO}$  emissions of  $\text{NH}_3/\text{H}_2$ /air mixtures under stoichiometric conditions with varying hydrogen ratios. Radiation reabsorption significantly influenced flame speed with a maximum enhancement of 17% observed at the lowest hydrogen ratio ( $\eta = 0.2$ ). The effect decreased as the hydrogen ratio increased. Radiation reabsorption promoted  $\text{NO}$  generation and emission, with the effect being more pronounced at lower hydrogen ratios. The promotion effect decreased monotonically with an increasing hydrogen proportion.

Nawaz et al.<sup>38</sup> further delved into the combustion characteristics and  $\text{NO}_x$  emissions of ammonia–hydrogen blends in spherically expanding laminar flames. The hydrogen concentration in the fuel blends was varied from 0 to 50%, and the equivalence ratios were adjusted from 0.5 to 1.5. The study found that  $\text{NO}_x$  emissions peak at lean conditions and decrease significantly for rich mixtures, with hydrogen addition tending to increase  $\text{NO}_x$  emissions, particularly at lean equivalence ratios. Figure 1 illustrates the average concentrations of  $\text{NO}$ ,  $\text{NO}_2$ , and  $\text{N}_2\text{O}$  emissions across different mixture compositions and equivalence ratios. The figure highlights the trend of  $\text{NO}_x$  emissions increasing with hydrogen fractions in lean mixtures.

Anasif et al.<sup>39</sup> evaluated the performance of various kinetic reaction mechanisms in predicting  $\text{N}_2\text{O}$  mole fractions in  $\text{NH}_3/\text{H}_2$  blends especially with the 70/30 vol % mixing ratio. The  $\text{NH} + \text{NO} \rightleftharpoons \text{N}_2\text{O} + \text{H}$  reaction was identified as being dominant in  $\text{N}_2\text{O}$  formation across all studied conditions. The consumption of  $\text{N}_2\text{O}$  was primarily through the reactions  $\text{N}_2\text{O} + \text{H} \rightleftharpoons \text{N}_2 + \text{OH}$  and  $\text{N}_2\text{O} (+\text{M}) \rightleftharpoons \text{N}_2 + \text{O} (+\text{M})$ . The study concluded that while the Klippenstein (2018) model generally predicts  $\text{N}_2\text{O}$  mole fractions accurately, its performance deteriorates under very lean conditions. The chemical reaction  $\text{NH} + \text{NO} \rightleftharpoons \text{N}_2\text{O} + \text{H}$  significantly contributes to the formation of  $\text{N}_2\text{O}$  under all of the tested conditions. The reduction of  $\text{N}_2\text{O}$  is primarily controlled by specific reactions involving H and NO.

Ariemma et al.<sup>40</sup> and Kovaleva et al.<sup>41</sup> explored the nonlinear dependency of  $\text{NO}_x$  emissions on the ammonia ratio in  $\text{NH}_3/\text{CH}_4$ /air laminar flames and emphasized the role of methane in boosting OH radical production, thereby increasing  $\text{NO}_x$  production through ammonia oxidation. For lean conditions, many reactions involving NH and  $\text{NH}_2$  species with O, H, NO, and  $\text{O}_2$  had a high sensitivity for NO without strongly affecting the laminar burning velocity. The latter study also reported HCN emissions with changing ammonia content. HCN was experimentally measured and found to be a significant pollutant at rich conditions ( $\phi = 1.20\text{--}1.35$ ;  $E_{\text{NH}_3} = 0.6\text{--}0.1$ ), similar to ammonia emissions. Okafor et al.<sup>42</sup> investigated the laminar burning velocity of premixed  $\text{NH}_3/\text{CH}_4$ /air mixtures, focusing on the influence of ammonia concentration on flame characteristics. A new detailed chemical kinetics model was developed that accurately predicted laminar burning velocities and  $\text{NO}$  emissions. The velocity decreased with increasing ammonia concentration with the highest velocity measured at 38.1 cm/s for methane–air mixtures at 1 atm, close to values reported in the literature. The burned gas Markstein length increased with the equivalence ratio and ammonia concentration, indicating increased flame stretch sensitivity. Wang et al.<sup>43</sup> measured the laminar burning velocities of  $\text{NH}_3/\text{CH}_4$ /air mixtures at elevated pressures and developed a kinetic mechanism that accurately models the combustion characteristics of these mixtures. The velocity decreased with an increasing ammonia concentration, with the highest velocities measured for methane–air mixtures. The study provided comprehensive data on the laminar burning velocities of  $\text{NH}_3/\text{CH}_4$ /air mixtures at elevated pressures, which are critical for the development of gas turbine combustors for these fuels. The CEU- $\text{NH}_3$ -Mech 1.1 mechanism showed improved accuracy in predicting combustion characteristics, especially under rich conditions and at elevated pressures.

The impact of oxygen-enriched conditions on the formation of  $\text{NO}_x$  in ammonia laminar flames has been a subject of recent investigations. Woo et al.<sup>44</sup> reported a nonmonotonic trend in  $\text{NO}_x$  emissions with varying oxygen ratios in ammonia-doped methane flames, with maximum emissions observed at an oxygen ratio of 0.7. Mei et al.<sup>45</sup> complemented this with an experimental and kinetic modeling study under oxygen enrichment and elevated pressure, identifying the interplay between oxygen content, equivalence ratio, and initial pressure on  $\text{NO}_x$  emissions. Moreover, numerous studies have investigated the combustion characteristics and emissions of DME–ammonia blends, which are a type of oxygenated fuel. Meng et al.<sup>46</sup> developed a detailed chemical reaction

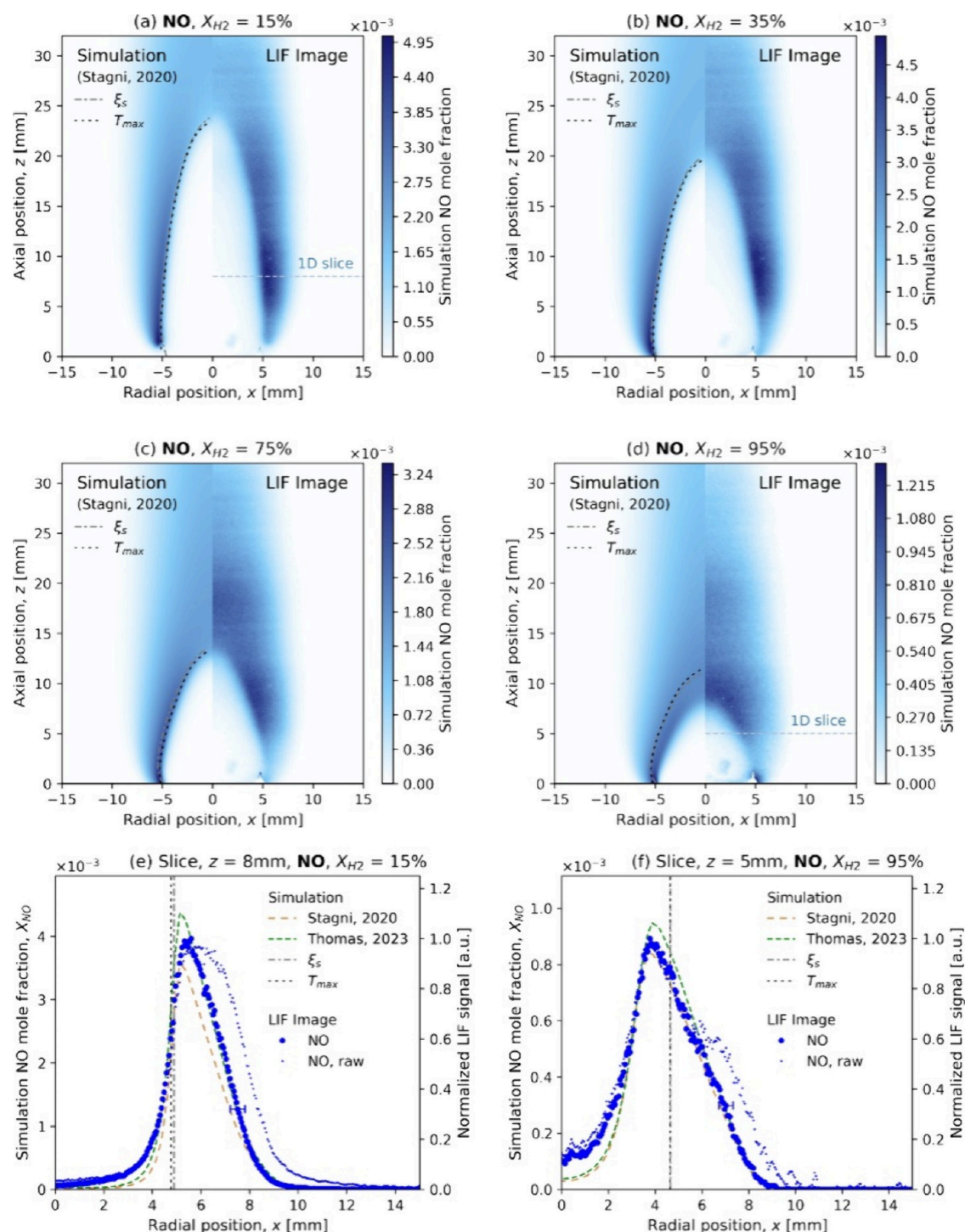


**Figure 2.** NO LIF images compared to simulation predictions for fuel hydrogen fractions of (a) 15, (b) 35, (c) 75, and (d) 95%. The species concentration profile for a 1D horizontal slice is also shown for (e)  $X_{H_2} = 15\%$  (at the height indicated in (a)) and (f)  $X_{H_2} = 95\%$  (at the height indicated in (d)). Reprinted with permission from ref 51. Copyright 2024 Elsevier.

mechanism for the dual-fuel combustion of  $NH_3/DME$ , which accurately predicted combustion behaviors in both laminar burning and ignition models, including combustion characteristics and emissions, particularly the formation and reduction of NO. The study found that adding up to 50% DME to ammonia promotes NO formation, leading to higher NO production. However, a blend with 75%  $NH_3$  and 25% DME (D25) generates more  $NH$  and  $NH_2$  radicals, promoting the NO reduction reaction and resulting in approximately 9% less

NO at an equivalence ratio of 0.7.  $CH_3$  radicals from DME can slightly increase NO production by promoting the conversion of HNO and  $NO_2$  to NO. Yu et al.<sup>47</sup> investigated the emission characteristics, particularly  $NO_x$ , CO, and unburned  $NH_3$ , of  $NH_3/DME/air$  premixed flames. They found that lean conditions and stoichiometric conditions favored NO formation, while rich conditions negatively impacted NO formation. Increasing the  $NH_3$  fraction from 50 to 90% in the fuel mixture effectively decreased NO emissions.  $NO_2$



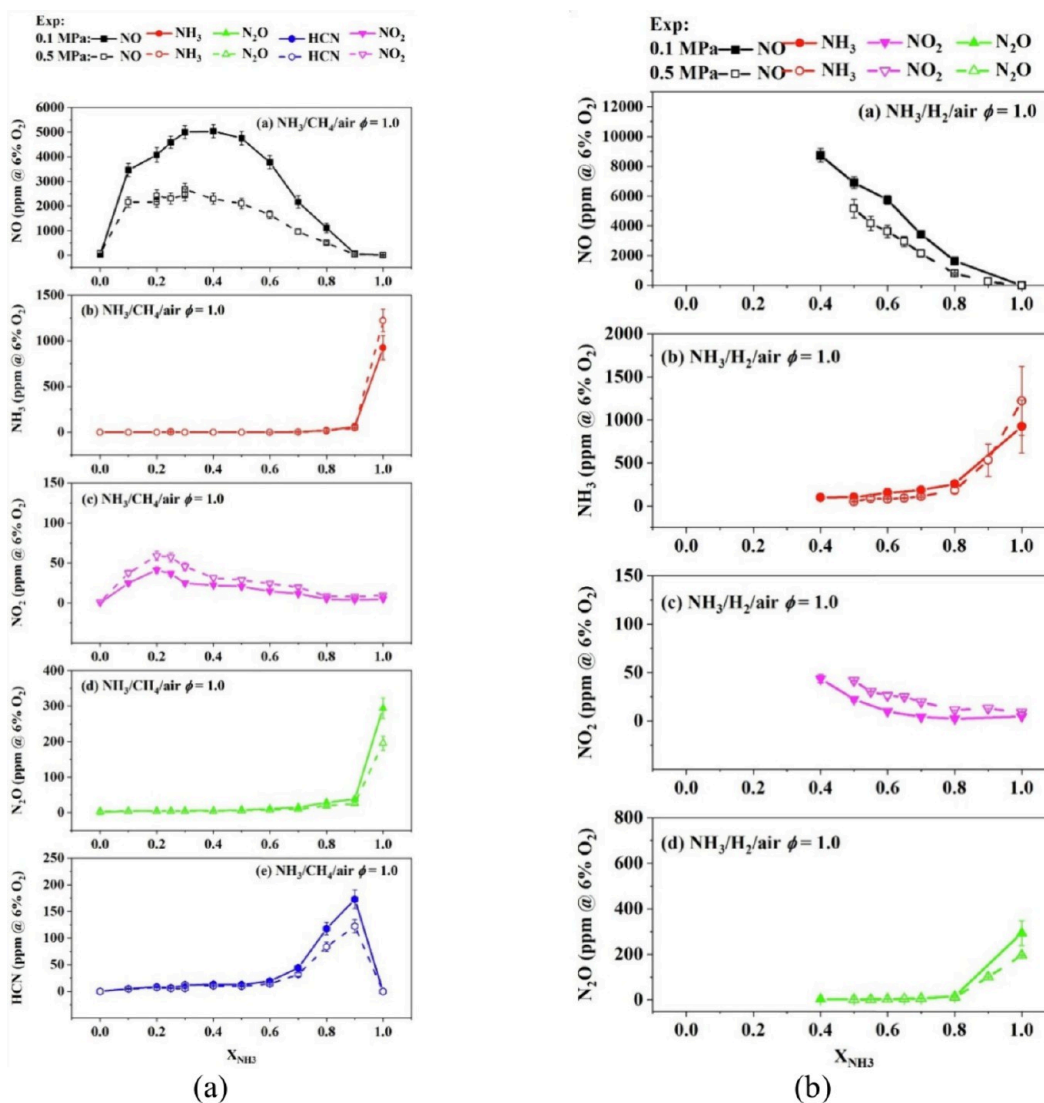


**Figure 3.** Measured and simulated  $\text{NO}$ ,  $\text{NH}_3$ ,  $\text{N}_2\text{O}$ ,  $\text{NO}_2$ , and  $\text{HCN}$  concentrations for the stoichiometric (a)  $\text{NH}_3/\text{CH}_4/\text{air}$  flame and (b)  $\text{NH}_3/\text{H}_2/\text{air}$  flame as a function of  $X_{\text{NH}_3}$  at 0.1 and 0.5 MPa (solid symbols, 0.1 MPa; open symbols, 0.5 MPa). Reprinted with permission from ref 52. Copyright 2024 Elsevier.

emissions followed a trend similar to that of  $\text{NO}$  but were approximately an order of magnitude lower in concentration. Rich conditions are more suitable for controlling  $\text{NO}$  emissions in  $\text{NH}_3/\text{DME}$  co-combustion. The study suggested that single-stage combustion may not be optimal for pollutant control in  $\text{NH}_3/\text{DME}$  co-combustion, and staged combustion strategies or  $\text{NO}_x$  post-treatment devices may be necessary. Alekseev et al.<sup>48</sup> investigated  $\text{NO}$  formation in  $\text{NH}_3/\text{DME}$  fuel mixtures and concluded that  $\text{NO}$  formation decreases with an increasing equivalence ratio ( $\phi$ ) and peaks at a certain  $\text{NH}_3$  percentage in the fuel mixture, after which it decreases with further increases in  $\text{NH}_3$  content. The study reported that, for the range of initial mixture parameters studied,  $\text{NO}$  formation in  $\text{NH}_3/\text{DME}$  flames is primarily determined by the  $\text{NH}_3$  submechanism, with the hydrocarbon component influencing radical concentrations and heat release.

For various  $\text{NH}_3$ -containing mixtures ( $\text{NH}_3/\text{air}$ ,  $\text{NH}_3/\text{H}_2/\text{air}$ ,  $\text{NH}_3/\text{CO}/\text{air}$ ,  $\text{NH}_3/\text{CH}_4/\text{air}$ , etc.), detailed kinetic models have been developed to predict the laminar flame speed and  $\text{NO}_x$  emissions, with validation against experimental data. The updated  $\text{NH}_3$  chemistry, particularly the  $\text{NNH}$  chemistry, was

found to be crucial for capturing the temperature dependence of  $\text{NH}_3/\text{air}$  flames and the influence of  $\text{H}_2$ ,  $\text{CO}$ , and  $\text{CH}_4$  on  $\text{NO}_x$  emissions.<sup>49</sup> Ramos et al.<sup>50</sup> investigated different ammonia/methane blends ( $X_{\text{NH}_3} = 0\text{--}0.7$ ) at three equivalence ratios (0.8, 0.9, and 1.0) in a laboratory-scale laminar flame burner. The experimental results indicated an initial rise in  $\text{NO}_x$  emissions as the ammonia content in the fuel mixture was raised to 50% with a decreasing trend afterward. This trend is consistent across the equivalence ratios studied (0.8, 0.9, and 1).  $\text{NO}_x$  emissions decrease as the equivalence ratio moves toward fuel-lean conditions, indicating that the combustion process becomes cleaner with less fuel relative to oxygen. The rate of production analysis indicates that the  $\text{HNO}$  pathway is crucial for  $\text{NO}$  formation, and its consumption is mainly driven by reactions with  $\text{N}$ ,  $\text{NH}$ , and  $\text{NH}_2$  radicals. The formation and consumption of  $\text{NO}$  are highly sensitive to the  $\text{H}_2/\text{O}_2$  chemistry, which determines the concentrations of the  $\text{O}$ ,  $\text{OH}$ , and  $\text{H}$  radicals. Sensitivity analysis revealed that reactions involved in the  $\text{H}_2/\text{O}_2$  submechanism, which regulates the amount of  $\text{O}$ ,  $\text{H}$ , and  $\text{OH}$  radicals as well as temperatures, most

affect the process of NO formation and consumption. In contrast to  $\text{NO}_x$ , CO and  $\text{NH}_3$  emissions were found to be quite low, indicating near-complete combustion of  $\text{CH}_4$  and  $\text{NH}_3$ .

Recently, Thomas et al.<sup>51</sup> investigated the structure and nitrogen oxide ( $\text{NO}_x$ ) formation in laminar diffusion flames of ammonia–hydrogen fuel blends with air. The experimental approach involved blending ammonia fuel with hydrogen to enhance fuel reactivity, covering a fuel composition range of 15–100% hydrogen by mole fraction. The flame structure was visualized using planar laser-induced fluorescence (PLIF) for NO, NH, and OH radicals as well as  $\text{OH}^*$  by filtered chemiluminescence. Numerical models were employed to predict species concentration profiles and were compared with experimental data. The study found that  $\text{NO}_x$  emissions, including NO,  $\text{NO}_2$ , and  $\text{N}_2\text{O}$ , decreased with increasing hydrogen content in the fuel blend. The authors also presented a detailed analysis of the reaction pathways contributing to NO creation and destruction, highlighting the importance of key reactions, such as HNO formation and the role of NH radicals. For high fuel hydrogen content, the measured NO profile shifted inward toward the fuel outlet, away from the peak temperature contour (see Figure 2), indicating a change in the flame structure and  $\text{NO}_x$  formation mechanisms.

The choice of fuel blend and operating conditions significantly impacts  $\text{NO}_x$  emissions in laminar ammonia flames. Hydrogen addition generally increases  $\text{NO}_x$  emissions, especially under lean conditions, due to increased flame speed and radical pool enrichment, with radiation reabsorption further promoting NO generation. In contrast,  $\text{NH}_3/\text{CH}_4$  blends initially increase  $\text{NO}_x$  emissions with rising ammonia content up to 50%, followed by a decrease, with lean conditions favoring lower  $\text{NO}_x$  emissions. The  $\text{NH}_3/\text{DME}$  blends show higher NO production up to 50% DME, but a blend with 75%  $\text{NH}_3$  and 25% DME reduces NO emissions under rich conditions due to increased NH and  $\text{NH}_2$  radicals. Oxygen enrichment can enhance  $\text{NO}_x$  emissions, but the effect can be complex and influenced by other factors. Optimizing fuel blends, operating conditions, and combustion strategies is crucial for minimizing  $\text{NO}_x$  emissions in ammonia-based combustion systems. For instance, while hydrogen addition can increase  $\text{NO}_x$  emissions, operating under fuel-rich conditions can mitigate this effect. Similarly, in  $\text{NH}_3/\text{DME}$  blends, increasing the ammonia concentration can effectively reduce the  $\text{NO}_x$  emissions. The impact of oxygen enrichment on  $\text{NO}_x$  emissions is more nuanced, with nonmonotonic trends observed in some cases. To minimize  $\text{NO}_x$  emissions, a careful balance must be struck among fuel selection, operating conditions, and combustion strategies.

Moreover, Wang et al.<sup>52</sup> presented a comprehensive study on the impact of elevated pressure and strain rate on  $\text{NO}_x$  emissions in laminar premixed flames of ammonia-enriched fuels. The research investigates the potential of combining elevated pressure and strain rate to reduce  $\text{NO}_x$  emissions in laminar premixed flames of  $\text{NH}_3/\text{CH}_4/\text{air}$  and  $\text{NH}_3/\text{H}_2/\text{air}$ . Utilizing a high-pressure heat flux burner and CHEMKIN software, the study measured and simulated  $\text{NO}_x$  emissions, including NO,  $\text{NO}_2$ ,  $\text{N}_2\text{O}$ ,  $\text{NH}_3$ , and HCN. Key findings indicate that increasing pressure generally decreases  $\text{NO}_x$  emissions, with the exception of  $\text{NO}_2$ , which sees an increase, as shown in Figure 3. Medium ammonia conditions are optimal for reducing the level of NO emissions through pressure enhancement. High strain rates were found to reduce

NO emissions in stoichiometric and rich conditions but increased NO emissions in lean conditions before the NO peak equivalence ratio. The research concludes that the combination of elevated pressure and strain rate can significantly reduce  $\text{NO}_x$  emissions while ensuring complete ammonia oxidation, particularly for medium ammonia content at equivalence ratios between 0.9 and 1.1. This finding is instrumental for the design of practical high-pressure burners that utilize ammonia blend flames to minimize the  $\text{NO}_x$  emissions.

Ammonia laminar flames offer insights into the complex interplay among fuel chemistry, flame dynamics, and pollutant formation. This section provides a comprehensive understanding of the  $\text{NO}_x$  emission characteristics of ammonia laminar flames under various conditions. The synthesis of experimental and computational studies has been instrumental in identifying key factors influencing  $\text{NO}_x$  formation and in developing predictive models. While significant strides have been made, the need for further research to refine emission reduction strategies remains. The integration of experimental data with computational models provides a robust framework for predicting and mitigating  $\text{NO}_x$  emissions in ammonia combustion systems, crucial for the design of efficient and environmentally friendly combustors.

### 2.3. Ammonia Swirl Flames. 2.3.1. Pure Ammonia.

Although the utilization of ammonia as a fuel offers a pathway to sustainable energy by reducing greenhouse gas emissions, the challenge of controlling  $\text{NO}_x$  emissions in these processes is nontrivial and requires a deep understanding of the underlying phenomena. This section reviews recent findings on the swirl flame of pure ammonia and its implications for  $\text{NO}_x$  emissions, drawing from various studies that have contributed to the understanding of the underlying chemical kinetics and combustion dynamics.

The formation of  $\text{NO}_x$  in ammonia swirl flames is a complex process influenced by various factors, including chemical kinetics and combustion dynamics. Klippenstein et al.<sup>53</sup> have explored the role of the NNH radical of  $\text{NO}_x$  formation in ammonia/air flames. Recognized as a key intermediate in thermal De- $\text{NO}_x$  processes, NNH is pivotal in the selective noncatalytic reduction of NO ( $\text{NNH} + \text{NO} = \text{N}_2 + \text{HNO}$ ), where ammonia acts as the reducing agent. This study investigated the potential energy surfaces of reactions involving NNH, revealing the impact of these reactions on NO formation ( $\text{N}_2 + \text{H} = \text{NNH}$ ,  $\text{NNH} + \text{O} = \text{NH} + \text{NO}$ ,  $\text{NH} + \text{O}_x = \text{NO} + \dots$ ) and reduction. The updated chemical kinetics model presented in this research has been instrumental in enhancing the understanding of NNH chemistry in thermal De- $\text{NO}_x$  processes. Complementing this, Hayakawa et al.<sup>54</sup> conducted a comprehensive experimental investigation into the  $\text{NO}_x$  characteristics of ammonia/air flames under varying conditions of equivalence ratio and pressure. The study employed numerical simulations to explore NO formation and reduction mechanisms, identifying the mole fraction of NO as being sensitive to changes in the equivalence ratio and pressure, indicating a decrease in the NO mole fraction with increasing equivalence ratio and pressure. The findings underscore the importance of the third-body reaction of  $\text{OH} + \text{H} + \text{M} = \text{H}_2\text{O} + \text{M}$  in NO reduction at high pressures and highlight the roles of  $\text{NH}_2$ , NH, and N in the postflame region of rich mixtures.

Garborg et al.<sup>55</sup> offered a detailed review of the various  $\text{NO}_x$  formation mechanisms, including thermal NO, prompt-NO, fuel-NO, and NO formation via  $\text{N}_2\text{O}$  or NNH; a



simplified reaction path diagram is shown in Figure 4. The review evaluates these mechanisms against experimental data

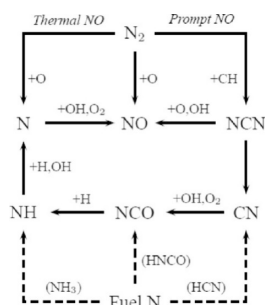


**Figure 4.** Simplified reaction path diagram illustrating the major steps in the formation of thermal NO, prompt NO, and fuel NO. Reprinted with permission from ref 55. Copyright 2018 Elsevier.

and discusses the accuracy of modeling predictions. Furthermore, it delves into in situ reduction methods such as humidification, selective noncatalytic reduction, and reburning techniques, which are critical for controlling NO<sub>x</sub> emissions in industrial applications. For example, Figure 5 shows a pathway

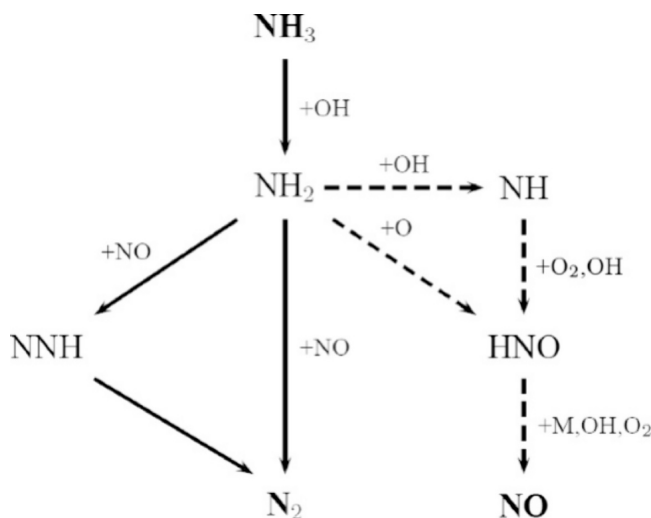


**Figure 5.** Reaction path diagram for the thermal De-NO<sub>x</sub> process. Dashed lines denote pathways only important at high temperatures. Reprinted with permission from ref 55. Copyright 2018 Elsevier.

diagram for the thermal De-NO<sub>x</sub> process in the presence of water vapor. Ammonia is converted to NH<sub>2</sub> by reaction with the O/H radical pool, primarily OH. The subsequent reaction between NH<sub>2</sub> and NO is the key step in the process via two product channels: NH<sub>2</sub> + NO = NNH + OH and NH<sub>2</sub> + NO = N<sub>2</sub> + H<sub>2</sub>O.

Pugh et al.<sup>56</sup> compared swirl-stabilized premixed and diffusion NH<sub>3</sub>–air flames, revealing that the diffusion flame configuration produced significantly lower NO concentrations at lean conditions, while the premixed flame is more favorable at higher equivalence ratios. The study also explored the use of secondary air and reactant humidification as methods to control NO<sub>x</sub> emissions, highlighting the need for careful control to avoid increased NO<sub>x</sub> production. Additionally, Okafor et al.<sup>57</sup> highlighted the significant influence of wall heat loss on the emission characteristics of premixed ammonia–air swirling flames. Their research shows that wall heat loss can

lead to contradictory emission trends, with substantial effects on the flame structure and NO<sub>x</sub> emissions. They advocate for strategies to reduce wall heat loss or extend the primary combustion zone to effectively control NH<sub>3</sub> and N<sub>2</sub>O emissions effectively. In a related study, Okafor et al.<sup>58</sup> examined the flame stability and emission control in two-stage micro gas turbine combustors using liquid ammonia spray combustion. Their findings underscore the importance of enhancing the flame in the primary combustion zone and reducing the combustor wall heat loss to control NO<sub>x</sub> emissions.

Enhancing ammonia combustion through oxygen enrichment is a strategic approach to achieving more efficient and cleaner energy conversion, particularly relevant for applications seeking to reduce carbon footprints. Liu et al.<sup>59</sup> proposed a strategy of using oxygen-enriched conditions to promote self-promoted fuel pyrolysis, which can lead to cleaner and more efficient ammonia combustion. Their findings suggest that oxygen enrichment significantly alters flame characteristics, with flames becoming more compact and stable as the oxygen content increases. This enrichment substantially expands the lean blowout (LBO) and rich blowout (RBO) limits of ammonia swirl flames, indicating a broader stable combustion window. Emissions of NO<sub>x</sub> and NH<sub>3</sub> were measured, revealing that the low NO<sub>x</sub>/NH<sub>3</sub> emission window also expands with increased oxygen levels, a critical factor for simultaneous pollutant control during combustion enhancement. The self-promoted ammonia pyrolysis under oxygen enrichment emerges as a promising approach for achieving clean and efficient ammonia combustion, effectively broadening both stable combustion and low NO<sub>x</sub>/NH<sub>3</sub> emission windows, which are essential for practical applications in gas turbines, furnaces, and boilers.

Building on this, Kim et al.<sup>60</sup> conducted a meticulous examination of the influence of oxygen-enriched conditions on the combustion behavior and emission profiles of NH<sub>3</sub>/air premixed flames. They observed that, under elevated oxygen levels, the flames exhibited not only increased propagation speeds but also reduced thicknesses. At a volume fraction of 35–40% O<sub>2</sub> in the nonfuel mixtures, the flames achieved a burning intensity comparable to that of conventional hydrocarbon/air flames, highlighting NH<sub>3</sub>'s potential as a carbon-free fuel alternative. The research also demonstrated that these O<sub>2</sub>-enriched NH<sub>3</sub>/air flames maintained stability against cellular instabilities at normal temperature and pressure with preferential diffusion playing a negligible role in any destabilizing effects. Despite these promising combustion characteristics, the study highlighted a critical concern: a significant increase in the level of local NO<sub>x</sub> emissions. This finding underscores the necessity for the development of effective strategies to mitigate NO<sub>x</sub> emissions in practical combustion systems employing O<sub>2</sub>-enriched NH<sub>3</sub>/air mixtures, ensuring that the environmental benefits of using ammonia as a fuel are fully realized.

The collective findings from these studies paint a complex picture of the interplay among combustion dynamics, chemical kinetics, and NO<sub>x</sub> emissions in pure ammonia swirl flames. The insights gained are invaluable for developing strategies aimed at minimizing NO<sub>x</sub> emissions while maintaining efficient combustion. As our understanding of these processes continues to evolve, further research is essential to refine these strategies and explore additional methods for controlling NO<sub>x</sub> emissions in practical applications.

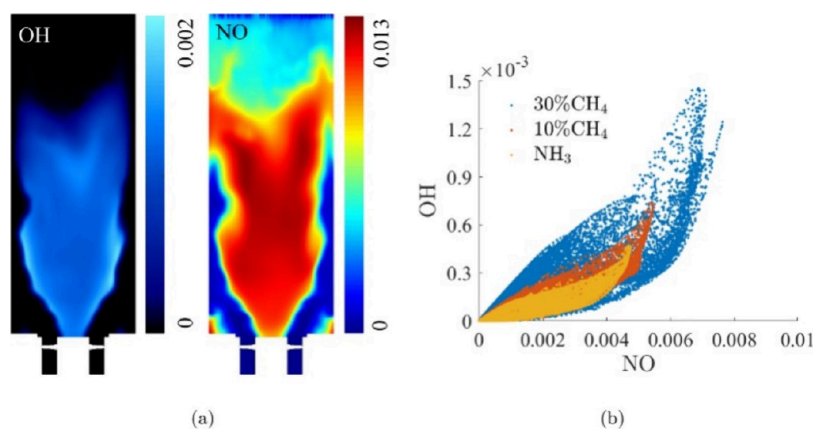


**Figure 6.** (a) Instantaneous distributions of the NO and OH mass fractions of the ammonia flame in the combustor. (b) Relationship of the local NO and OH mass fractions. The flame is operated at  $\phi = 0.7$  and  $U = 5$  m/s. Reproduced with permission from ref 69. Copyright 2021 Elsevier.

**2.3.2. Ammonia/Hydrocarbon Fuels.** The swirl flames of ammonia and hydrocarbon fuels present a rich tapestry of chemical kinetics and thermodynamic interactions that significantly influence  $\text{NO}_x$  emissions. This section endeavors to weave together the findings from various studies, elucidating the multifaceted nature of this challenge and the strategies devised to address it.

The pioneering works of Tian et al.<sup>61</sup> and Mendiara and Glarborg<sup>62</sup> shed light on the combustion dynamics of ammonia–hydrocarbon mixtures and the mechanisms that govern the  $\text{NO}_x$  emissions. Tian et al.<sup>61</sup> focused on the combustion of ammonia with methane under low-pressure conditions and illuminated the role of  $\text{NH}_2$  and  $\text{NH}$  radicals in the selectivity of NO or  $\text{N}_2$  formation, identifying key reactions that govern  $\text{NO}_x$  generation. Notably, the reactions  $\text{NH}_2 + \text{O} = \text{HNO} + \text{H}$  and  $\text{NH} + \text{NO} = \text{N}_2 + \text{O}$  are identified as crucial in the generation of  $\text{NO}_x$ . They discovered that, as the  $\text{NH}_3$  to  $\text{CH}_4$  mole ratio increases, the reaction zone expands and the levels of  $\text{H}_2\text{O}$ , NO, and  $\text{N}_2$  rise, while  $\text{H}_2$ , CO,  $\text{CO}_2$ , and  $\text{NO}_2$  decrease. This suggests that higher ammonia concentrations may lead to greater  $\text{NO}_x$  emissions. Additionally, they found that the temperature profiles of the flames decrease with an increased  $\text{NH}_3/\text{CH}_4$  mole ratio due to the reduction of  $\text{CH}_4$ , which can affect the formation and reduction pathways of  $\text{NO}_x$ . The reactions  $\text{H} + \text{O}_2 = \text{O} + \text{OH}$  and  $\text{NH}_2 + \text{O} = \text{HNO} + \text{H}$  emerge as significant contributors to NO formation, whereas  $\text{NH}_2 + \text{NO} = \text{N}_2 + \text{H}_2\text{O}$  and  $\text{NH} + \text{NO} = \text{N}_2\text{O} + \text{H}$  are instrumental in NO consumption. Mendiara and Glarborg,<sup>62</sup> on the other hand, investigated the impact of high  $\text{CO}_2$  concentrations on ammonia oxidation during the oxy-fuel combustion of methane. Their findings indicate that high  $\text{CO}_2$  levels enhance NO formation under reducing conditions but inhibit it under stoichiometric and lean conditions. The presence of  $\text{CO}_2$  as a bulk gas was found to facilitate NO formation due to an increased OH/H ratio and higher CO levels that enhance HNCO formation, while reactions leading to HNO and NH are inhibited under high  $\text{CO}_2$  levels due to reduced concentrations of O and H radicals, leading to an increased probability of forming  $\text{N}_2$  instead of NO.

Building upon these foundational studies, subsequent research has delved deeper into the factors influencing  $\text{NO}_x$  emissions. Valera-Medina et al.<sup>63</sup> explored the emission characteristics of premixed ammonia–methane swirling flames, noting a reduction in  $\text{NO}_x$  and  $\text{CO}_2$  emissions with increasing

equivalence ratio, while CO, THC, and unburned  $\text{NH}_3$  emissions increased. Xiao et al.<sup>64</sup> expanded on this by examining methane–ammonia flames across a wide range of mixing ratios, finding that the addition of ammonia to methane-rich mixtures enhances  $\text{NO}_x$  emissions, while high ammonia content in fuel mixtures has a De- $\text{NO}_x$ ing effect. They also noted that fuel-bound  $\text{NO}_x$  formation is more sensitive to ammonia content than thermal  $\text{NO}_x$ , particularly in regions with a low ammonia content. Li et al.<sup>65</sup> and Okafor et al.<sup>66</sup> further highlighted the critical factors influencing  $\text{NO}_x$  emissions in  $\text{NH}_3/\text{CH}_4$  combustion. For example, Li et al.<sup>65</sup> highlighted the HNO pathway as the predominant driver of  $\text{NO}_x$  formation in  $\text{NH}_3/\text{CH}_4$  combustion, with a sharp increase in  $\text{NO}_x$  emissions observed with  $\text{NH}_3$  addition up to a 20% dilution. They also emphasized the effectiveness of air staging in reducing  $\text{NO}_x$  emissions. Okafor et al.<sup>66</sup> underscored the role of OH radicals in fuel  $\text{NO}_x$  production and advocated for a rich-lean combustion strategy to achieve low emissions. Moreover, Zhang et al.<sup>67</sup> reported non-monotonic NO and  $\text{NO}_2$  emissions trends for different methane–ammonia blends, with the highest NO emissions observed for a 50/50 vol %  $\text{CH}_4/\text{NH}_3$  blend at stoichiometry. They suggested operating the combustor under rich conditions and avoiding an  $\text{NH}_3$  mole fraction of 0.5 to control the  $\text{NO}_x$  emissions.

Subsequently, An et al.<sup>68</sup> and Zhang et al.<sup>69</sup> investigated the effects of methane and hydrogen additives on  $\text{NO}_x$  emissions. To be specific, An et al.<sup>68</sup> found that cofiring methane with ammonia in premixed swirling flames increases  $\text{NO}_x$  emissions, with a peak at a 40%  $\text{NH}_3$  mole fraction. Zhang et al.<sup>69</sup> examined the effects of methane and hydrogen additives on  $\text{NO}_x$  emissions in ammonia/air flames within a swirl combustor, finding that small amounts of these additives can stabilize the flame without significantly increasing  $\text{NO}_x$  emissions. A positive correlation between OH and NO concentrations is displayed in Figure 6, indicating a temperature-dependent relationship.

Early studies<sup>70,71</sup> identified reactions such as  $\text{CH} + \text{N}_2 = \text{HCN} + \text{N}$  and  $\text{CH} + \text{N}_2 = \text{NCN} + \text{N}$  as critical initiation steps toward prompt NO formation. NCN eventually reacts with H radicals to convert into HCN, which then reacts with the O radicals to produce NCO. NCO converts into NH radicals that produce atomic nitrogen. Glarborg et al.<sup>55</sup> reported a rapid increase in HCN concentration at rich conditions ( $\phi > 1.2$ ),

highlighting the role of amine radicals and NO recycling back to HCN.

The influence of the pressure and temperature on NO<sub>x</sub> emissions has been a subject of interest for the NH<sub>3</sub>/CH<sub>4</sub> swirl flame. The study by Xiao et al.<sup>72</sup> has shown that increased pressure leads to a reduction in NO and CO emissions, while increased initial temperature results in an augmentation of emissions. As the methane mole fraction in the fuel mixture increases, the NO<sub>x</sub> concentration in the flame also increases. This trend is consistent across different equivalence ratios, indicating that methane acts as a promoter for NO<sub>x</sub> formation. Sensitivity analyses were conducted to identify key reactions impacting NO<sub>x</sub> conversion. The results show that the reactions  $H + O_2 = O + OH$  (promoting) and  $NH_2 + NO = N_2 + H_2O$  and  $NH + NO = N_2O + H$  (inhibiting) play significant roles in NO<sub>x</sub> chemistry across different fuel compositions and equivalence ratios. The presence of methane in ammonia fuels leads to enhanced combustion intensities, as indicated by increased temperatures, heat release rates, and concentrations of important intermediate radicals such as OH, H, and O. The pressure is identified as a more significant factor affecting the NO<sub>x</sub> kinetics under practical engine operational conditions. Somarathne et al.<sup>73</sup> investigated the impact of OH concentration and temperature on NO<sub>x</sub> emissions in turbulent nonpremixed methane/ammonia/air swirl flames at high pressure. Their study indicated that adjusting the equivalence ratios to far-rich conditions could significantly reduce the level of NO<sub>x</sub> emissions. They also noted that local NO and OH concentrations and temperature distributions were similar to those in NH<sub>3</sub>/air flames, with the highest NO<sub>x</sub> emissions occurring at an energy fraction of NH<sub>3</sub> between 20 and 30%.

Recently, Mashruk et al.<sup>74</sup> investigated methane/ammonia/hydrogen ternary blends in a swirl burner. They observed minimum N<sub>2</sub>O and NO<sub>2</sub> emissions under rich conditions, with significant NO emissions at high methane mixtures due to the availability of OH radicals. The study also noted that NH<sub>3</sub> slip increased initially with decreasing methane content but then dropped as the hydrogen content increased, indicating the dominance of hydrogen chemistry.

The use of DME as a combustion promoter in ammonia flames is advantageous due to its high reactivity and ability to enhance flame stability and reduce emissions. Meng et al.<sup>46</sup> found that fuel NO<sub>x</sub> dominates the total NO<sub>x</sub> production in NH<sub>3</sub>/DME combustion. Adding up to 50% DME to ammonia promotes the NO formation reaction, leading to higher NO production. The study found that a higher ammonia content in the blend (as in D25, 75% NH<sub>3</sub>/25% DME) generates more NH and NH<sub>2</sub> radicals, promoting the NO reduction reaction. Lower DME content also results in fewer H/O/OH active radicals, inhibiting NO generation. Yu et al.<sup>75</sup> applied the fuel staging method to mitigate the issue of NO<sub>x</sub> emissions of the NH<sub>3</sub>/DME/air flame. The NO removal efficiency initially increased with temperature and then decreased, with optimal reaction temperatures at 950 °C for an equivalence ratio of the primary stage ( $\phi_{pri}$ ) at 0.9 and 900 °C for  $\phi_{pri}$  at 0.75. The NO removal efficiency improved with longer residence times and increased the number of secondary NH<sub>3</sub> injections. NH<sub>3</sub> slip was significant at lower temperatures but decreased dramatically above 950 °C due to NH<sub>3</sub> oxidation. The fuel staging method, with optimization of parameters like temperature, residence time, and NH<sub>3</sub> injection, can significantly reduce NO<sub>x</sub> emissions from NH<sub>3</sub>/DME cocombustion, with a

maximum NO removal efficiency of 55.2% achieved in this study.

Lian et al.<sup>76</sup> investigated the impact of CO<sub>2</sub> exhaust gas recirculation (EGR) on the flame characteristics and NO<sub>x</sub> emissions of premixed NH<sub>3</sub>/DME swirl flames. CO<sub>2</sub> EGR significantly affects flame morphology, making the flame weaker and increasing its height, which indicates reduced flame stability. The lean blowout (LBO) limit increases with an increasing CO<sub>2</sub> EGR rate, suggesting that higher CO<sub>2</sub> concentrations make the flame less stable. CO<sub>2</sub> EGR reduces the maximum mole fraction of the OH radical, affecting the flame's chemiluminescence intensity and distribution. NO<sub>x</sub> emissions decrease with an increasing CO<sub>2</sub> EGR rate due to the thermal effect of CO<sub>2</sub>, which reduces the flame temperature and thus the formation of thermal NO<sub>x</sub>. Yu et al.<sup>47</sup> investigated the effects of partial precracking of NH<sub>3</sub> and the use of DME as a combustion promoter on flame macrostructures, LBO characteristics, and exhaust emissions, including NO<sub>x</sub>, CO, and unburned NH<sub>3</sub>. As the precracking ratio of NH<sub>3</sub> increases, the flame height shortens, OH fluorescence intensifies, and core jet velocities amplify, leading to a significant reduction in the LBO limit, indicating enhanced combustion. NO and NO<sub>2</sub> emissions increase with a larger precracking ratio, while CO and unburned NH<sub>3</sub> emissions increase sharply under fuel-rich conditions due to insufficient oxygen. The study reveals a trade-off between NO and NH<sub>3</sub> emissions, with relatively low NO/NH<sub>3</sub> emissions observed under slightly rich conditions ( $\phi = 1.0$ – $1.1$ ). The partial precracking strategy effectively enhances NH<sub>3</sub> combustion, but it also increases NO<sub>x</sub> emissions. The study suggests that burning the partially precracked NH<sub>3</sub> directly rather than separating N<sub>2</sub> from the mixtures is more feasible due to deteriorating effects on NO<sub>x</sub> emissions.

Moreover, unburned ammonia emissions are a critical aspect of the emissions profile for combustion systems. Ammonia at the exhaust can lead to the formation of particulate matter via ammonium sulfides and nitrates, thus impacting the environmental quality. It is essential to design combustion systems that mitigate ammonia slip to avoid nuisances and reduce particulate matter.

This section underscores the multifaceted nature of NO<sub>x</sub> emissions in the swirl flames of ammonia and hydrocarbon fuels. It highlights the critical interplay between fuel composition, chemical kinetics, combustion dynamics, and the environment. The findings provide a foundation for developing advanced combustion strategies and emission control technologies, ensuring sustainable and efficient energy systems.

**2.3.3. Ammonia/Hydrogen Fuels.** The quest for decarbonization in the power sector has led to the exploration of ammonia–hydrogen blends as cleaner alternatives to fossil fuels. The combustion of these blends, particularly in swirl flame configurations, presents unique challenges and opportunities for NO<sub>x</sub> emission control. Initial studies by Joo et al.<sup>77</sup> and Li et al.<sup>78</sup> established the potential of ammonia substitution to enhance the safety of hydrogen use. They observed a decrease in NO<sub>x</sub> production with an increased ammonia slip as flames transitioned from stoichiometric to rich conditions. This reduction was attributed to lower flame temperatures, which favor NO<sub>x</sub> reduction mechanisms. Valera-Medina et al.<sup>79</sup> extended the research by examining lean premixed combustion of a 50/50 vol % NH<sub>3</sub>/H<sub>2</sub> blend in swirling flames. Their findings indicated a significant reduction



in  $\text{NO}_x$  emissions with decreasing equivalence ratios, achieving as low as  $\sim 100$  ppm wet NO at  $\phi = 0.40$ .

A pivotal sensitivity analysis by Tian et al.<sup>61</sup> and Xiao et al.<sup>80</sup> identified the reaction  $\text{NH}_2 + \text{O} = \text{HNO} + \text{H}$  as a key promoter of NO formation, highlighting the influence of increasing ammonia concentration in the fuel blend on NO exhaust concentrations. Further studies by Xiao et al.<sup>81</sup> revealed that  $\text{NO}_x$  emissions decrease with increasing pressure, suggesting that the use of ammonia/hydrogen blends in gas turbines could result in reduced  $\text{NO}_x$  emissions under practical operating conditions. This finding underscores the potential of pressure as a key parameter in optimizing combustion processes for lower emissions.

Further investigations were made by Khateeb et al.<sup>82</sup> and Zhu et al.<sup>18</sup> into various lean ammonia/hydrogen swirling flames at  $Re = 5000$  and under atmospheric conditions. These studies showed significant NO reduction under lean conditions for low turbulent ammonia–hydrogen flames, as shown in Figure 7. However, they did not address  $\text{NO}_2$ ,  $\text{N}_2\text{O}$ , and  $\text{NH}_3$

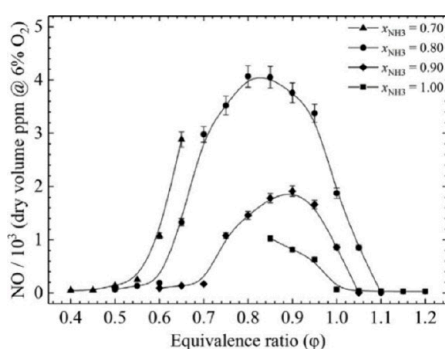


**Figure 7.** Measured exhaust NO mole fraction in ammonia–hydrogen–air flames in parts per million (ppm) as a function of equivalence ratio for  $X_{\text{NH}_3} = 0.70$  (triangles),  $0.80$  (circles),  $0.90$  (diamonds), and  $1.00$  (squares) for  $S_g = 1.00$  and  $Re = 5000$ . Results are normalized for a  $6\%$   $\text{O}_2$  mole fraction. Reproduced with permission from ref 82. Copyright 2020 Elsevier.

emissions, leading to the comprehensive study by Mashruk et al.<sup>83</sup> where the authors have investigated different ammonia/hydrogen blends at a fixed lean equivalence ratio ( $\phi = 0.65$ ) with different thermal powers and  $Re$  under atmospheric conditions (Figure 8). They reported a decrease in NO and  $\text{NO}_2$  emissions but an increase in  $\text{N}_2\text{O}$  production with a higher ammonia content in the fuel mixtures. This trend was more pronounced at elevated thermal powers or Reynolds numbers, highlighting the role of radical formation rates, particularly  $\text{NH}$ ,  $\text{OH}$ , and  $\text{NH}_2$ . The reaction  $\text{NH} + \text{NO} = \text{N}_2\text{O} + \text{H}$  was pinpointed as the primary  $\text{N}_2\text{O}$  source in the flame, with postflame  $\text{N}_2\text{O}$  consumption occurring primarily through  $\text{N}_2\text{O} + \text{H} = \text{N}_2 + \text{OH}$  and  $\text{N}_2\text{O} (+\text{M}) = \text{N}_2 + \text{O} (+\text{M})$ .

The influence of humidification on  $\text{NO}_x$  production was initially explored by Pugh et al.<sup>84</sup> in  $\text{NH}_3/\text{H}_2$  flames. They found that the addition of steam reduced  $\text{NO}_x$  concentrations (see Figure 9) by limiting thermal pathways and enhancing NO consumption in the postflame zone. The application of staged combustion, with secondary airflow, improved fuel burnout and further reduced  $\text{NO}_x$  emissions. An increase in combustor pressure up to  $0.185$  MPa resulted in a significant reduction in  $\text{NO}_x$  concentrations, primarily due to enhanced  $\text{NH}_2$  formation, which subsequently consumed NO in the postflame zone. The research demonstrates that  $\text{NO}_x$

emissions from premixed swirling  $\text{NH}_3/\text{H}_2$  flames can be significantly reduced through a combination of elevated pressure, reactant humidification, and staged combustion techniques. However, a careful balance is needed to avoid increasing unburned  $\text{NH}_3$ , which could eventually lead to higher  $\text{NO}_x$  formation in the secondary reaction zone.

Moreover, the potential of humidified ammonia/hydrogen systems using rich-quench-lean (RQL) technology was investigated by Mashruk et al.,<sup>85</sup> demonstrating its efficacy in emission reduction at high power outputs. Sensitivity analyses identified HONO, HNO, and  $\text{NO}_2$  as critical species for NO formation, with  $\text{NH}_2$  playing a vital role in NO consumption. The interplay of chemical reactions in ammonia/hydrogen combustion was found to be complex, but the RQL system's combination with humidified atmospheres effectively lowered emissions through species recombination and reduced combustion temperatures. As shown in Figure 10, these two studies illustrated show the  $\text{NO}_x$  formation/reburn routes in a  $70/30$  vol %  $\text{NH}_3/\text{H}_2$  blend studied by Mashruk et al. at lean ( $\phi = 0.65$ )<sup>83</sup> and rich conditions ( $\phi = 1.20$ ),<sup>85</sup> respectively, in swirling turbulent flames. Ammonia reacts with OH radicals to produce  $\text{NH}_2$  radicals in both rich and lean conditions, which converts to HNO directly by reacting with O radicals and via NH radicals by reacting with OH. Nitroxyl (HNO) is the main source of fuel NO production in ammonia flame through reactions with molecular oxygen and H and O radicals, as well as through disassociation processes.<sup>31</sup>

Subsequent studies<sup>13,86</sup> recommended an optimal equivalence ratio of  $1.20$  for two-stage burner configurations, balancing emissions performance and combustion efficiency. The reactions involving NH radicals were also highlighted as significant contributors to NO and  $\text{N}_2\text{O}$  production, with the latter being predominantly converted to  $\text{N}_2$  through reactions with H radicals and the third-body reaction  $\text{N}_2\text{O} (+\text{M}) = \text{N}_2 + \text{O} (+\text{M})$ . These reactions, along with the conversion of  $\text{N}_2\text{O}$  to  $\text{N}_2$ , are critical in managing  $\text{NO}_x$  emissions in ammonia/hydrogen swirl flames. Other prominent sources of NO reduction are through the chain branching reaction  $\text{NH}_2 + \text{NO} = \text{NNH} + \text{OH}$  and the terminating reaction  $\text{NH}_2 + \text{NO} = \text{N}_2 + \text{H}_2\text{O}$ .<sup>87,88</sup>

Moreover, Shi et al.<sup>89</sup> studied the effects of partial precracking of ammonia on flame macrostructures, lean blowout (LBO) characteristics, and exhaust emissions in a gas turbine model combustor. The results demonstrated that increasing the precracking ratio ( $\gamma$ ) leads to a more compact and stable flame, as evidenced by the shorter flame height, intensified OH fluorescence, and amplified core jet velocities. Consequently, the LBO limit is significantly reduced, indicating enhanced  $\text{NH}_3$  combustion. However, the trade-off between NO and  $\text{NH}_3$  emissions becomes more pronounced with higher precracking ratios, as NO and  $\text{NO}_2$  emissions increase substantially while  $\text{NH}_3$  emissions decrease. The study also found that separating  $\text{N}_2$  from the partially precracked  $\text{NH}_3$  mixtures can lead to increased  $\text{NO}_x$  emissions, suggesting that direct burning of the partially precracked  $\text{NH}_3$  is a more favorable approach. Overall, the partial precracking strategy presents a promising avenue for improving  $\text{NH}_3$  combustion characteristics in gas turbine model combustors, but careful consideration must be given to the trade-off between  $\text{NO}_x$  and  $\text{NH}_3$  emissions.

In summary, this section offers a comprehensive understanding of the chemical kinetics governing the  $\text{NO}_x$  emissions in ammonia/hydrogen swirl flames. By integrating these

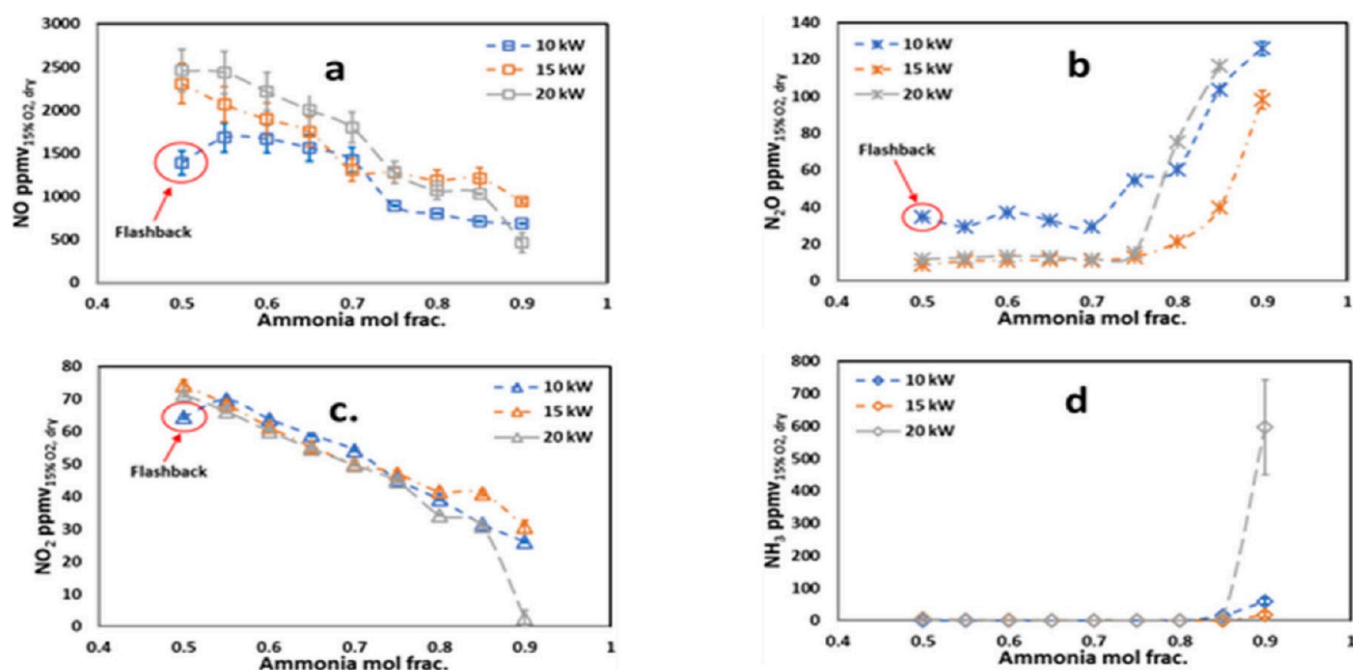


Figure 8. Sampled NO (a), N<sub>2</sub>O (b), NO<sub>2</sub> (c), and NH<sub>3</sub> (d) emissions at different thermal powers and  $\phi = 0.65$ . From ref 83. CC BY 4.0.

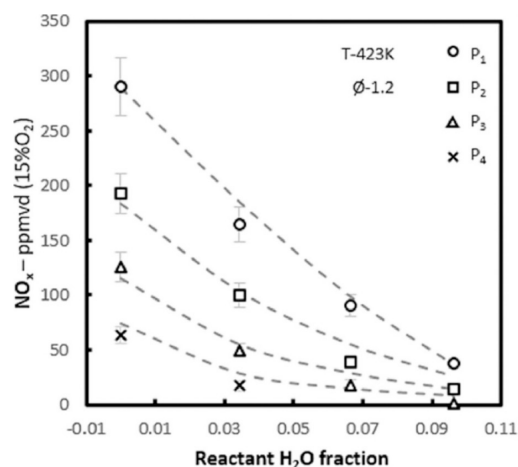


Figure 9. Experimental (symbols) and modeled (lines) NO<sub>x</sub> concentrations against reactant water fraction with increased pressure ( $\phi = 1.2$ ). From ref 84. CC BY 4.0.

findings into a cohesive narrative, we can better grasp the interplay of factors influencing NO<sub>x</sub> emissions and develop targeted strategies to mitigate these emissions in practical combustion systems.

**2.3.4. Ammonia–Coal Cofiring.** Ammonia–coal cofiring is also a promising technology that large power generation companies are evaluating mainly in Asia. Replacement of coal appears to have many benefits related not only to CO<sub>2</sub> abatement but also to mitigation of nitrogen oxide emissions and higher radiation outputs. Cui et al.<sup>90</sup> investigated NO<sub>x</sub> (i.e., NO, N<sub>2</sub>O, NO<sub>2</sub>) emissions from ammonia–coal cofiring using different pulverized coal concentrations. It was found that the reducing effect of unburned ammonia led to the rapid decrease of N<sub>2</sub>O in the last stages of combustion, while the combustion of char caused the reduction of NO<sub>2</sub>. The results also demonstrated that when coal was decreased, the oxygen concentration increased with the formation of NO and NO<sub>2</sub>.<sup>91</sup>

Further studies also elucidated the importance of water content which after decomposition produced large pools of OH radicals, capable of impacting the reconversion of NO<sub>x</sub> species.<sup>92</sup>

Fan et al.<sup>93</sup> used a fixed-bed reactor for their studies on the pore surface impact on NO<sub>x</sub> emissions using ammonia–coal blends. Chars with the largest porosity showed a maximum NO reduction efficiency of >90%, while smaller porosities denoted lower reduction efficiencies of ~80%, hence with the finding that enriched micropores with large pore volume and surface area could increase the adsorption capacity of coal. Therefore, more ammonia could be adsorbed on the surface of the coal, hence promoting overall NO<sub>x</sub> reduction reactions. Further studies by the group also showed that using additives can have an impact on NO mitigation, with Fe<sub>2</sub>O<sub>3</sub>, Fe<sub>3</sub>O<sub>4</sub>, and Cu<sub>2</sub>O in the fly ash having an improved increase in NO reduction efficiency by nearly 30%. However, Chen et al.<sup>94</sup> showed that Fe can have adverse impacts on the reduction of NO due to the potential absorption of NH<sub>x</sub> free radicals that promote NO consumption.

Attention has also been paid to the ammonia–coal ratios. A reactor network, representing an IHI burner (Figure 11) and three different modes of ammonia injection, was used for that purpose (Figure 12). Results found that low CO<sub>2</sub> and NO<sub>x</sub> could be produced by the reduction of coal and various processes such as ammonia De-NO<sub>x</sub>ing, lower temperatures, and char–NO reducing effects, respectively. Additional work<sup>95</sup> showed that the increase of water content from ammonia combustion could also reduce CO by the water gas shift reaction, H<sub>2</sub>O + CO → H<sub>2</sub> + CO<sub>2</sub>.

The work also addressed the difference in reaction paths between the 20 and 80% cases with the 40 and 60% scenarios, as shown in Figure 12. NO emissions are considerably reduced at 20% due to postcombustion reactions, while at 80% there are more effective reactions that do not involve NO production and that lead to N<sub>2</sub> via NH<sub>i</sub> recombination. Although 40 and 60% NO at the flame are kept low via reactions that produce

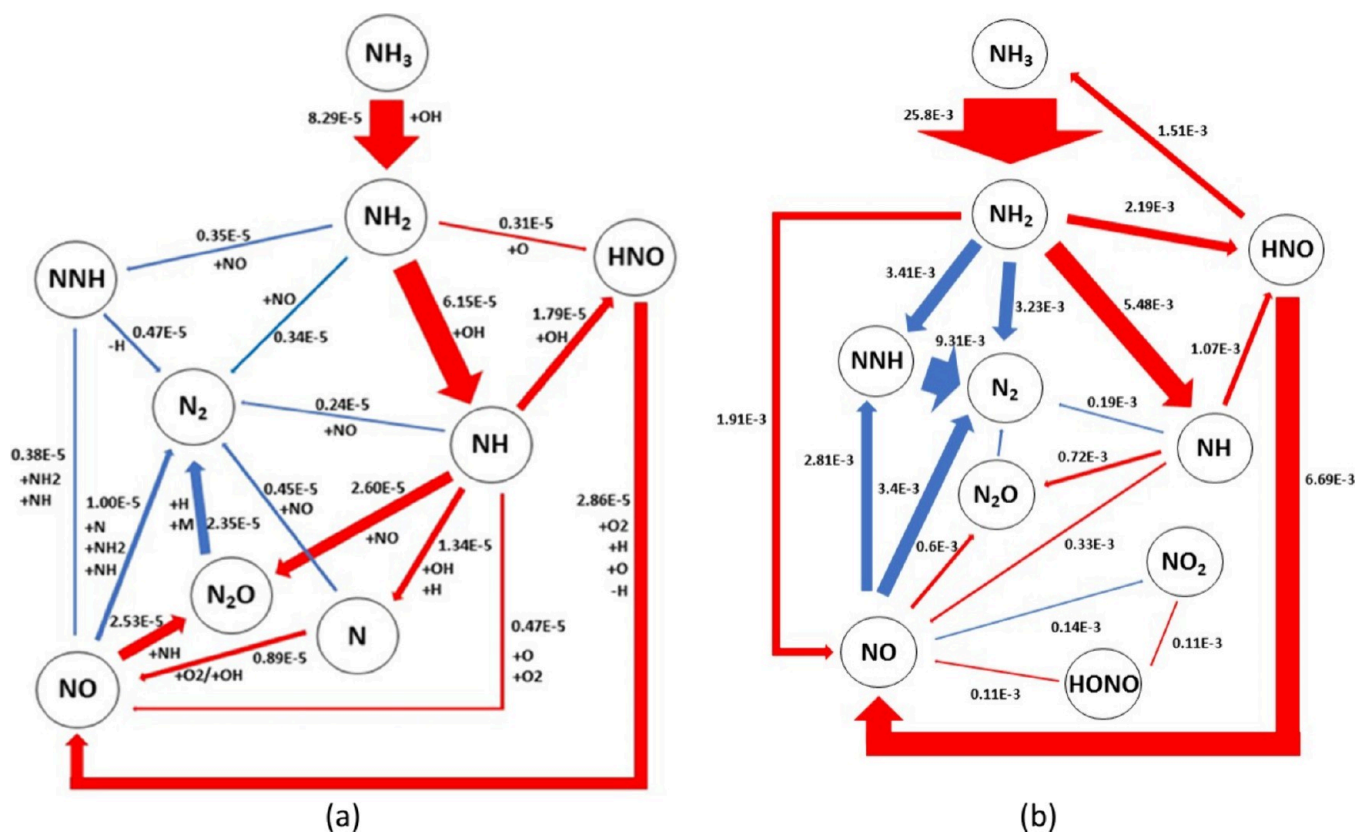


**Figure 10.** (a) Fuel  $\text{NO}_x$  formation and reburn pathways under lean conditions ( $\phi = 0.65$ ). Reproduced from ref 83. Copyright 2022 Elsevier. (b) Fuel  $\text{NO}_x$  formation and reburn pathways under rich conditions ( $\phi = 1.20$ ). Reproduced with permission from ref 85. Copyright 2021 Elsevier.

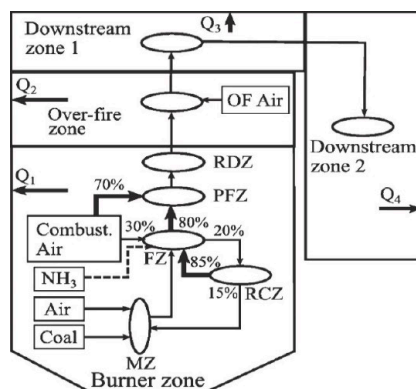


**Figure 11.** Reactor network representing a pulverized coal fired boiler with  $\text{NH}_3$  cofiring. MZ, mixing zone; FZ, flame zone; RCZ, recirculation zone; PFZ, postflame zone; RDZ, reduction zone; OF Air: overfire air. Q1–Q4: local heat absorption in each zone. Reprinted with permission from ref 96. Copyright 2020 Elsevier.

$\text{N}_2\text{H}_2$  and  $\text{NNH}$ , the higher temperatures in the postcombustion zone elevate thermal  $\text{NO}_x$ .

Fundamental analyses of the temperature dependency of  $\text{NO}$  have also been conducted when coal is cofired with ammonia. Jiang et al.<sup>97</sup> used a high-temperature fixed-bed reactor and conducted ammonia/coal cofiring experiments. Results showed that between 0 and 10% blending ratios, as the temperature increases,  $\text{NO}_x$  reaches a peak in a shorter time. An interesting pattern is that the peak fluctuates, from low  $\text{NO}_x$  emissions at  $\sim 1000$  °C, peaking at 1200 °C, to then decay and reach minimum values at 1500 °C. This behavior is believed to be caused by the increase of  $\text{NH}_i$  free radicals,

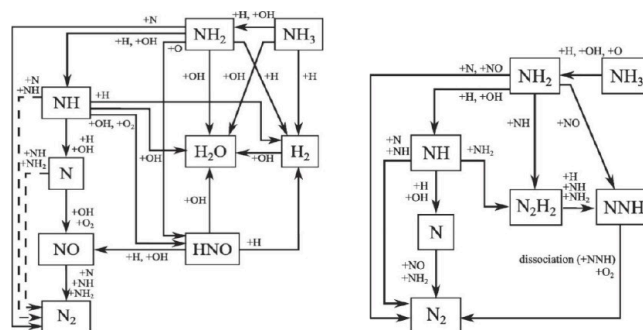


**Figure 12.** Comparison between ammonia–coal reactions at (left) 20 and 80% (dashed line) and (right) 40 and 60% ammonia contents. Reprinted with permission from ref 96. Copyright 2020 Elsevier.

hence contributing to the reduction of  $\text{NO}$ . Similarly, the reduction of oxygen would have an impact on  $\text{NO}_x$  emissions, as previously described in other types of flames. Niu et al.<sup>98</sup> showed that the reduction of oxygen content has a remarkable impact on the reduction of  $\text{NO}$ . Analyses showed that a decrease from 4.24 to 2.35% causes a drop in up to 36% nitrogen emissions. Furthermore, Fan et al.<sup>93</sup> found that  $\text{NH}_3$  has a De- $\text{NO}_x$ ing effect under oxygen-depleted atmospheres. The studies showed that, at 0% oxygen content and 1300 °C, the highest reduction efficiency was close to 50%.

The impact of different fuels on  $\text{NO}_x$  emissions in ammonia swirl flames varies significantly based on fuel composition and combustion conditions. Pure ammonia flames produce high  $\text{NO}_x$  emissions due to thermal  $\text{NO}_x$  formation at high temperatures, with radicals such as  $\text{NH}$  and  $\text{NH}_2$  playing a crucial role. While hydrogen addition can generally reduce



$\text{NO}_x$  emissions, especially under lean conditions, hydrocarbons like methane and DME can have more complex effects. Ammonia/methane blends initially increase  $\text{NO}_x$  emissions with added ammonia, but higher concentrations may reduce the level of  $\text{NO}_x$  due to enhanced reduction pathways.  $\text{CO}_2$  as a diluent generally reduces  $\text{NO}_x$  emissions under lean conditions. Ammonia/DME blends show increased  $\text{NO}_x$  emissions with added DME due to its high reactivity, though higher ammonia content can reduce  $\text{NO}_x$  through enhanced reduction reactions. Fuel staging and optimized combustion parameters can significantly reduce the level of  $\text{NO}_x$  in  $\text{NH}_3/\text{DME}$  flames. Ammonia/hydrogen blends offer lower  $\text{NO}_x$  emissions, especially at lean conditions. However, the formation of other nitrogenous species such as  $\text{N}_2\text{O}$  must be managed. Each fuel blend presents unique advantages and challenges, necessitating optimized combustion parameters to achieve low  $\text{NO}_x$  emissions.

**2.4. Plasma-Assisted Combustion.** In the literature, various strategies have been explored to address the high  $\text{NO}_x$  and  $\text{N}_2\text{O}$  emissions of ammonia combustion. A notable method involves blending ammonia ( $\text{NH}_3$ ) with hydrogen ( $\text{H}_2$ ), which improves the burning velocity owing to hydrogen's higher mass diffusivity.<sup>5</sup> While this approach mitigates some of the issues inherent in traditional  $\text{NH}_3$  combustion, hydrogen production itself poses challenges. Additionally, increasing hydrogen's volume fraction from 0 to 30% in fuel-lean mixtures can significantly escalate  $\text{NO}_x$  emissions. It has also been observed that combusting  $\text{NH}_3/\text{H}_2$  blends under extremely lean conditions can induce thermoacoustic instabilities, flame instabilities, and elevated emissions of  $\text{NO}$  and  $\text{N}_2\text{O}$ .<sup>8</sup> Over the past decade, nonequilibrium (or nonthermal/cold) plasma technology has shown substantial promise in boosting ignition, expanding flammability limits, accelerating low-temperature oxidation, and cutting emissions in combustion.<sup>99,100</sup> This technology leverages the disparity between the translational and internal degrees of gas molecules and electrons to facilitate robust momentum and energy transfer at lower temperatures, effectively exciting and dissociating target molecules with minimal heat loss or energy inefficiency. Furthermore, nonequilibrium plasma enhances combustion by generating chemically reactive species at low temperatures, such as high-energy electrons, excited species, and ions. The degree to which nonequilibrium plasma enhances combustion is heavily influenced by specific plasma properties, such as electron temperature and electron number density. These critical plasma characteristics are determined by the reduced electric field ( $E/N$ ), which represents the ratio of the electric field strength to the molecular number density. The subject, novel and with limited published literature, opens the possibility of using advanced systems to control and mitigate  $\text{NO}_x$  emissions in ammonia flame systems.

There are two recent review papers<sup>101,102</sup> that extensively discuss plasma-assisted ammonia combustion, though we will not go into detail on these here. All the experimental and numerical studies on plasma-assisted ammonia combustion give clear evidence that plasma-assisted ammonia flames are feasible to improve the combustion process while producing less  $\text{NO}_x$  compared to conventional ammonia flames. However, the level of  $\text{NO}_x$  mitigation can be affected by a series of factors. Some that have been identified so far are plasma discharge gas, plasma type, equivalence ratio, and plasma conditions (applied voltage and pulse repetition frequency). Choe et al.<sup>103</sup> addressed the variation of  $\text{NO}_x$

concentrations with discharge voltage and discharge power at a constant equivalence ratio,  $\phi = 0.94$ , as shown in Figure 13.

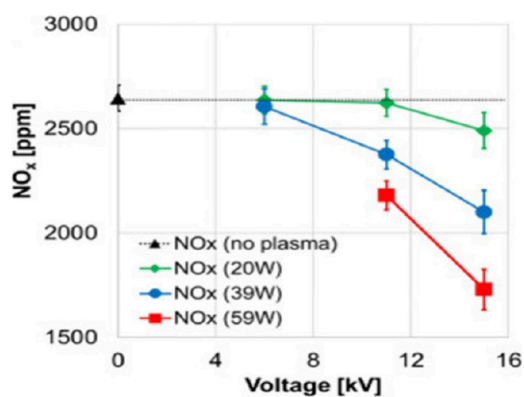
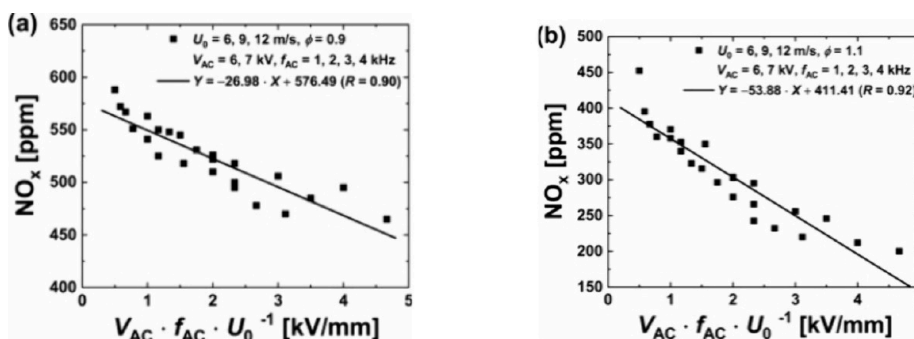


Figure 13.  $\text{NO}_x$  variation with discharge power and discharge voltage. Reproduced with permission from ref 103. Copyright 2021 Elsevier.

$\text{NO}_x$  concentrations were reduced with nanosecond pulsed discharge plasma, and further reductions were achieved with the increase of both discharge voltage and discharge power. The  $\text{NO}_x$  suppression was linked to the reaction of  $\text{NO}$  with abundant  $\text{NH}_2^*$  generated by plasma through the thermal De- $\text{NO}_x$  process.<sup>104</sup> Tang et al.<sup>105</sup> reported the limited effect of plasma on  $\text{NO}_x$  ( $\text{NO}$  and  $\text{NO}_2$ ) emissions in a range of equivalence ratios from 0.76 to 1.00, due to the added effect of thermal  $\text{NO}$  emission induced by the gliding arc discharges. However, the effect became more prevalent in lean ammonia flames, where  $\text{NO}_x$  emissions dropped to less than 100 ppm at  $\phi = 0.57$ . The authors discussed the reduction of the possible reaction of unburnt  $\text{NH}_3$  with  $\text{NO}_x$ . Kim et al.<sup>106</sup> extended the investigation of plasma-flame coupling to rich ammonia flames. It was found that the  $\text{NO}_x$  suppression with and without plasma remained negligible at fuel-rich conditions,  $\phi = 1.2$ – $1.3$ , and became remarkable at  $\phi \leq 1$ . By applying plasmas,  $\text{NO}_x$  concentrations dropped from 691 to 487 ppm at  $\phi = 0.9$ . The authors also found a negative correlation between  $\text{NO}_x$  concentration and the product of discharge voltage, applied frequency, and the inverse of the flow residence time, implying that  $\text{NO}_x$  could be further reduced by increasing discharge power and by reducing the residence time, as shown in Figure 14.

Lin et al.<sup>107</sup> reported that plasmas could reduce  $\text{NO}$  emissions below 100 ppm in lean ammonia flames when air served as a discharge gas. In the case of ammonia being used as a discharge gas, plasma-assisted ammonia flames produced  $\text{NO}$  concentrations below 100 ppm (at a particular flow rate), regardless of the equivalence ratio. The authors speculated that applying discharges to the ammonia stream might produce a rich mixture of  $\text{H}^*$ ,  $\text{NH}^*$ , and  $\text{NH}_2^*$  that play a vital role in  $\text{NO}$  consumption.

Recently researchers at Princeton University for the first time studied plasma-assisted ammonia oxidation at room temperature with a focus on unveiling nonequilibrium  $\text{NO}_x/\text{N}_2\text{O}$  reaction pathways by combining in situ laser diagnostics using a miniature plasma reactor and kinetic plasma modeling using the 0D hybrid ZDPlasKin–CHEMKIN solver.<sup>108,109</sup> Their study revealed that nonequilibrium plasma regulates  $\text{NO}_x$  production through the generation of  $\text{O}/\text{H}/\text{N}$  atoms from electron-impact dissociation and the quenching of excited states.  $\text{N}_2\text{O}$  is produced via a dual-step process, beginning with



**Figure 14.** Correlation between  $\text{NO}_x$  and  $V_{AC}f_{AC}U_0^{-1}$  for (a)  $\phi = 0.9$  and (b)  $\phi = 1.1$ . Reproduced with permission from ref 106. Copyright 2022 Elsevier.

the formation of amine radicals by electron-impact reactions, which then combine with  $\text{NO}_x$  to form  $\text{N}_2\text{O}$ . This process leads to efficient and eco-friendly ammonia oxidation, enhancing reactivity and minimizing emissions of  $\text{NO}_x$  and  $\text{N}_2\text{O}$  by optimizing the mixture compositions and plasma parameters. Findings demonstrate that plasma discharge notably boosts ammonia ignition at lower temperatures and decreases ignition delay, especially under fuel-lean conditions, in contrast to fuel-rich autoignition scenarios. They outlined three approaches to optimize plasma operations for effective ammonia oxidation and reduced pollutant emissions based on nonequilibrium  $\text{N}_2\text{O}/\text{NO}_x$  chemistry. First, using fuel-rich conditions was recommended for plasma-aided low-temperature ammonia oxidation to maximize electron energy directed toward ammonia dissociation. Second, it emphasized the importance of maintaining an optimal  $E/N$  ratio to ensure efficient energy use primarily for ammonia dissociation, avoiding energy losses to nitrogen excitation or dissociation. Lastly, it suggested that modulating the discharge frequency can help control the formation and transformation of intermediate species, optimizing the chemical reaction pathways.

In the context of the gas turbine setting, Kim et al.<sup>110</sup> explored the synergetic effects of nonthermal plasma and methane ( $\text{CH}_4$ ) addition on enhancing ammonia/air premixed flames and  $\text{NO}_x/\text{CO}$  emission characteristics. They experimentally investigated the changes in flame behavior by varying the equivalence ratio, mixture velocity, and methane content in the fuel mix. The  $\text{NO}_x$  and CO emissions in  $\text{NH}_3/\text{air}$ ,  $\text{NH}_3/\text{H}_2/\text{air}$ , and  $\text{NH}_3/\text{CH}_4/\text{air}$  flames with/without nonthermal plasma (NTP) are shown in Figure 15. It can be seen that the addition of  $\text{CH}_4$  notably intensifies streamer generation compared to  $\text{H}_2$ , primarily due to the role of positive ions from  $\text{CH}_4$  in streamer formation. This intensified streamer activity not only improves ammonia combustion when

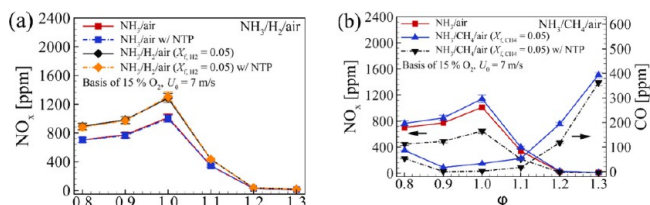


**Figure 15.** Variations in  $\text{NO}_x$  emission as a function of  $\phi$  for  $\text{NH}_3/\text{air}$ ,  $\text{NH}_3/\text{H}_2/\text{air}$  and  $\text{NH}_3/\text{CH}_4/\text{air}$  premixed flames with and without NTP. Reproduced with permission from ref 110. Copyright 2024 Elsevier.

combined with  $\text{CH}_4$  but also significantly broadens the lean blowout limits of  $\text{NH}_3/\text{CH}_4/\text{air}$  flames compared with those without NTP application. The study also demonstrates that streamer intensity correlates linearly with the equivalence ratio, methane fraction, and mixture velocity across a wide range of these variables. Additionally, the use of NTP notably decreases both  $\text{NO}_x$  and CO emissions. These findings highlight the potential of using NTP in tandem with  $\text{CH}_4$  addition as a more effective means to stabilize turbulent premixed  $\text{NH}_3/\text{air}$  flames and reduce harmful emissions, leveraging their synergistic effects.

The research reviewed shows that using nonequilibrium plasma in ammonia combustion effectively enhances the laminar burning velocity by improving the decomposition of ammonia and increasing the equivalence ratio and  $E/N$ , with significant support from hydrogen atoms generated during plasma discharges. Moreover, adjusting the pulse energy density, while keeping  $E/N$  constant, drastically reduces the ignition delay time and significantly increases the burning velocity. The introduction of nonequilibrium plasma also shortens the ignition delay time by generating reactive OH radicals. Furthermore, nonequilibrium plasma broadens the lean blowout limit, enhancing performance marginally better than when hydrogen is used. It also lowers  $\text{NO}_x$  emissions, particularly when the discharge power and voltage are increased. Specifically, plasma-assisted ammonia combustion reduces  $\text{NO}_x$  formation significantly, primarily by hastening the conversion of  $\text{NH}_3$  to  $\text{N}_2$ , thus minimizing the precursors available during ignition that contribute to  $\text{NO}_x$  production.

**2.5. Ammonia Combustion in Internal Combustion Engines.** Internal combustion engines are extremely versatile, in terms of both the fuel that can be used and its applications. The earliest successful attempts to use ammonia as a fuel for cars and buses goes back to the 1930s–1940s.<sup>10,111</sup> In the 1960s, U.S. institutions investigated the potential of ammonia as an alternative fuel using cooperative fuel research (CFR) engines. This led to a set of publications which demonstrated the feasibility, not without challenges, to run ICE on ammonia-based fuel.<sup>112–115</sup> The interests of the industry and academia only took off in the late 2000s as limits on carbon emissions were becoming more stringent to look for alternatives to hydrocarbon fuels. Major engine manufacturers of the shipping industry such as Wärtsilä and MAN Energy Solutions have announced their first operational ammonia-based engines in 2024.<sup>116,117</sup>

Compared to standard fuels like gasoline and diesel or even hydrogen, most of ammonia's properties make it hard to burn.<sup>118</sup> Ammonia possesses a narrow flammability limit,

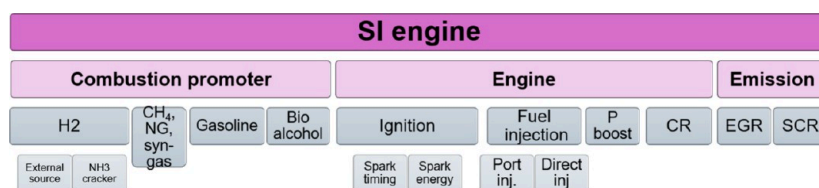


Figure 16. Optimization pathways investigated in the literature for SI engines.

especially compared to hydrogen, and its resistance to autoignition is very high with an autoignition temperature of 651 °C (against 254 °C for diesel and 370 °C for gasoline).<sup>20</sup> This makes the use of ammonia in a compression ignition (CI) engine very challenging, and very high compression ratios (>35:1) are needed to ignite it.<sup>115</sup> Therefore, the research mainly approached the use of ammonia in CI engines via dual-fuel operations to compensate for that issue.<sup>119</sup>

The very low flame speed (laminar flame speed is 7 cm/s<sup>120</sup>) slows down the combustion process. Therefore, using a combustion promoter like hydrogen will be key to maintaining a stable combustion and ensure ignition of the mixture in spark ignition (SI) engines. However, ammonia properties are also an advantage regarding knock in SI engines thanks to the very high octane number (>130).<sup>121</sup> Additionally, the heat of vaporization (1370 kJ/kg)<sup>122</sup> is very high compared to the range for gasoline (180–350 kJ/kg),<sup>123</sup> reinforcing knock resistance as spontaneous ignition is unlikely to occur. Although unlikely, knock should not be disregarded especially when considering ammonia fuel blends because optimization solutions like boosting or increase of compression ratio could make it possible.<sup>124</sup> Another important aspect is the higher fuel consumption when using ammonia. Diesel has a lower heating value of 45 MJ/kg and ammonia only has half that amount with 18.8MJ/kg, meaning that fuel consumption should be expected to be twice that of a standard fossil fuel.<sup>118</sup>

Because of ammonia's characteristics, its utilization as a fuel in internal combustion engines is challenging. Yet, recent publications proved that it can be achieved with relatively limited changes to the engine itself, which is encouraging, as it shows that retrofit of an existing ICE is possible. The main issue to be addressed in the transition of ICEs toward using ammonia is related to NO<sub>x</sub> emission mitigation while maintaining adequate performance.

**2.5.1. SI Engines.** The current trend is to favor utilization of ammonia with spark ignition engines to take advantage of the high octane number and because of the reasonable compression ratio thanks to the ignition via a spark plug. However, the slow flame speed of pure ammonia poses problems to maintain stable combustion for a range of operational conditions, and the need for a combustion enhancer has been repeatedly reported in the literature.<sup>112,114,121–123,125,126</sup> The spectrum of fuels used to promote ammonia combustion includes gasoline, alcohol, methane, natural gas, syngas, and hydrogen.

Overall, an SI engine based on ammonia shows the following trends with respect to combustion enhancement:<sup>112,121,126,127</sup>

At low load, a higher amount of fuel promoter is needed, whereas it is possible to operate on pure ammonia at high loads. Regarding engine speed, at high speed it is difficult if not impossible to maintain stable combustion, and a fuel promoter is needed. The spark timing must be advanced compared with standard fuel operation to allow time for the flame to

propagate. Finally, cold start operation requires a higher amount of fuel promoter than once the engine is warmed up.

Other strategies for performance improvements (and reduce NO<sub>x</sub> emission) have also been explored such as boosting the intake pressure using a turbo or a supercharger and increasing the compression ratio (CR), which has shown good results.<sup>112,128–131</sup> The study of different fuel injection strategies either in the intake port (majority of the publications) or by direct injection in the cylinder is also being considered. These strategies are also used in the frame of emission mitigation, where understanding of the ammonia combustion process is essential. Selective catalytic reduction (SCR) is a commonly proposed aftertreatment solution,<sup>129,131,132</sup> and EGR in combination with rich operation could provide interesting results.<sup>125,126,129</sup> A summary of all the optimization strategies which are currently investigated is provided in Figure 16.

Gasoline/ammonia blend experiments have shown that a mixture of 30% gasoline and 70% ammonia reached a heat release rate 25% lower than for standard gasoline operation and could provide a similar result if optimized with an intake pressure boosting device.<sup>121,133</sup> An earlier spark timing was necessary compared with 100% gasoline to ensure stable combustion.

Methane, natural gas,<sup>133,134</sup> and more recently syngas<sup>128</sup> have also shown interesting results and are attractive as they can be obtained from sustainable sources. Operation with 50% natural gas was achieved easily, thus reducing by 28% the CO<sub>2</sub> emissions.<sup>218</sup> In the case of syngas,<sup>128</sup> the performance was lower than with pure methane but boosting the intake pressure by 20% then gave similar results. Ammonia slip was relatively important in the exhaust in the case of syngas.

**2.5.2. CI Engines.** The early studies on compression ignition engines highlighted the difficulty in igniting pure ammonia. The very high compression ratios necessary were not deemed practical and did not provide satisfactory results.<sup>115,135</sup> Two methods to work around that issue have been proposed: dual fuel (similar to the use of a fuel promoter with SI engines) and the implementation of a spark-assisted operation. The most explored route is the dual-fuel route, used in a small amount to trigger the ignition. Early studies performed in the 1960s tested up to 45 additives (fuel promoter),<sup>114</sup> and for CRs up to 25:1, acetylene was preferred, whereas above that value hydrogen performed better. Acetylene was also considered less convenient because of the higher amount required. The more recent studies mostly focus on diesel (and biodiesel), dimethyl ether (DME), and hydrogen.<sup>118,120,136,137</sup>

Various combustion modes have been tested covering homogeneous charge compression ignition (HCCI), partially premixed compression ignition (PPCI), and reactivity-controlled compression ignition (RCCI). Stable combustion with HCCI was obtained with a blend of 70% ammonia and 30% H<sub>2</sub>, but efficiency is lower and optimization such as increasing the CR, boosting the intake pressure, and boosting the crevice are needed.<sup>118</sup> For RCCI, ammonia is used as the



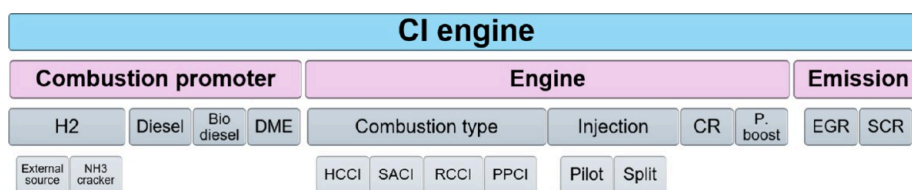


Figure 17. Optimization pathways investigated in the literature for CI engines.

Table 1. Main Emission Trend Observed for Blend of Ammonia/Other Fuel, Compared to Pure Fossil Fuel from Experimental Results in the Literature<sup>a</sup>

emission	blend					
	SI engine			CI engine		
	H <sub>2</sub>	NH <sub>3</sub> /CH <sub>4</sub> (NG)	NH <sub>3</sub> /syngas	gasoline	DME	diesel
NH <sub>3</sub>	for increasing ER: stable until ER ~ 1; increase when ER > 1; decrease with increasing H <sub>2</sub> content	increase	increase	increase	increase	increase
NO <sub>x</sub>	for increasing ER: NO <sub>x</sub> increases until ER ~ 0.7–0.8; NO <sub>x</sub> decrease for richer mixture	increase	slight increase	increase	increase	usually decrease

<sup>a</sup>Note that the trend may change depending on a particular engine operation type, especially for CI engines.

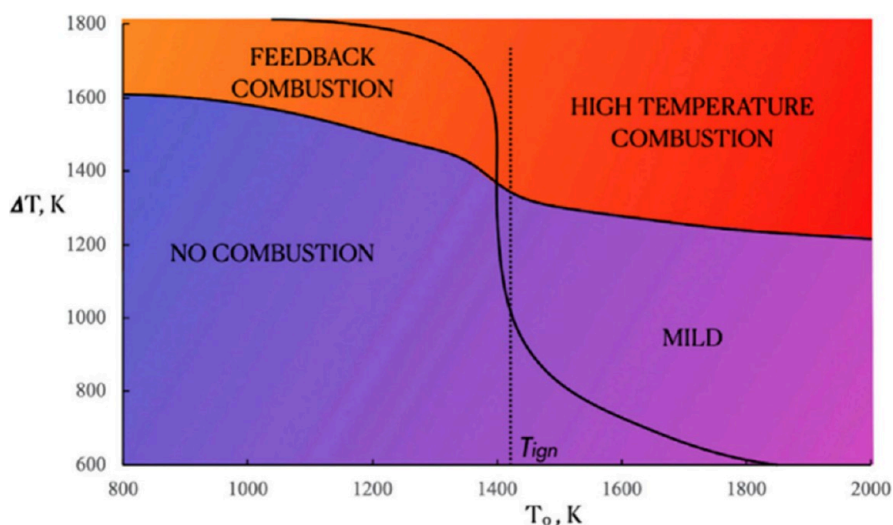


Figure 18. Combustion mode behavior of pure NH<sub>3</sub> in the hot-fuel–diluted-fuel configuration at  $P = 1$  atm. From ref 146. CC BY 4.0.

low reactivity fuel and the fuel promoter (only diesel has been tested) is used as high reactivity fuel.<sup>136,138</sup> The diesel pilot injection timing advance plays an important role in reducing emissions of NH<sub>3</sub> and N<sub>2</sub>O. However, lower brake efficiency has been reported.<sup>138</sup>

The other route of spark-assisted compression ignition (SACI) was first mentioned by Starkman et al.<sup>115</sup> in 1968, and in 2021, Mounaim-Rousselle et al.<sup>139</sup> attempted again to use that method. The results obtained were promising at different engine speeds and low loads and allowed pure ammonia.

Like for SI engines, emission can be mitigated by using an EGR, but Pochet et al.<sup>140</sup> reported a negative impact on the combustion efficiency. He suggested to investigate combining EGR with boosted pressure and maximizing the stroke-to-bore ratio to overcome that problem.<sup>28</sup> SCR is also proposed as a downstream solution to limit emissions. The optimization pathways are summarized in Figure 17.

**2.5.3. Emissions Trends for Ammonia Use in ICE.** The two major emission contributors are NO<sub>x</sub> (including N<sub>2</sub>O) and ammonia (NH<sub>3</sub>). To a lesser extent, hydrocarbons (HC),

carbon monoxide (CO), carbon dioxide (CO<sub>2</sub>), and hydrogen (H<sub>2</sub>) can also be found.

For NO<sub>x</sub>, the main trend is that for lean combustion (equivalence ratio ER < 1) more NO<sub>x</sub> are produced, whereas NO<sub>x</sub> production decreases when the operation shifts toward rich combustion (ER > 1),<sup>118,120,138,141</sup> the opposite behavior is seen for ammonia slip in the exhaust. Overall, NO is in a greater amount but N<sub>2</sub>O is also present, which is critical given its very high global warming potential. Upstream NO<sub>x</sub> reduction methods are being studied via understanding the ammonia combustion characteristics.<sup>138,142</sup> However, with the current performance obtained, it is expected that SCR will be necessary to keep NO<sub>x</sub> emissions below regulation levels.

The presence of ammonia in the exhaust is attributed to the crevice mechanism suggested by Westlye et al.,<sup>131</sup> and ammonia slip is more important when operating in rich condition. HC, CO<sub>2</sub>, and CO are also present in the case where the fuel promoter is based on hydrocarbons. Behaviors with emissions vary depending on the engine operation mode. For instance, Niki reported that, for RCCI engine operation, HC, NO<sub>x</sub>, and CO increased whereas NH<sub>3</sub> and N<sub>2</sub>O

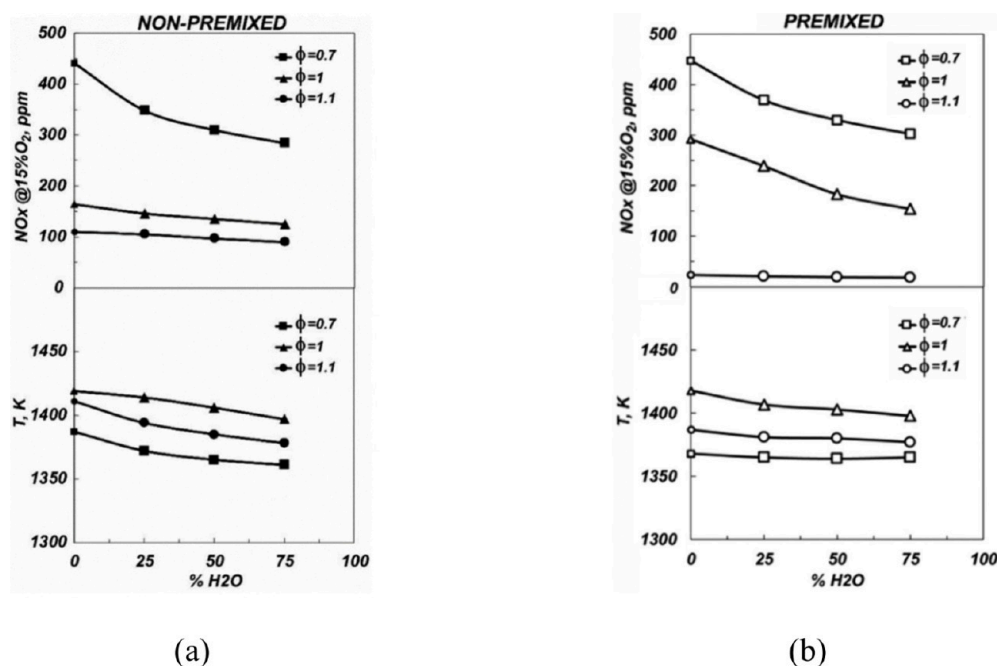


**Figure 19.** Effect of water addition (% H<sub>2</sub>O) on reactor temperatures ( $T$ ) and NO<sub>x</sub> emissions for varying equivalence ratio at  $P_{\text{thermal}} = 7$  kW: (a) nonpremixed; (b) premixed. Reproduced with permission from ref 147. Copyright 2021 Elsevier.

decreased.<sup>138</sup> In another publication, Niki suggested that split injection decreased CO and HC.<sup>136</sup> The emission trends for NO<sub>x</sub> and NH<sub>3</sub> are presented in Table 1.

The main challenge in limiting both NO<sub>x</sub> and ammonia emissions will be to find the sweet spot regarding several aspects that include appropriate fuel blend, injection/ignition method, combustion control, and postcombustion mitigation strategy.

**2.6. Moderate or Intense Low-Oxygen Dilution (MILD) Combustion.** MILD combustion, also termed flameless combustion, has shown a great potential to mitigate the thermal NO<sub>x</sub> problem in NH<sub>3</sub> combustion. Combustion processes are called MILD when the reactant mixture inlet temperature ( $T_{\text{in}}$ ) is higher than the mixture's autoignition temperature ( $T_{\text{ign}}$ ) and the maximum temperature increase ( $\Delta T = T_{\text{out}} - T_{\text{in}}$ ) after ignition is lower than the  $T_{\text{ign}}$ .<sup>143</sup> The dilution effect can be obtained with effective recirculation, creating a large reaction zone with a relatively uniform temperature field, often leading to limited thermal NO<sub>x</sub> emissions.<sup>144</sup>

**2.6.1. MILD Combustion of Pure NH<sub>3</sub>.** MILD combustion holds great potential for direct NH<sub>3</sub> combustion since the oxidation process happens based on the local distributed  $T_{\text{ign}}$  rather than the flame propagation mechanism. Furthermore, it can happen outside the flammability limits due to effective dilution with flow recirculation while achieving reduced thermal NO<sub>x</sub> emissions with moderate reactor temperatures.<sup>145</sup> These features of MILD combustion offer solutions to low laminar burning velocity, narrow flammability limits, and high thermal NO<sub>x</sub> emission problems of conventional NH<sub>3</sub> combustion. The MILD combustion mode in the case of pure NH<sub>3</sub> combustion can be further clarified in Figure 18, with a comparison to traditional combustion modes. The lines separating each combustion mode are computed from heat release and temperature curves.<sup>146</sup> It is seen that the  $\Delta T$  for the MILD combustion zone is always lower than the  $T_{\text{ign}}$ .

The research on the MILD combustion of NH<sub>3</sub> is still in its early stages and limited. Sorrentino et al.<sup>145</sup> investigated MILD combustion of pure NH<sub>3</sub> for the first time using a cyclonic burner configuration. The reactor temperature was kept above 1250 K in all experiments, while stability and emission control were achieved for temperatures higher than 1300 K. The minimum NO<sub>x</sub> levels of lower than 100 ppmv were achieved near stoichiometric conditions (slightly fuel-lean to fuel-rich). It was also noted that unburned NH<sub>3</sub> content higher than 1000 ppmv was obtained for equivalence ratios above 1.1. Ariemma et al.<sup>147</sup> studied the effects of water (H<sub>2</sub>O) addition for MILD NH<sub>3</sub> combustion in a cyclonic burner configuration. It was found that the H<sub>2</sub>O addition reduces NO<sub>x</sub> emissions for both premixed and nonpremixed configurations without compromising process stability. The NO<sub>x</sub> reduction was more pronounced for fuel-lean conditions with increasing H<sub>2</sub>O content, as shown in Figure 19.

Rocha et al.<sup>148</sup> investigated three NO<sub>x</sub> reduction methods in modern stationary gas turbines, namely, dry-low emissions (DLE), rich-burn, quick-quench, and lean-burn (RQL), and MILD combustion, numerically at a pressure of 20 bar and an inlet temperature of 500 K. The study revealed a strong correlation between NO<sub>x</sub> emissions and the exhaust-gas-recirculation ratio (EGR), indicating a logarithmic decrease in NO<sub>x</sub> emissions with higher EGR levels. It was reported that NO<sub>x</sub> emissions lower than 50 ppmv were possible in highly diluted cases. Recently, Liu et al.<sup>149</sup> carried out a regime classification study in well-stirred reactor (WSR) combustion. In this study, MILD combustion was classified as a subregime of flameless combustion where NO<sub>x</sub> emissions were lower than 100 ppmv. Furthermore, regarding NO production, the HNO route was found to be the most important producer by contributing more than 94% of the NO in the MILD combustion of NH<sub>3</sub>. Mohammadpour et al.<sup>150</sup> numerically studied the furnace wall temperature and dilution effects in a furnace. Regarding NO<sub>x</sub> emissions, it was found that the NO<sub>x</sub> emissions reduce significantly when the wall temperatures are

reduced and/or the diluent levels in the oxidizer are elevated. Conversely,  $\text{N}_2\text{O}$  production exhibits an opposing trend, decreasing as the  $\text{NO}_x$  levels diminish. Recently, Shi et al.<sup>151</sup> showed that the MILD  $\text{NH}_3$  combustion reproduces significantly lower  $\text{NO}_x$  emissions compared to premixed  $\text{CH}_4/\text{NH}_3/\text{air}$  combustion due to lower  $\text{O}_2$  concentrations, which subsequently lowers the O, H, and OH radical pool concentrations. Another conclusion was the existence of a critical  $\text{NH}_3$  flow rate under a certain MILD combustion condition. If the critical value is exceeded, then  $\text{NO}_x$  emissions increase significantly. Guintini et al.<sup>152</sup> investigated  $\text{NH}_3$  MILD combustion in a cyclonic reactor configuration at stoichiometric conditions numerically. The work mainly focused on providing a reliable computational framework to reduce uncertainties arising from kinetics, cyclonic flow, and MILD combustion conditions. Regarding the  $\text{NO}_x$  emissions, Nakamura et al.<sup>153</sup> and Li<sup>154</sup> kinetic mechanisms were found to perform well in terms of relative error compared to experiments. Very recently, Wang et al.<sup>155</sup> studied the MILD combustion of a premixed  $\text{NH}_3/\text{air}$  jet flame in hot coflow for varying conditions numerically. Ammonia/air mixtures have wider reaction zones and lower heat release rates resulting in the development of a MILD combustion regime more easily compared to  $\text{CH}_4/\text{air}$  mixtures. Furthermore, it was seen that MILD combustion reduces the  $\text{NO}_x$  emissions of  $\text{NH}_3/\text{air}$  combustion by 2 orders of magnitude compared to the conventional combustion regime. Also, stoichiometric conditions were found to be the optimal case for  $\text{NO}_x$  and unburned  $\text{NH}_3$ .

**2.6.2. MILD Combustion of Mixtures of  $\text{NH}_3$  with Other Fuels.** In traditional combustion, blending  $\text{NH}_3$  with other fuels such as hydrogen ( $\text{H}_2$ ), methane ( $\text{CH}_4$ ), syngas, and alcohols is a common practice to enhance certain combustion properties of  $\text{NH}_3$ .<sup>156,157</sup> Lewandowski et al.<sup>158</sup> explored the  $\text{NO}_x$  emissions in MILD combustion of binary  $\text{NH}_3$ ,  $\text{H}_2$ , and  $\text{CH}_4$  blends in a WSR setting. For  $\text{NH}_3/\text{H}_2$  blends, it was concluded that  $\text{H}_2$  content of 10–20 vol % in  $\text{NH}_3$  results in a significant reduction in  $\text{NO}_x$  emissions as well as  $T_{\text{ign}}$ . For  $\text{NH}_3/\text{CH}_4$  blends, it was seen that  $\text{NO}_x$  emissions decrease monotonically as the  $\text{CH}_4$  content increases. Another important finding for  $\text{NH}_3$  blends was the necessity of significant dilution levels, with  $\text{O}_2$  levels around 2–6%, which is necessary to keep  $\text{NO}_x$  emissions under 100 ppmv. Similar observations were made in the work of Czyzewski and Slefarski for the co-combustion of ammonia with methane as well as with  $\text{CH}_4/\text{H}_2/\text{CO}_2$  mixture in a semi-industrial chamber for 150 kW burner thermal power.<sup>159,160</sup> The lowest emissions, not even exceeding 100 ppmv, were obtained under slightly fuel-lean conditions for an equivalence ratio of 0.95 (1%  $\text{O}_2$  in dry exhaust gas). Mousavi et al.<sup>161</sup> studied MILD combustion of  $\text{NH}_3/\text{H}_2/\text{CH}_4$  ternary mixtures with low  $\text{NH}_3$  concentrations (up to 20 vol %) numerically using a modified eddy dissipation concept (EDC) model. Ammonia addition to the  $\text{H}_2/\text{CH}_4$  mixture resulted in more complete combustion by increasing the flow residence times. Interestingly, addition of  $\text{NH}_3$  increased the reactivity of the mixture unlike the conventional combustion mode. NO emissions were reported to increase sharply near the inlet but then decrease downstream with the addition of  $\text{NH}_3$ . Finally, the most important pathway for  $\text{NO}_2$  generation was found to be  $\text{NO} + \text{HO}_2 = \text{NO}_2 + \text{OH}$ . Kuang et al.<sup>162</sup> investigated the combustion characteristics of various fuel blends containing  $\text{NH}_3$ ,  $\text{CH}_4$ ,  $\text{H}_2$ ,  $\text{N}_2$ , and  $\text{CO}_2$  in different combustion modes

numerically. The MILD combustion and oxy-fuel MILD combustion modes demonstrated relatively lower NO emissions, specifically for oxy-fuel MILD combustion. Furthermore, the  $\text{CO}_2$  dilution strengthened the MILD combustion state in all scenarios. Similar to their previous work,<sup>162</sup> Mousavi et al.<sup>163</sup> used a modified EDC to investigate syngas/ $\text{NH}_3/\text{CH}_4$  mixtures in the MILD combustion regime to investigate stability and  $\text{NO}_x$  emissions. It was reported that increasing the syngas content in  $\text{NH}_3$  MILD combustion reduced  $\text{NO}_x$  and  $\text{N}_x\text{O}$  emissions and resulted in more complete combustion. Kiani et al.<sup>164</sup> experimentally investigated the effect of  $\text{NH}_3$  addition to nonpreheated syngas MILD combustion in a furnace configuration. The mole fraction of  $\text{NH}_3$  was varied between 0.34 and 0.66 at an equivalence ratio of 1.0 for a syngas composition of 0.7;  $[\text{H}_2]/([\text{H}_2] + [\text{CO}]) = 0.7$ . It was reported that the NO emissions vary between 200 and 400 ppmv and show an increasing trend as the  $\text{NH}_3$  content increases. Later, Jiang et al.<sup>165</sup> studied syngas/ $\text{NH}_3$  MILD combustion in a novel burner by 20 different experiments. It was reported that low  $\text{NO}_x$  emissions could be achieved without any  $\text{NH}_3$  leakage at certain  $\text{NH}_3$  flow rates and furnace temperatures ( $T_{\text{furnace}} = 1428 \text{ K}$  and  $V_{\text{NH}_3} \leq 5.72 \text{ SLM}$ ,  $T_{\text{furnace}} = 1467 \text{ K}$  and  $V_{\text{NH}_3} \leq 8.10 \text{ SLM}$ ). Ariemma et al.<sup>166</sup> studied the binary  $\text{NH}_3/\text{alcohol}$  mixtures for methanol, ethanol, and 1-butanol in a cyclonic flow burner. Overall, blending alcohols with  $\text{NH}_3$  provides a stable combustion over a wider range of conditions. The  $\text{NO}_x$  emissions were found to be higher than pure  $\text{NH}_3$  but lower than  $\text{NH}_3/\text{CH}_4$  MILD combustion, especially for fuel-lean conditions where  $\text{NH}_3$  slip is lower.

The published literature showed the feasibility of MILD combustion technology in achieving ultralow  $\text{NO}_x$  emissions (<100 ppmv). However, several challenging aspects, such as the necessity of high levels of dilution and low thermal energy density, might pose problems in terms of design and operation.

### 3. INSIGHTS INTO CHEMICAL KINETICS MECHANISMS FOR $\text{NH}_3$ -BASED FUELS

Over the past six decades, many investigations have been carried out to provide a chemical kinetics mechanism that can interpret the chemical transformation of  $\text{NH}_3$  fuels under gas-phase conditions. These improvements are based on experimental investigations from previous studies, and the results were applied to fit the proposed models. Since the first kinetic reaction mechanism best describing the chemical conversion of  $\text{NH}_3$  oxidation was proposed by Miller et al.,<sup>167</sup> it has served as the foundation for subsequent efforts to improve kinetic reaction mechanisms.

Despite numerous improvements considering a wide range of operational conditions, equivalence ratios, and mixing ratios in binary flames of  $\text{NH}_3$ -based fuels, predictive capabilities still face limitations.<sup>168,169</sup> This is especially evident in studies focused on  $\text{NH}_3\text{--H}_2$  flames, where prediction accuracy decreases as the hydrogen fraction exceeds 40% in the flame.<sup>49</sup> The investigation by Girhe et al.<sup>170</sup> on  $\text{NH}_3$  and  $\text{NH}_3/\text{H}_2$  combustion revealed that the kinetic model proposed by Mei et al.<sup>36</sup> aligns well with the experimental results of Alzueta et al.,<sup>171</sup> who conducted flow reactor measurements to study  $\text{NH}_3/\text{NO}$  interactions. However, the model effectively captures the reduction of NO at the initiation temperature with a decreasing equivalence ratio, a scenario that other tested mechanisms have struggled to replicate. However, the model



exhibits poor performance in pyrolysis<sup>170</sup> and fails to accurately predict the laminar burning velocity (LBV) at high temperatures under fuel-rich conditions, as noted by Shawnam et al.<sup>172</sup>

Establishing a reliable kinetic model that accurately predicts experimental outcomes remains a challenging task. The accuracy of the predictions is fundamentally dependent on the quality and precision of experimental measurements. Limitations in measurement technology have led to a limited understanding of fuel chemistry under combustion conditions, which affects the data used to improve flame kinetics.<sup>49</sup> Setting aside the kinematic differences among the models, which arise due to the lack of experimental data on the rate coefficients of key reactions, further investigation and adaptation of these coefficients within the kinetic reaction mechanisms are required. Notably, the rate constant of the critical reaction  $\text{NH}_2 + \text{N}_2\text{O} \rightarrow \text{N}_2\text{H}_2 + \text{NO}$  remains highly uncertain, as reported by Cornell et al.<sup>173</sup> To address this gap, Wang et al.<sup>174</sup> recently investigated this reaction under different conditions of  $\text{NH}_3/\text{N}_2\text{O}$  flames, aiming to refine and update their kinetic model. As a result, chemical kinetics models constantly require refinement and updates to incorporate new experimental observations. Consequently, this section outlines the most widely used reaction mechanisms for  $\text{NO}_x$  prediction, highlighting their differences, limitations, and applicability under various conditions and combustion systems.

**3.1. Nitrogen Oxide Formation Pathways.** The abundance of radicals such as H, OH, and  $\text{O}_2$  significantly influences the combustion environment, promoting the formation of NO through interactions with the ammonia decomposition radicals HNO, NH, and N, which are essential to the pathways leading to NO formation. A study by Alnasif et al.<sup>175</sup> analyzed the performance of 67 kinetic reaction mechanisms in predicting NO concentrations at various equivalence ratios and atmospheric conditions (Figure 20).

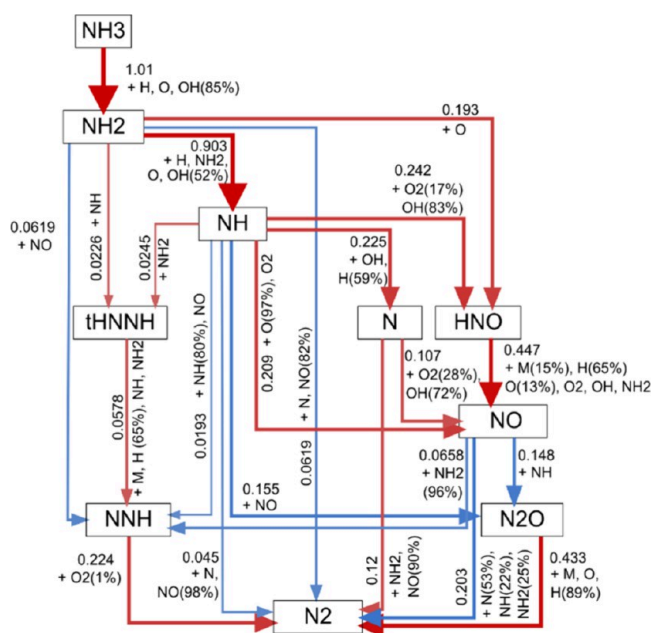


**Figure 20.** NO pathways at flame temperature ( $T = 1770 \text{ K}$ ) and at  $\phi = 0.8$  based on the predictions of the Glarborg kinetic model. Red and blue lines refer to fuel  $\text{NO}_x$  pathways and NO return pathways, respectively. From ref 175. CC BY 4.0.

The review emphasizes the variation between reaction mechanisms, a description that will not be addressed in this review. Further analyses within such a paper targeted a 70/30 vol %  $\text{NH}_3/\text{H}_2$  premixed flame, highlighting the challenges of using various mechanisms and their resolution processes. The study identified two primary reactions,  $\text{HNO} + \text{H} \leftrightarrow \text{NO} + \text{H}_2$  and  $\text{HNO} + \text{OH} \leftrightarrow \text{NO} + \text{H}_2\text{O}$ , as major pathways in the HNO to NO conversion, contributing to increased NO production. Furthermore, the study noted that these reactions display opposite trends as the equivalence ratio ( $\phi$ ) increases. Additionally, the reactions  $\text{N} + \text{OH} \leftrightarrow \text{NO} + \text{H}$  and  $\text{N} + \text{O}_2 \leftrightarrow \text{NO} + \text{O}$  also significantly impact NO formation and are highly dependent on the temperature. Their influence accelerated at higher temperatures, particularly under stoichiometric conditions where temperatures peak, a finding also supported by Hayakawa et al.<sup>54</sup> in their study on the oxidation of pure ammonia flames. Furthermore, the study by Singh et al.<sup>176</sup> demonstrated the significance of the reaction  $\text{NH} + \text{O}_2 \leftrightarrow \text{HNO} + \text{O}$  in increasing NO concentrations, a finding confirmed by Alnasif et al.<sup>177</sup> study as one of the most influential reactions in NO formation, according to the tested kinetic model of Nakamura.<sup>178</sup> This reaction produces the important key radical HNO, which serves as a crucial intermediate in NO production.

Increasing the hydrogen content in the binary fuel of  $\text{NH}_3/\text{H}_2$  premixed flames can affect the kinetic chemistry of the  $\text{NO}_x$  formation. According to study by Zhang et al.,<sup>179</sup> increasing hydrogen enrichment accelerates the production of oxygenated radical pools, thereby speeding up NO formation by strengthening the chain branching reaction  $\text{O}_2 + \text{H} \leftrightarrow \text{OH} + \text{O}$  and the chain propagation reaction  $\text{OH} + \text{H}_2 \leftrightarrow \text{H} + \text{H}_2\text{O}$ . This leads to an increased generation of H, OH, and O radicals that react with ammonia decomposition products (i.e., NH,  $\text{NH}_2$ , NNH, and N) to form NO, a finding also confirmed by Singh et al.<sup>176</sup>

The impact of pressure on the  $\text{NO}_x$  concentration has been studied to determine if the chemical reactions related to NO formation in the reaction zone are pressure dependent. According to research by Hayakawa et al.,<sup>54</sup> increasing pressure significantly accelerates the reaction rates of key reactions such as  $\text{NH} + \text{NO} \leftrightarrow \text{N}_2\text{O} + \text{H}$ ,  $\text{NH} + \text{OH} \leftrightarrow \text{HNO} + \text{H}$ ,  $\text{H} + \text{O}_2 \leftrightarrow \text{O} + \text{OH}$ ,  $\text{NH}_2 + \text{O} \leftrightarrow \text{HNO} + \text{H}$ , and  $\text{OH} + \text{H} + \text{M} \leftrightarrow \text{H}_2\text{O} + \text{M}$ . Notably, the reaction  $\text{OH} + \text{H} + \text{M} \leftrightarrow \text{H}_2\text{O} + \text{M}$  showed the most substantial relative increase. This suggests that OH and H radicals are rapidly consumed in the third-body reaction to form stable  $\text{H}_2\text{O}$  and play a vital role in NO formation, as emphasized in studies by Miller et al.<sup>167,180</sup> Consequently, as the pressure increases, the peak NO concentration decreases due to the limited formation of NO, driven by the consumption of OH and H radicals.

When it comes to coal and ammonia cofiring, the reaction mechanism is complex and includes radicals such as  $\text{NH}_i$  ( $i = 0, 1, 2$ ), HNO, HNCO, and NCO.<sup>181</sup> Glarborg et al.<sup>182</sup> approached the topic, and as depicted later, the group identified the mechanism behind the increase and decrease of NO emissions when both molecules are employed. Further, tar has been acknowledged as a nitrogen carrier in coal. When the temperature is up to 1400 K, tar undergoes rapid pyrolysis to produce HCN.<sup>182</sup> HCN, as previously described, is an important intermediate of the formation of  $\text{NO}_x$ , as it can be converted into HNO under the following high temperature reactions.<sup>182</sup>

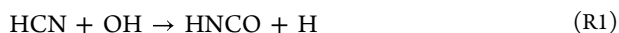


Figure 21 shows the dominating reaction paths involved in the conversion of N-containing species in ammonia/coal

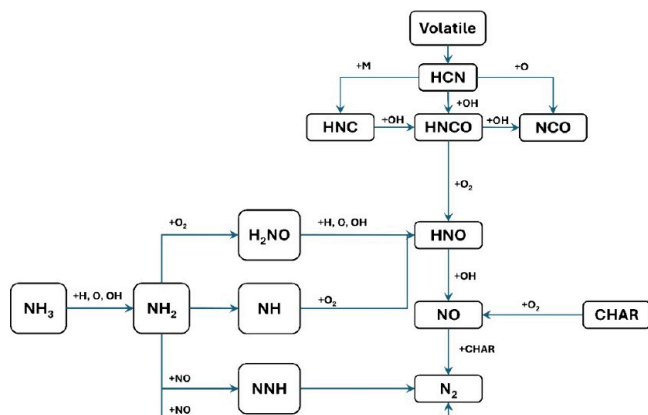


Figure 21. Reaction path of volatiles, ammonia, and char.<sup>183</sup>

cofiring with emphasis on the paths followed by HNO. Interestingly, as the ammonia ratio increases, the molecule starts competing for oxygen, thus suppressing HNO. Other NO reactions (R3, R4, and R5) increase until a point where further  $\text{NH}_3$  intake starts De- $\text{NO}_x$ ing the combustion system.<sup>182</sup>



**3.2. Nitrogen Oxide Consumption Pathways.** According to the study of Alnasif et al.,<sup>177</sup> The key reactions  $\text{NH}_2 + \text{NO} \leftrightarrow \text{N}_2 + \text{H}_2\text{O}$ ,  $\text{NH}_2 + \text{NO} \leftrightarrow \text{NNH} + \text{OH}$ ,  $\text{NH} + \text{NO} \leftrightarrow \text{N}_2\text{O} + \text{H}$ ,  $\text{NH} + \text{NO} \leftrightarrow \text{N}_2 + \text{OH}$ , and  $\text{N} + \text{NO} \leftrightarrow \text{N}_2 + \text{O}$  are the most influential reactions in consuming the NO concentration; see Figure 1. The study revealed that the reduction of NO was primarily due to  $\text{NH}_2$ ,  $\text{NH}$ , and  $\text{N}$  radicals, which are accelerated in excess from  $\text{NH}_3$  under rich conditions. This key finding is also confirmed by Glarborg et al.<sup>184</sup> In scenarios under conditions with 60% hydrogen enrichment, both  $\text{NH}$  and  $\text{NH}_2$  radicals serve as De- $\text{NO}_x$  agents. They consume NO to form  $\text{N}_2\text{O}$  and  $\text{NNH}$  through the reactions  $\text{NH} + \text{NO} \leftrightarrow \text{N}_2\text{O} + \text{H}$ ,  $\text{NH}_2 + \text{NO} \leftrightarrow \text{NNH} + \text{OH}$ , and  $\text{NH} + \text{NO} \leftrightarrow \text{NNH} + \text{O}$ .<sup>184</sup>

$\text{N}_2\text{O}$  has been identified in a study by Glarborg et al.<sup>185</sup> as an important intermediate in the thermal De- $\text{NO}_x$  process. Studies conducted by Miller and Glarborg<sup>186,187</sup> have identified the reactions  $\text{NH}_2 + \text{NO}_2 \leftrightarrow \text{N}_2\text{O} + \text{H}_2\text{O}$  and  $\text{NH} + \text{NO} \leftrightarrow \text{N}_2\text{O} + \text{H}$  as the two main sources of  $\text{N}_2\text{O}$  production. Similarly, research by Klippenstein et al.<sup>53</sup> reveals that the formation of  $\text{N}_2\text{O}$  is significantly influenced by both temperature and oxygen content in the gas mixture. This study demonstrated that the peak concentration of  $\text{N}_2\text{O}$  shifts from lower to higher temperatures as the concentration of the phosphorus compounds in  $\text{O}_2$  increases.

The consumption of  $\text{N}_2\text{O}$  primarily occurs through the hydrogen abstraction reaction  $\text{N}_2\text{O} + \text{H} \leftrightarrow \text{N}_2 + \text{OH}$ , and through dissociation in the presence of a third body (M) via the reaction  $\text{N}_2\text{O} (+\text{M}) \leftrightarrow \text{N}_2 + \text{O} (+\text{M})$ , which is highlighted

by the study of Glarborg et al.<sup>185</sup> The pathways for  $\text{N}_2\text{O}$  consumption are clearly illustrated in Figure 20, as explained by the study conducted by Alnasif.<sup>175</sup>

**3.3. Assessment of Kinematic Differences among Reaction Mechanisms.** Previous studies have shown that while various kinetic models perform well across different equivalence ratios, some mechanisms only demonstrate good performance with minor discrepancies under specific conditions of  $\phi$ . However, their performance significantly deteriorates when the equivalence ratio either decreases or increases. This apparent good performance might result from coincidental alignments with certain data, rather than accurately reflecting the true kinetic modeling of  $\text{NO}_x$  concentration estimation. This indicates a lack of reliability and accuracy in scientific modeling and highlights a deficiency in the performance of ammonia kinetic models.

Alnasif et al.<sup>175</sup> highlighted in their previous study on burner-stabilized stagnation flames for a 70/30 (vol %)  $\text{NH}_3/\text{H}_2$  mixture that the kinetic model of Nakamura et al.<sup>153</sup> and the model of Glarborg et al.<sup>55</sup> perform well from fuel-lean to stoichiometric conditions, showing good agreement with experimental measurements. This suggests that the key reactions influencing the kinetic behavior of NO formation and consumption are effectively captured in the tested mechanisms. However, disparities were observed in the mechanism of Glarborg et al. under conditions nearing  $\phi = 1.2$ , indicating the necessity for enhancements in the rate parameters to more accurately depict the chemical transformation of the relevant reactions for NO.

The study also highlighted the significant roles of key reactions such as  $\text{HNO} + \text{OH} \rightleftharpoons \text{NO} + \text{H}_2\text{O}$  and  $\text{HNO} + \text{H} \rightleftharpoons \text{NO} + \text{H}_2$  in NO formation and reactions  $\text{NH}_2 + \text{NO} \rightleftharpoons \text{N}_2 + \text{H}_2\text{O}$ ,  $\text{NH} + \text{NO} \rightleftharpoons \text{N}_2 + \text{OH}$ , and  $\text{NH}_2 + \text{NO} \rightleftharpoons \text{NNH} + \text{OH}$  in NO reduction. Their roles are determined based on the abundance of the radicals H, OH, and O in the flame.<sup>70,176</sup>

According to the analysis conducted by Mulvihill et al.,<sup>188</sup> the key reaction  $\text{N}_2\text{O} + \text{H}_2 \rightleftharpoons \text{N}_2 + \text{H}_2\text{O}$  considerably impacts  $\text{N}_2\text{O}$  consumption within Zhang's kinetic model.<sup>189</sup> However, this reaction is not considered influential in the Klippenstein kinetic model.<sup>190</sup> Mulvihill et al.<sup>188</sup> report that the reaction  $\text{N}_2\text{O} + \text{H}_2 \rightleftharpoons \text{N}_2 + \text{H}_2\text{O}$  has negligible importance in  $\text{NO}_x$  modeling. The study determined that the rate constant for this reaction must be significantly reduced by a factor of 30 from the value used in Zhang's model. This indicates that the actual rate of the reaction  $\text{N}_2\text{O} + \text{H}_2 \rightleftharpoons \text{N}_2 + \text{H}_2\text{O}$  is much lower than previously estimated. The study also revealed that, whether this reaction was completely removed from the model or its rate constant was reduced by a factor of 30, the outcomes were identical. This suggests that the presence or absence of this reaction does not significantly alter the model's predictions, underscoring that this reaction is not crucial in  $\text{NO}_x$  modeling.

The study by Cornell et al.<sup>173</sup> has brought significant attention to the role of  $\text{N}_2\text{O}$  in ammonia oxidation at low temperatures. This research involved conducting jet stirred reactor (JSR) experiments using an  $\text{NH}_3/\text{N}_2\text{O}/\text{N}_2$  mixture at intermediate temperatures (850–1180 K) and utilized the model of Glarborg<sup>191</sup> to validate their results and address the data gap concerning  $\text{N}_2\text{O}$ 's role in the ammonia oxidation process. The study reported that the kinetic model of Glarborg<sup>191</sup> aligns with the experimental measurements of  $\text{N}_2\text{O}$  mole fractions when the rate constant of the key reaction  $\text{N}_2\text{H}_2 + \text{NO} \rightleftharpoons \text{N}_2\text{O} + \text{NH}_2$  is reduced by a factor of 10,

compared to its original value reported by Dean and Bozzelli.<sup>192</sup> Furthermore, the study revealed that the predictions of Glarborg's model, whether including the key reaction  $\text{N}_2\text{H}_2 + \text{NO} \rightleftharpoons \text{N}_2\text{O} + \text{NH}_2$  or not, are nearly identical. This suggests that previous experimental data sets used for validation may not have effectively tested this specific reaction in Glarborg's model.<sup>191</sup> As a result, this study underscored the importance of a more accurate determination of the rate constant in future research.

The low-pressure-limit rate constant of the reaction  $\text{N}_2\text{O} + \text{M} \rightleftharpoons \text{N}_2 + \text{O} + \text{M}$  has been thoroughly investigated by Mulvihill et al.<sup>193</sup> using a shock-tube configuration for mixtures of 0.2%  $\text{N}_2\text{O}/\text{Ar}$ . This study aimed to provide more accurate and reliable data for the reaction  $\text{N}_2\text{O} + \text{M} \rightleftharpoons \text{N}_2 + \text{O} + \text{M}$  in the temperature range 1550–2500 K at 1.3 atm. A detailed kinetic analysis was conducted, accounting for nonideal pressure variations. The study determined that, over the temperature range 1550–2500 K, the rate constant of  $\text{N}_2\text{O} + \text{M} \rightleftharpoons \text{N}_2 + \text{O} + \text{M}$  was best fit by the expression  $k = 1.01 \times 10^{15} \exp(-30050/T)$ , with  $k$  in  $\text{cm}^3 \text{mol}^{-1} \text{s}^{-1}$  and  $T$  in kelvin. By integrating these results with previous low-temperature data measured in flow/static reactors, the best fit over the temperature range 850–2500 K was found to be  $k = (1.04 \pm 0.04) \times 10^{15} \exp((-30098 \pm 90)/T)$ .

The key findings of Mulvihill et al.<sup>193</sup> differ from those included by the kinetic models,<sup>153,190,194</sup> which are based on the review studies by Baulch et al.,<sup>195</sup> and from Zhang's kinetic model<sup>189</sup> that is derived from the experimental studies of Javoy et al.<sup>196</sup> The study's findings highlight that the concentration of  $\text{N}_2\text{O}$  is significantly influenced by the key reaction  $\text{N}_2\text{O} + \text{M} \rightleftharpoons \text{N}_2 + \text{O} + \text{M}$ , suggesting that this reaction plays a major role in determining the  $\text{N}_2\text{O}$  concentration under specific conditions. Therefore, considering these key findings, updating the rate parameters and incorporating the results from the tested conditions, along with low-temperature data from previous studies, will enhance the prediction accuracy of the kinetic models.

**3.4. Recently Improved Kinetic Models for Nitrogen Oxide Chemistry.** Numerous kinetic reaction mechanisms considering the chemical kinetics of  $\text{NO}_x$  have been introduced. These mechanisms vary in their mechanistic and kinematic aspects, leading to differences in their predictive outcomes, even though their rate parameters are continuously updated. One of the primary issues that can constrain the kinetic model in certain conditions is the development of the model focused on a specific combustion system under specific operational conditions. Restricting the kinetic model to these conditions can impact its predictive performance, particularly in terms of alignment with experimental observations.

A kinetic model for nitrogen chemistry in combustion was developed by Glarborg et al.,<sup>191</sup> based on previous work,<sup>53,184,197</sup> and validated using experimental data from the literature. This model accurately predicts NO formation and consumption across a broad range of conditions. It was later refined by the same author,<sup>198</sup> maintaining the rate coefficients and thermodynamic data from the original model.<sup>191</sup> Enhancements included updating the  $\text{NH}_3/\text{NO}_2/\text{O}_2$  reaction subset based on experimental observations from batch reactors (580–690 K) and flow reactors (850–1350 K) within the  $\text{NH}_3/\text{NO}_2$  system. These updates were supplemented with new flow reactor results, examining the impact of  $\text{O}_2$  addition at the same temperatures. The findings are crucial for modeling ignition and  $\text{N}_2\text{O}$  emissions in ammonia combustion. The

results align with the theoretical study by Klippenstein et al.<sup>199</sup> and are consistent with low-temperature measurements by Lindholm and Hershberger<sup>200</sup> and Sun et al.<sup>201</sup>

Zhang et al.<sup>179</sup> developed a model based on the recent study by Mei et al.,<sup>45</sup> adopting the hydrogen mechanism from Glarborg's studies,<sup>202</sup> which was based on comprehensive experimental data on hydrogen combustion. This model incorporates several chemical reactions ( $\text{H} + \text{O}_2 + \text{H}/\text{O}/\text{OH} = \text{products}$ ), additions not originally included in Glarborg's hydrogen mechanism. The base model was validated using experimental data from a jet-stirred reactor (JSR) that tested  $\text{NH}_3/\text{H}_2$  mixtures at atmospheric pressure, with hydrogen content ranging from 0 to 70 vol %. The experimental conditions covered temperatures from 800 to 1280 K and equivalence ratios of 0.25 and 1. Speciation data for  $\text{NH}_3$ ,  $\text{H}_2\text{O}$ ,  $\text{NO}$ , and  $\text{N}_2\text{O}$  were utilized to verify the reliability of the submechanisms for  $\text{NO}$  and  $\text{N}_2\text{O}$ , which are crucial intermediates in ammonia oxidation. The key findings of their study indicate that increasing the  $\text{H}_2$  content causes the reaction  $\text{NH}_3 + \text{H} \leftrightarrow \text{NH}_2 + \text{H}_2$  to proceed in the reverse direction, converting the  $\text{NH}_2$  radical back into an H atom. These newly formed H atoms then initiate further reactions, specifically  $\text{H} + \text{O}_2 \leftrightarrow \text{O} + \text{OH}$  and  $\text{H} + \text{O}_2 (+\text{M}) \leftrightarrow \text{HO}_2 (+\text{M})$ , which produce O, OH, and  $\text{HO}_2$  radicals. Additionally,  $\text{NH}_2$  and  $\text{H}_2\text{NO}$  radicals serve as chain carriers, transforming one  $\text{HO}_2$  and one H radical into two OH radicals, thereby enhancing OH production. This process promotes the consumption of ammonia ( $\text{NH}_3$ ) and influences the  $\text{NO}_x$  formation.

The study by Singh et al.<sup>176</sup> introduces a new kinetic reaction model for  $\text{NH}_3/\text{H}_2/\text{air}$  flames based on the kinetic model previously developed by Shrestha et al.<sup>169</sup> This model takes into account the chemistry of  $\text{NH}_2$ ,  $\text{H}_2\text{NO}$ ,  $\text{HO}_2$ ,  $\text{N}_2\text{H}_x$ ,  $\text{NNH}$ ,  $\text{HNO}$ , and  $\text{NO}_x$  emissions in a hydrogen-enriched environment and their effects on the overall pathways. Additionally, the study considers reactions of  $\text{NO}$  and  $\text{NO}_2$  with  $\text{NH}_2$  radicals due to their impact on the ammonia oxidation process. Their study underscores the significant impact of the chain branching reaction  $\text{O}_2 + \text{H} \rightarrow \text{OH} + \text{O}$  on the overall chemistry, greatly affecting  $\text{NH}_3/\text{H}_2/\text{air}$  oxidation and emissions. It also highlights the role of  $\text{HNO}$  in  $\text{NO}$  production, especially through the reaction  $\text{NH} + \text{O}_2 \rightarrow \text{HNO} + \text{O}$ , which is critical for  $\text{NO}$  formation. Furthermore, the study found that, at higher levels of hydrogen enrichment, reactions involving  $\text{NH}_2$ ,  $\text{NH}$ ,  $\text{NNH}$ , and  $\text{HNO}$  subspecies also markedly influence the oxidation and  $\text{NO}_x$  chemistry in both pure ammonia and hydrogen-enriched ammonia flames.

According to the study of Meng et al.,<sup>203</sup> which introduced a novel potential  $\text{NO}_x$  formation mechanism involving the breaking of the N–N bond through reactions with  $\text{HNNO}$ , the research collectively refers to *trans*- $\text{HNNO}$ , *cis*- $\text{HNNO}$ , and  $\text{ONHN}$  isomers of  $\text{HNNO}$ . These  $\text{HNNO}$  forms are produced through the pressure-dependent reaction  $\text{H} + \text{N}_2\text{O} (+\text{M}) \rightleftharpoons \text{HNNO} (+\text{M})$ . They engage in various reactions with common combustion species, leading to  $\text{NO}_x$  production. The study highlights that at lower temperatures and higher pressures  $\text{HNNO}$  becomes the preferred product of the  $\text{H} + \text{N}_2\text{O}$  reaction. The study also investigated  $\text{HNNO}$  interactions with common combustion species like  $\text{O}_2$  and clarified that, while these reactions mainly convert  $\text{HNNO}$  back to  $\text{N}_2\text{O}$ , they are relatively slow. This slowness makes interactions with radical species more probable, resulting in high  $\text{NO}_x$  yields.



Table 2. Definitions for Different Combustion Configurations

	PV	test case	ref
CH <sub>4</sub> /NH <sub>3</sub> /air	$PV_1 = -100 \left( \frac{Y_{CO_2}}{M_{CO_2}} + \frac{Y_{H_2O}}{M_{H_2O}} + \frac{Y_{O_2}}{M_{O_2}} + \frac{Y_{H_2}}{M_{H_2}} \right)$	swirling flames	147
	PV <sub>2</sub> = enthalpy		
CH <sub>4</sub> /NH <sub>3</sub> /air	PV <sub>1</sub> = Y <sub>CO<sub>2</sub></sub> + Y <sub>CO</sub>	swirling flames	216
	PV <sub>2</sub> = enthalpy		
coal NH <sub>3</sub>	PV = Y <sub>CO<sub>2</sub></sub> + Y <sub>CO</sub> + Y <sub>H<sub>2</sub></sub> + Y <sub>H<sub>2</sub>O</sub>	cofiring of ammonia with pulverized coal	217
coal NH <sub>3</sub>	PV = Y <sub>CO<sub>2</sub></sub> + Y <sub>H<sub>2</sub></sub> + Y <sub>H<sub>2</sub>O</sub>	laminar counterflow diffusion flames of pulverized coals	218
NH <sub>3</sub> /air	PV <sub>1</sub> = Y <sub>N<sub>2</sub></sub> + Y <sub>H<sub>2</sub></sub> + Y <sub>H<sub>2</sub>O</sub>	laminar premixed flame	219
	PV <sub>2</sub> = mixture fraction		
NH <sub>3</sub> /H <sub>2</sub> /air	$PV_1 = \frac{Y_{N_2}}{M_{N_2}} + \frac{Y_{H_2O}}{M_{H_2O}} - \frac{Y_{H_2}}{M_{H_2}} - \frac{Y_{NH_3}}{M_{NH_3}}$	turbulent cracked ammonia flame	220
	PV <sub>2</sub> = enthalpy		

In line with Meng et al.<sup>203</sup> study, Lee et al.<sup>204</sup> research confirmed the significant role of the HNNO mechanism in NO<sub>x</sub> formation at high pressures and low temperatures. This confirmation was based on experimental measurements involving H<sub>2</sub>, O<sub>2</sub>, N<sub>2</sub>, N<sub>2</sub>O, NO, and Ar in jet stirred reactor experiments, which provided strong experimental support for the NO<sub>x</sub> formation route via HNNO. The study compared these measurements with highly validated kinetic models<sup>53,70,189,191,205</sup> for the N<sub>2</sub>O, H<sub>2</sub>, H<sub>2</sub>O, and O<sub>2</sub> species mole fraction measurements. While the tested kinetic models varied in predicting the onset temperature for reactivity, they generally reproduced the qualitative features of temperature-dependent reactivity. However, for NO, NO<sub>x</sub>, and NH<sub>3</sub>, none of the models captured the observed behavior, predicting negligible amounts of NO and NO<sub>x</sub> at lower temperatures (below ~950 K). In contrast, the model incorporating HNNO pathways predicted significant NO and NH<sub>3</sub> formation at these lower temperatures (~800–950 K), unlike models without HNNO. Therefore, including the HNNO pathway in NO<sub>x</sub> formation models marks a significant improvement in accurately predicting and understanding NO<sub>x</sub> emissions in combustion systems.

#### 4. REDUCED CHEMISTRY FOR AMMONIA SYSTEM BASED ON LOW-DIMENSIONAL MANIFOLD CONCEPT

The chemical kinetics of the ammonia/air system, enriched with hydrogen or methane, involves over 30 species reacting in several hundreds to thousands of reactions. Utilizing detailed chemical kinetics for turbulent flame simulations results in high computational costs due to the high dimensionality and stiffness of the governing equations for species.<sup>206</sup> Consequently, efforts have been focused on reducing the computational time by developing model reduction techniques for chemical kinetics. Various approaches include the intrinsic low-dimensional manifold (ILDMM),<sup>207</sup> computational singular perturbation (CSP),<sup>208</sup> global quasi-linearization (GQL),<sup>209</sup> reaction–diffusion manifold (REDIM),<sup>210</sup> flamelet-generated manifold (FGM),<sup>211</sup> flamelet/progress variable (FPV),<sup>212</sup> and others (refer to ref 206).

In ref 213, the CSP method was utilized to identify fast species that can be considered to be in quasi-steady state. For instance, the CSP tool determined that NH<sub>2</sub> and HO<sub>2</sub> reach a quasi-steady state. In ref 214, the CSP method was applied to a perfectly stirred reactor (PSR) for a premixed ammonia/air

system. Analysis of chemical time scales revealed NH and H<sub>2</sub>O as two species with short chemical time scales for the PSR model, making them prime candidates for steady-state species. Further CSP analysis demonstrated that the chemical time scales of OH and NH<sub>2</sub> radicals are 2 orders of magnitude shorter than those of major species such as N<sub>2</sub>O, N<sub>2</sub>, O<sub>2</sub>, and H<sub>2</sub>.

The chemical kinetics were further analyzed using the GQL method, which is capable of globally studying fast and slow chemical processes. In ref 215, the GQL reduction method was applied to the CRECK mechanism, comprising 203 elementary reactions and 30 species. It was demonstrated that, for reproducing ignition delay times with high accuracy (<5% error), a 17-dimensional GQL reduced chemistry is adequate. Additionally, to capture the low-temperature reaction of ammonia with NO<sub>x</sub>, a 16-dimensional GQL reduced chemistry is necessary.

In turbulent reacting flows, reduced chemistry based on the low-dimensional manifold concept offers computational efficiency, typically involving only two or three progress variables. The flamelet model shows a balance between accuracy and computational cost, making it a practical choice for simulating turbulent combustion across various engineering applications. For instance, the FGM model has been integrated with LES<sup>68</sup> or RANS<sup>216</sup> to simulate swirling flames in NH<sub>3</sub>/CH<sub>4</sub>/air systems. One of the most challenging aspects of the flamelet model is defining progress variables (PVs), which are used to parametrize the thermokinetic states. Various definitions for different combustion configurations are listed in Table 2.

The choice of suitable progress variables aims at predicting the NO<sub>x</sub> emissions accurately. In most cases listed above, the transport equations for NO<sub>x</sub> species must be considered due to their related slow chemical reactions. It was found in ref 72 that the prediction of NO<sub>x</sub> emissions can be improved by considering the NO transport equation in the simulation. However, if one considers the multidimensional cylindrical ammonia/hydrogen flames in which flame stretch exists, as studied in ref 219, the preferential effect has significantly influenced NO<sub>x</sub> emission, and the other selection of progress variables must be used to capture the NO<sub>x</sub> concentration. To summarize, for an accurate prediction of NO<sub>x</sub> emissions, a great deal of attention must be paid to the selection of suitable progress variables in the flamelet model for the turbulent ammonia flame simulation.

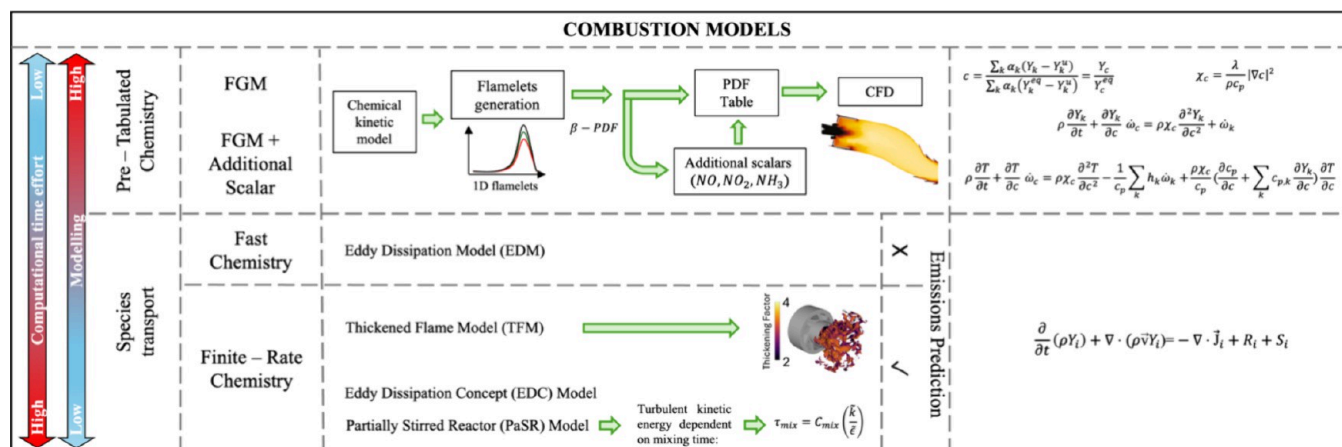


Figure 22. Combustion models comparison in terms of computational time effort and modeling.

## 5. CFD MODELING: AN OVERVIEW

In computational fluid dynamics, reactive simulations play a crucial role in understanding the formation of  $\text{NO}_x$  from ammonia combustion. Ammonia chemistry proves to be more challenging than that of fuels commonly utilized in gas turbines,<sup>10,221</sup> such as natural gas and hydrogen, especially in terms of comprehensively resolving mechanisms related to  $\text{NO}_x$  emissions, as previously depicted. To improve the combustor design procedures by investigating the complexities of pollutant emission formation paths, a proper definition of the ammonia combustion mechanisms, combined with various turbulence closures like Reynolds-averaged Navier–Stokes (RANS), large eddy simulation (LES), and direct numerical simulation (DNS) is required. RANS approaches have been widely used as a standard predictive tool for combustion applications at the industrial level. Even though they remain an attractive choice for providing quick indications and trends, reliable predictions of pollutant emissions require the adoption of detailed chemistries integrated with an efficient turbulence–chemistry interaction model obtained by performing detailed LES. Conversely, at the state of the art, DNS is totally unfeasible for  $\text{NO}_x$  prediction along industrial geometries due to the formidable computational costs. Nevertheless, its application to academic cases is essential to shed some light on the complex mechanism of the fuel bound formation.

The complexity and the computational cost of the simulation are primarily determined by the selected combustion model; thus, it is essential to distinguish between two applicable approaches in reactive CFD, as reported in Figure 22. Models based on the transport of the primitive variables (so-called species transport) resolve the combustion using a chemical mechanism that could account for several chemical species and hundreds/thousands of reactions. Such an approach can provide highly accurate predictions by tracking individual chemical species within the computational domain. However, this approach is computationally expensive due to the need to solve many coupled differential equations, especially in the LES context. The adoption of such a solution strategy along industrial geometries is very hard to implement, unless skeletal chemistries derived from detailed chemistry sets are used.

In the species transport category, the eddy dissipation concept (EDC) and partially stirred reactor (PaSR) combustion models should be mentioned. The former,

proposed by Magnussen,<sup>222</sup> is a finite-rate chemistry combustion model, widely applied for the simulation of combustion systems, although it requires not negligible computational costs. The PaSR model, proposed by Chomiak et al.,<sup>223</sup> represents a perfectly stirred reactor (PSR) with imperfect mixing. Like EDC, PaSR conceptualizes combustion as a series of reaction and mixing steps within locally uniform regions with the definition of a reacting volume fraction based on local estimations of chemical and mixing time scales.

On the other side, pretabulated chemistry approaches like flamelet-generated manifold (FGM)<sup>211</sup> represent a good trade-off between accuracy and computational efficiency. In fact, the combustion is modeled through a low-dimensional manifold derived from the chemical kinetics while the turbulence–chemistry interaction is usually calculated through a  $\beta$ -PDF function of auxiliary variables like mixture fraction and progress variable.<sup>224</sup> By precomputing 1D flamelets, prechemistry significantly reduces the computational costs. However, it may not capture all of the combustion features that are accessible when solving the species transport approach. As an example, computation of the characteristic chemical time scale is generally one of the variables that is used to define the progress variable. By using FGM it is not possible to capture the trends of those species, like  $\text{NO}_x$ , whose formation time scale is quite different from the other, much faster, species. As it will be pointed out in the literature review, pretabulated approaches struggle in the  $\text{NO}_x$  prediction even when coupled with high-fidelity turbulence models like LES.<sup>80</sup>

Recently, a new approach combining CFD and chemical reactor networks (CRNs)<sup>225</sup> has received significant attention, with the goal of reducing simulation time and computational effort. CRN represents a hybrid approach that combines zero-dimensional perfectly stirred reactors (PSRs) with one-dimensional plug-flow reactors (PFRs). Ehrhardt et al.<sup>226</sup> were the first to introduce this approach, which consists of three main steps: (a) A reactive CFD simulation is performed, possibly limiting as much as possible the computational effort, for example using global kinetic scheme. The CFD results are then postprocessed using a set of global criteria to separate the combustor into chemically and physically homogeneous zones. The cells that satisfy the same criteria are clustered together to form the zones of the reactor network. (b) A perfectly stirred reactor (PSR) or a plug-flow reactor (PFR) is associated with each zone according to the local flow conditions. The links and the exchanges of the main physical quantities between the

reactors are established by computing the mass fluxes between adjacent zones. (c) Last, the CRN is solved with a detailed chemical reaction mechanism to obtain an accurate prediction of pollutant emissions. The CRN model is significantly less computationally intensive compared to the above-described approaches, and therefore, it can efficiently be used to perform many simulations, comparing several chemical kinetics models. Obviously, the reliability of the CRN predictions is strongly dependent on the accuracy of the underlying CFD simulation that in any case must be able to capture the main features of the flame, such as its morphology, length, and position inside the combustor.

In the next section, a comprehensive review will report the main works present in the literature employing the approaches here described, aiming at highlighting the main findings as well as their limitations.

**5.1. Comprehensive Review on NO<sub>x</sub> Emission Evaluation by CFD.** As for the pretabulated chemistry models, an interesting solution strategy to overcome the issue related to the different time scales between NO<sub>x</sub> and the species used for the definition of the progress variable is represented by the solution of additional scalar transport equations associated with NO<sub>x</sub> whose source terms are pretabulated as well, with the advantage to decouple the NO<sub>x</sub> equation from the remaining set of transport equations. This approach has been adopted by Cerutti et al.,<sup>227</sup> where an initial feasibility study on introducing ammonia into industrial gas turbines by combining LES and FGM combustion models and NO<sub>x</sub> emissions was investigated. It was confirmed that fuel-bound NO<sub>x</sub> plays a dominant role in pollutant emissions. The simulations captured the key physical trends, revealing appropriate tools for assessing the feasibility of introducing hydrogen–ammonia mixtures in gas turbine combustors. An et al.<sup>68</sup> employ such method for modeling the FGM combustion in a fully premixed swirled flame investigated through an LES: the research is focused on the impact of different NH<sub>3</sub> concentrations blended with CH<sub>4</sub>. While excellent agreement with the data is retrieved in terms of flame position and velocity field, the prediction of NO<sub>x</sub> is not fully satisfactory. Despite a significant improvement of the results obtained through the decoupling approach if compared to the pretabulated NO mass fraction, as shown in Figure 23, the model results in a marginal error only when low percentages of NH<sub>3</sub> (by volume) are present in the mixture. Conversely, when the fuel-bound NO<sub>x</sub> pathways are preponderant over the thermal pathways, the error increases significantly. A huge overprediction of the emission is noticeable, as the numerical model predicts NO<sub>x</sub> values 1000 ppm higher than the reference data. The same numerical approach is employed by Wang et al.<sup>228</sup> focusing on a nonpremixed flame. The fuel gas is obtained by ammonia cracking, and two different concentrations of NH<sub>3</sub> are investigated, namely 56 and 75%. Detailed radial NO profiles measured at several axial distances from the injector are used to measure the performance of the LES employing Okafor's mechanism.<sup>42</sup> Interestingly, there is a very good match in the sections close to the injector, while the prediction degrades moving downstream. It can be seen that the LES overpredicts the data by about 50% at the last reported cross section. Honzawa et al.<sup>229</sup> focus their investigation through LES on the effect of heat losses on NO<sub>x</sub> production in a perfectly premixed test rig including this effect in the FGM model. The LES simulations are performed for a NH<sub>3</sub>–CH<sub>4</sub> blend, providing an assessment also for

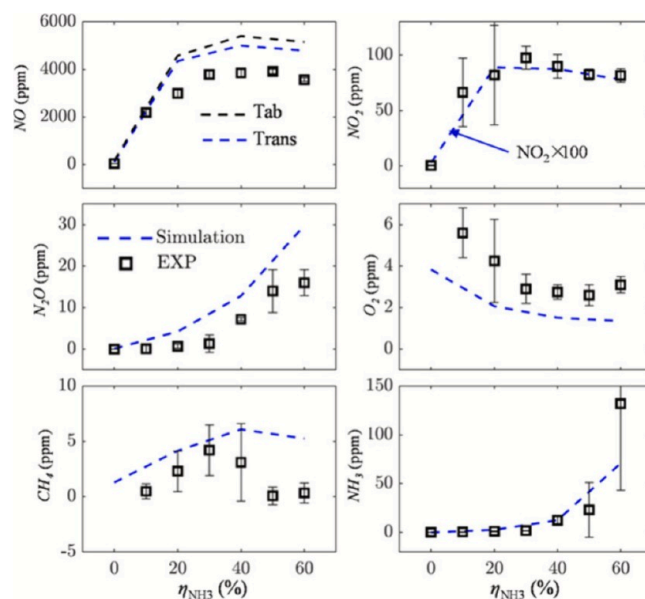


**Figure 23.** In figure of NO (ppm), comparison of NO transported values and pretabulated values with experiments. Comparison of experimentally and numerically derived values of NO, NO<sub>2</sub>, N<sub>2</sub>O, O<sub>2</sub> and unburnt fuel (CH<sub>4</sub> and NH<sub>3</sub>) emissions as a function of NH<sub>3</sub> fraction. Reproduced with permission from ref 68. Copyright 2021 Elsevier.

unburnt CO. Despite a significant improvement of NO<sub>x</sub> prediction obtained through the nonadiabatic model, demonstrating the sensitivity of the fuel-bound NO<sub>x</sub> to the heat loss, the difference with the reference data is still significant: while in the rich regime the model overpredicts the emission with a factor of 1.5, in the lean regime NO<sub>x</sub> are up to 5 times the experimental value. An interesting finding coming from this study is that all of the chemical mechanisms that have been tested behave in a similar way.

A different approach was attempted by Yadav et al.,<sup>217</sup> conducting LES modeling of cofiring of ammonia with pulverized coal in a single-burner test furnace and studying the nonadiabatic effects using a three mixture fractions flamelet/progress variable (3Z-FPV) methodology. A six-variables tabulation method based on nonpremixed flamelets was introduced. To parametrize the thermochemical space, the model used three mixture fractions—ammonia, coal volatiles, and char off-gases—as well as the variances of mixture fraction, reaction progress variable, and total enthalpy. A direct comparison between the adiabatic and the nonadiabatic models was shown and compared with the available experimental data. The results demonstrate that the NO emissions and temperature are slightly underestimated in the nonadiabatic case, while an opposite situation (overprediction) is noticed in the adiabatic case. Aiming at obtaining hydrogen from the cracking process, two ammonia cracking ratios of 14 and 28% at a pressure of 5 bar were examined by Wang et al.<sup>228</sup> The authors explored the effect of the ammonia cracking ratio on the flame structure and NO formation mechanism. The chemical kinetics schemes of Ootomo et al.,<sup>70</sup> Okafor et al.,<sup>42</sup> Mathieu et al.,<sup>230</sup> and Jiang et al.<sup>231</sup> were compared to determine the best solution for replicating these operating conditions. The FGM approach was employed in the context of large eddy simulations, and the results were compared with experimental data available in ref 232. It was shown that with



increasing cracking ratio the flame reactivity is enhanced but also the generation of NO is increased. Good correlations between numerical simulation and experimental data have been obtained, particularly in the flame zone, while the error becomes not negligible downstream from the fuel inlet section.

The higher accuracy of the species transport models over the pretabulated ones is demonstrated by Meloni et al.,<sup>233</sup> by investigating the effect of rising operating pressure along an extremely lean NH<sub>3</sub>–H<sub>2</sub> blend. Here, a perfect match of the NO emission is obtained at atmospheric pressure, while a 15% lower concentration is obtained at the maximum operating pressure of 2 bar. Bioche et al.<sup>234</sup> use LES to predict the flame characteristics and the NO<sub>x</sub> emissions using the PRECCINSTA burner. A dynamic Smagorinsky and TFLES models are used for the subgrid scale and the turbulent combustion models, respectively. They found an emission minimum point at a rich condition ( $\phi = 1.46$ ) for  $X_{H_2} = 0.46$ , corresponding to  $X_{NO_x} \approx X_{NH_3} \approx 300$  ppmv. The same computational domain (PRECCINSTA) was used by Shen et al.<sup>235</sup> employing CFD simulations to investigate wet ammonia combustion characteristics and the NO<sub>x</sub> formation mechanisms using LES. The effects of the equivalence ratio and the amount of hydrogen in the mixture have been analyzed in terms of fluid dynamics variables and emissions. The partially stirred reactor (PaSR) is used as a combustion model with finite-rate chemistry. A sensitivity analysis showed the influence of various parameters on NO<sub>x</sub> emissions, velocity, and temperature fields, providing valuable information for optimizing wet ammonia combustion systems. However, the lack of validation against experimental data limits the reliability of the findings. As for the flame morphology, the wet combustion leads to the liftoff of the flame, while an attached flame to the bluff body is identified for the dry flame. The rich condition shows the superiority of controlling NO and N<sub>2</sub>O emissions via the reburning of NO downstream. However, the unburnt ammonia remains at problematic levels due to the limited residence time in the combustion chamber. Finally, a POD analysis was carried out to extract the coherent structures and ascertain the nonlinear turbulence–chemistry coupling mechanism. Indlekofer et al.<sup>236</sup> carried out a comprehensive study that exploits the use of large eddy simulations in conjunction with detailed chemical kinetics to assess a rich–lean staging strategy applied to the combustion of partially cracked ammonia. A CRN model is developed and tuned against the LES results with the goal to gain more detailed insights about the chemical pathways. The analysis of the results obtained from both numerical modeling approaches, LES and CRN, confirmed the experimental findings and predicted a significant reduction in NO<sub>x</sub> emissions compared to the nonstaged case. The two-staged combustion is also investigated by Okafor et al.<sup>66</sup> for methane–ammonia–air diffusive flames using LES coupled with the PaSR combustion model; the optimum equivalence ratio in primary zone was found to vary from 1.30 to 1.35 as the ammonia fuel fraction decreased from 0.30 to 0.10.

Moving to methodologies requiring lower computational effort, Füzési et al.<sup>237</sup> employed a RANS turbulence model coupled with a partially stirred reactor for the analysis of a lean premixed swirl-stabilized burner operating at atmospheric pressure. The analysis involves a blend of NH<sub>3</sub>–H<sub>2</sub> at several equivalence ratios (up to 0.9) and H<sub>2</sub> shares (up to 20 vol %). The comparison with data at 10% H<sub>2</sub> reveals that the trend of NO (predicted through Okafor's mechanism<sup>42</sup>) is satisfactorily

predicted. It was shown that NO rises with the equivalence ratio, and a mean error of about 15% was measured across the investigated conditions. Mikulčić et al.<sup>238</sup> and Chaturvedi et al.<sup>225</sup> performed atmospheric RANS simulations with a finite-rate combustion model for premixed NH<sub>3</sub>–CH<sub>4</sub> and NH<sub>3</sub>–H<sub>2</sub> blends, respectively. In both cases, the CFD is coupled with a chemical reactor network investigating several chemical mechanisms. In the former work, three of the most common chemistry sets used in the literature for ammonia combustion are analyzed. All the mechanisms showed a satisfying agreement with the reference data only for ultrarich conditions, while a huge overprediction can be identified in lean conditions for any employed chemistry set. Furthermore, a non-negligible difference can be observed among the mechanisms under the same operating condition. Very similar trends are obtained in Chaturvedi et al.,<sup>225</sup> with a significant overpredictions of the data at lean conditions for all the investigated chemistry sets. Such a gap is progressively reduced moving close to the stoichiometric and rich conditions. Mazzotta et al.<sup>239</sup> used RANS simulations coupled with detailed chemistry, specifically EDC and PaSR combustion models, to compare the effects of pressure on NO<sub>x</sub> emissions derived from ammonia–hydrogen blends as a results of high ammonia cracking. In particular, a mixture consisting in 25% NH<sub>3</sub>–75% H<sub>2</sub> (by volume) was analyzed. The increase in pressure from 0.11 to 0.2 MPa resulted in a reduction of 65% in NO<sub>x</sub> emissions. A comparison of various kinetic schemes in laminar burning velocity, ignition delay time, and emissions was carried out, aiming at selecting the most suitable one to be used in subsequent CFD simulations. The choice of chemical kinetics model resulted to be a key parameter in terms of prediction of combustion and emission characteristics. However, even if the numerical results derived by both EDC and PaSR predicted the experimental NO<sub>x</sub> emissions with small errors, the computational time turned out to be prohibitive due to the combustion model being based on detailed chemistry to obtain a narrow range of results. A similar approach to the latter was analyzed by Viguera-Zuniga et al.<sup>240</sup> using RANS simulations coupled with the EDC model on hydrogen–ammonia mixtures. The model demonstrated good accuracy in the prediction of the consumption and production of ammonia under atmospheric conditions. However, the results confirmed the poor capabilities in the prediction of nitrogen oxide emissions and hydrogen reactivity with an overestimation of both parameters. The effect of pressure is investigated by Somaratne et al.<sup>241</sup> for premixed ammonia–air flames: the increase in pressure from 0.1 to 0.5 MPa results in a reduction of NO from 700 to 200 ppm. Sun et al.<sup>242</sup> employed RANS coupled with the EDC combustion model to analyze the combustion and emission characteristics of premixed ammonia and hydrogen flames in a swirling flow configuration. The effects of the equivalence ratio and hydrogen content in the mixture for NO emissions were investigated. The increase in the equivalence ratio leads a decrease in NO emissions for  $\phi > 1.1$ , while unburned NH<sub>3</sub> increases in rich condition, at  $\phi > 1.3$ . As the hydrogen content is increased, unburnt NH<sub>3</sub> is decreased dramatically, while NO generation is increased. As  $X_{H_2}$  is increased, NO emission is increased significantly at a lower  $\phi$ , while it is increased slightly or even remains unchanged at a higher  $\phi$ .

The formation and distribution of nitrogen oxides (NO<sub>x</sub>), including NO, NO<sub>2</sub>, and N<sub>2</sub>O, are crucial due to their

environmental impact, and CFD has become an indispensable tool for predicting and analyzing the distribution of these species within the flame structure and the overall combustion device to try to identify and reduce the most impactful  $\text{NO}_x$ -forming reactions. Direct numerical simulation (DNS) offers a unique capability to quantify these radicals with high precision, capturing the intricate interactions between turbulence and chemical reactions. In particular, DNS provides a detailed spatial distribution of  $\text{NO}$ ,  $\text{NO}_2$ , and  $\text{N}_2\text{O}$  within the flame front, allowing for the identification of regions with high pollutant formation. In contrast, large eddy simulation (LES), while effective for larger scales, lacks the resolution needed to accurately capture these finer-scale species distributions. However, the introduction of hydrogen into an ammonia-based flame front introduces a greater degree of uncertainty about the formation of  $\text{NO}$ ,  $\text{NO}_2$ , and  $\text{N}_2\text{O}$ . This uncertainty is primarily due to the difficulty in modeling mixtures with  $Le \neq 1$ , necessitating a deeper analysis of preferential and differential diffusion.<sup>219,243</sup> Tian et al.<sup>244</sup> analyzed turbulent ammonia/air premixed flames to investigate the influence of the equivalence ratio on the flame structure and  $\text{NO}$  formation characteristics using DNS and analyzing the role of preferential diffusion. It was found that  $\text{NO}$  is high in the product of the lean case, as well as  $\text{NO}_2$ , even if it is 3 times smaller. In contrast,  $\text{NH}_3$  is higher in the product of the rich case. The effect of molecular diffusion on the turbulent premixed  $\text{NH}_3/\text{H}_2/\text{air}$  flame structure and  $\text{NO}$  production were investigated by Chi et al.<sup>245</sup> by performing four different DNSs, highlighting the need to include the molecular diffusion and the Soret effect to better capture the flame structure, in particular in the prediction of the  $\text{NO}$  production and turbulent flame speed. Osipova et al.<sup>246</sup> investigated experimentally and numerically the flame structure of premixed ammonia/hydrogen flames at 4 and 6 atm while varying the equivalence ratio between 0.8 and 1.2. According to experimental data and numerical simulations,  $\text{NO}$  was the most abundant nitrogen-containing species in the postflame zone, while  $\text{N}_2\text{O}$  and  $\text{NO}_2$  concentrations were negligible. Transitioning to rich conditions ( $\phi = 1.2$ ) reduced  $\text{NO}$  concentrations in the postflame zone as well as peak  $\text{NO}$  and  $\text{N}_2\text{O}$  concentrations in the reaction zone.

**5.2. Final Considerations.** To date, the prediction of  $\text{NO}_x$  emissions in mixtures with ammonia via CFD is still an inaccurate and challenging topic, especially due to the difficult prediction of  $\text{NO}$  and  $\text{NO}_2$  formation from fuel-bound  $\text{NO}_x$  mechanisms. The combustion models that are most effective, and within a feasible error range, are those that couple detailed chemistry using species transport models (EDC or PaSR) with unsteady simulations (LES) to predict the formation of slow chemical species; however, the computational effort required is prohibitive. Models based on pretabulated chemistry coupled with LES simulations are a compromise between accuracy and computational time, using the addition of scalar transport equations to predict  $\text{NO}$  and unburned fuel emissions. The fluid-dynamic fields derived from high-fidelity CFD simulations can then be used in a CFD–CRN approach, which is significantly less computationally intensive compared to the pretabulated and species transport approaches and can efficiently be used to perform sensitivity studies.

The predictive capability of CFD models is found to vary significantly based on the combustion regime, as evidenced by the state-of-the-art analysis. This disparity can be attributed to several factors. First, the chemical kinetics model is found to be a significant contributor to this discrepancy, as there is

currently no single model that is valid for all operating conditions.<sup>170</sup>

In the case of perfectly premixed flames, where the chemistry is controlled (apart from preferential diffusion effects), the models are generally easier to solve, and the existing models give satisfactory results and a higher probability of capturing  $\text{NO}_x$  emissions, especially for very lean ( $\phi \ll 1$ ) or very rich ( $\phi \gg 1$ ) combustion. For  $\phi \gg 1$ , the  $\text{NO}_x$  chemistry is overconstrained due to the lack of  $\text{O}_2$ , allowing good emission prediction; for  $\phi \ll 1$ , there are fewer advantages from a chemical/modeling perspective. In addition, the mesh can be more easily calibrated to resolve the flame front (species transport models) or to minimize the error in modeling subgrid effects (pretabulated chemistry models).

However, in multiregime combustion (stratified or non-premixed flames), where combustion is controlled by mixing/diffusion as well as chemistry, flame thickness resolution becomes a significant challenge for the accurate prediction of  $\text{NO}_x$  formation, with a lower probability of capturing  $\text{NO}_x$  emissions compared to premixed cases. This problem is further enhanced in lean conditions, where flame thickness is minimal. Conversely, in rich diffusion flames, the flame fronts are significantly thicker, making the prediction of  $\text{NO}_x$  formation more feasible and the chemistry more constrained. From a combustion model perspective, it is more difficult to accurately describe the flame front using species transport due to its smaller size (especially in the diffusive regime). In general, very fine meshes must be used to capture the mixing. On the other hand, pretabulated chemistry models have another disadvantage: they can hardly account for multiregime combustion.

## 6. MACHINE LEARNING FOR $\text{NO}_x$ PREDICTION

Machine learning (ML) has emerged as a promising tool for predicting  $\text{NO}_x$  emissions, offering an alternative to traditional experimental methods and computational fluid dynamics (CFD) simulations, provided there are sufficient high-quality data. Its application spans across various combustion systems, including boilers,<sup>247</sup> thermal power plants,<sup>248</sup> gas turbines,<sup>249</sup> and engines,<sup>250</sup> predominantly focusing on fuels such as coal,<sup>247,248</sup> natural gas,<sup>249</sup> diesel,<sup>250</sup> and biomass.<sup>251</sup> However, its utilization for the  $\text{NO}_x$  prediction of  $\text{NH}_3$  combustion remains limited.

In one of the early works, Li et al.<sup>251</sup> utilized images of flame radicals such as  $\text{OH}^*$ ,  $\text{CN}^*$ ,  $\text{CH}^*$ , and  $\text{C}_2^*$  as a training data set to predict  $\text{NO}_x$  emissions from biomass combustion. The ML model was chosen to be a deep denoising autoencoder (DDAE) which in essence adds noise to the original images and reconstructs the uncorrupted version. The reconstructed images were then compared to the output from a gas analyzer to measure the error. It was reported that the root-mean-square error obtained from the  $\text{NO}_x$  predictions were as low as 2 ppm. Ye et al.<sup>252</sup> used historical operational data in conjunction with data generated from CFD simulations to predict  $\text{NO}_x$  emissions in a coal-fired power plant. Three ML models, namely, artificial neural network (ANN), gradient boosted regression trees (GBRT), and support vector regression (SVR), were compared to find the best suitable framework. Through a Shapley additive interpretation analysis, the most important features playing a role in  $\text{NO}_x$  production were identified. Finally, the correlation coefficient ( $R^2$ ) of the model was reported to be 0.98. Yuan et al.<sup>248</sup> applied an ensemble ML method to predict  $\text{NO}_x$  emissions in a coal-fired power plant. Initially, the input feature space consisted of 31

auxiliary variables and then was reduced to 12 variables using principal component analysis and mutual information. Then, three base learners, namely, ANN, decision trees (DT), and SVR were used to create a linear regression based meta-model for  $\text{NO}_x$  prediction. The reported  $R^2$  values ranged between 0.87 and 0.95, showing good prediction accuracy. Yan et al.<sup>253</sup> predicted the  $\text{NO}_x$  emissions from a coal bed methane fueled rich-quench-lean combustor using XGBoost, NGboost, and random forests. The model used only four parameters: air mass flow rate, air inlet temperature, swirler angle, and lean burn zone length of the combustor. It was reported that the inlet air temperature had the highest importance in  $\text{NO}_x$  production while the swirler angle had no impact on  $\text{NO}_x$  emissions. Later, Zhang et al.<sup>254</sup> applied least-squares SVR (MLS-SVR) to predict  $\text{CO}_2$ , CO, and  $\text{NO}_x$  emissions from a biodiesel- $\text{H}_2$  fueled compression ignition engine. The input features for the model were chosen to be thermophysical parameters of the fuel (calorific value, cetane number, density, and viscosity), engine variables (speed and load), and fuel  $\text{H}_2$  content. The model was then used to analyze  $\text{NO}_x$  emissions at different engine speeds and loads using the ML model. Overall, the prediction accuracy of the model was satisfactory ( $R^2 > 0.99$ ). Even though successful applications of ML to the  $\text{NO}_x$  prediction of various fuels and combustion systems are present in the literature, applications to  $\text{NH}_3$  combustion systems remain limited.

In a relatively recent first attempt, Saleem et al.<sup>255</sup> leveraged published literature data to develop artificial neural network (ANN) models for predicting  $\text{NO}_x$  emissions from a range of fuels including  $\text{NH}_3$ ,  $\text{H}_2$ , natural gas, kerosene, and their binary blends. It was noted that the  $\text{NO}_x$  emissions were highly sensitive to the equivalence ratios for all fuels. Notably, the developed model is agnostic to geometric variations within combustors, exhibiting robust performance with an achieved coefficient of  $R^2$  higher than 0.95, making it suitable for a wide range of applications. Subsequently, Mao et al.<sup>256</sup> utilized ANNs to predict  $\text{NO}_x$  emissions from  $\text{NH}_3/\text{H}_2$  combustion across a wide range of operating conditions. Their approach employed training data derived from a chemical reactor network (CRN) model, incorporating perfectly stirred reactors (PSRs), partially stirred reactors (PaSRs), and plug flow reactors (PFRs) to emulate a rich-quench-lean (RQL) two-stage combustion system. Among the tested ANN models, the backpropagation-ANN approach yielded the highest accuracy ( $R^2 = 0.998$ ), effectively supplanting the CRN network for  $\text{NO}_x$  emission predictions. Very recently, Xing and Jiang<sup>257</sup> developed neural network potentials (NNPs) to investigate  $\text{NO}_x$  and  $\text{N}_2\text{O}$  formation during  $\text{NH}_3$  and  $\text{NH}_3/\text{H}_2$  combustion. The NNPs were used to replace computationally costly reactive molecular dynamics (RMD) simulations. It was reported that the addition of  $\text{H}_2$  to  $\text{NH}_3$  increased the NO and  $\text{NO}_2$  emissions in  $\text{NH}_3/\text{H}_2$  blends while  $\text{N}_2\text{O}$  was reduced.

The use of  $\text{NH}_3$  as an alternative fuel in compression ignition engines has gained significant attention due to its potential to reduce carbon emissions. However, the challenges associated with  $\text{NH}_3$  combustion, particularly  $\text{NO}_x$  emissions, necessitate advanced optimization and control strategies. Recent studies have explored the application of ML to predict and optimize the  $\text{NH}_3$  combustion performance and emissions in compression ignition engines. Data generation typically involves modified single-cylinder or multicylinder engines operated under various conditions. For instance, Elumalai et al. utilized a single-cylinder common rail engine running on

$\text{NH}_3$ -biodiesel dual fuel at 80% load and 1500 rpm.<sup>258</sup> Similarly, Mi et al. investigated an  $\text{NH}_3$ -diesel dual-fuel engine across different  $\text{NH}_3$  energy fractions.<sup>259</sup> These studies systematically vary parameters such as injection timing, pressure, and fuel composition while measuring performance metrics and emissions by using advanced instrumentation.

Several ML approaches have been employed to model and predict engine performance and emissions. Response surface methodology (RSM) is commonly used for developing regression models and identifying optimal operating conditions. Artificial neural networks (ANNs) have gained popularity due to their ability to capture complex nonlinear relationships in engine data. Elumalai et al. compared RSM and ANN models, finding that the ANN approach produced more accurate predictions across various engine responses.<sup>258</sup> It was reported that the ANN model predicted all engine responses with  $R^2 > 0.99$ , demonstrating excellent reproducibility of experimental data.<sup>258</sup> When validated against experimental results, these models typically show error rates in the range of 1–5%, which is considered acceptable for engine applications. These models are also used for multiobjective optimization to find the best trade-offs between performance and emissions. Elumalai et al.<sup>258</sup> used RSM combined with a desirability function approach to optimize split injection parameters, achieving a 12.33% increase in brake thermal efficiency while reducing most emissions, though  $\text{NO}_x$  emissions increased by 15.62%.

Future research directions include developing more comprehensive models that account for transient engine operation, as most current studies focus on steady-state conditions. In a recent study, Arivalagan et al. demonstrated the potential of long short-term memory (LSTM) networks for capturing temporal dependencies in engine performance data.<sup>260</sup> They investigated the emissions from a compression ignition engine using  $\text{NH}_3$ -diesel fuel blends. The trained LSTM network successfully captured the  $\text{NO}_x$  emissions depending on the fuel blend, engine speed, and crank angles.

The utilization of ML presents an opportunity to expedite the design iteration processes significantly compared to conventional experimental and CFD approaches. Despite notable achievements in other fuel types, the studies focusing on ML applications for  $\text{NH}_3$ -fueled combustion systems remain scarce. Nevertheless, the reported predictive accuracies of the models in recent studies underscore the potential of ML in  $\text{NH}_3$  combustion for  $\text{NO}_x$  prediction.

## 7. CHALLENGES AND PERSPECTIVES

Ammonia, as a renewable and clean fuel, holds significant potential for industrial applications. However, the challenges associated with  $\text{NO}_x$  emissions from ammonia combustion require further research and development. This review provides a comprehensive analysis of the combustion characteristics,  $\text{NO}_x$  emission trends, and underlying mechanisms, contributing to a better understanding of the roles of ammonia in sustainable energy and clean fuels.

Despite extensive research, several gaps hinder the broad implementation of ammonia as a fuel. Current kinetic models, while improved, still show discrepancies in predicting  $\text{NO}_x$  emissions across various combustion conditions. More accurate models are needed to capture the complex chemistry of ammonia combustion. There is also a need for more comprehensive experimental data, especially under conditions that mimic real-world applications, to validate and refine the



computational models. The development of advanced diagnostic tools to measure key species and intermediates in ammonia flames can provide deeper insights into combustion processes. Looking ahead, pivotal research directions include developing novel strategies for  $\text{NO}_x$  reduction, improving CFD models by integrating detailed chemistry and turbulence interactions, and expanding experimental research to cover a broader range of operational parameters. Employing cutting-edge experimental techniques and hybrid experimental–computational approaches can create a synergistic methodology, leveraging the strengths of both to advance the field. By addressing these challenges and pursuing the outlined research directions, significant strides can be made toward the sustainable and efficient use of ammonia as a fuel, with minimal environmental impact.

The field of plasma-assisted  $\text{NH}_3$  combustion presents both significant challenges and promising opportunities, with advancements in several key areas likely to drive the field forward. Future research should focus on developing detailed models that can accurately predict the effects of plasma on  $\text{NH}_3$  combustion dynamics and emission formation under diverse conditions. Advances in computational techniques have the potential to accelerate the generation of critical data for reaction mechanisms, although experimental validation remains challenging to ensure model accuracy. Another important research direction involves exploring novel plasma configurations and discharge types to further enhance combustion performance and emission control. The integration of advanced diagnostics and real-time control systems for plasma-assisted combustion also represents a crucial area for future development. Advancements in plasma-assisted combustion could benefit greatly from collaboration between the high-temperature combustion and low-temperature plasma communities. Furthermore, although current research has primarily focused on  $\text{NO}_x$  emissions, future studies should expand to comprehensively address other potential pollutants and their formation mechanisms in plasma-assisted  $\text{NH}_3$  combustion. Additionally, there is a pressing need to investigate the scalability of plasma-assisted-combustion technologies for practical implementation in gas turbines and other large-scale energy systems. This includes addressing challenges related to plasma stability, uniformity, and energy efficiency in high-power applications. Lastly, as the field progresses, there is a need for standardized methodologies and metrics to facilitate meaningful comparisons between different plasma-assisted-combustion strategies and conventional approaches.

While MILD combustion of  $\text{NH}_3$  and its mixtures shows promise for ultralow  $\text{NO}_x$  emissions, several challenges and research gaps remain. The necessity for high levels of dilution and a low thermal energy density poses significant design and operational challenges, particularly for practical applications. Future research should focus on optimizing reactor designs to achieve stable MILD combustion conditions while maintaining a high thermal efficiency. There is a need for more comprehensive studies on the effects of pressure, as most current research is limited to atmospheric conditions. The interplay between  $\text{NH}_3$  and various cofuels (e.g.,  $\text{H}_2$ ,  $\text{CH}_4$ , syngas, alcohols) in MILD conditions requires further investigation, especially regarding emission control and combustion stability. Advanced diagnostic techniques and high-fidelity numerical simulations are needed to better understand the complex chemical kinetics and flow patterns

in  $\text{NH}_3$  MILD combustion. The development of more accurate and comprehensive chemical kinetics mechanisms for  $\text{NH}_3$  and its blends under MILD conditions is crucial. Future work should also explore the scalability of  $\text{NH}_3$  MILD combustion systems from laboratory scale to industrial applications. Additionally, the potential of MILD combustion in mitigating other pollutants, such as  $\text{N}_2\text{O}$ , deserves attention. Lastly, interdisciplinary research combining combustion science with materials engineering could lead to innovative reactor designs and materials capable of withstanding the unique conditions of  $\text{NH}_3$  MILD combustion.

The modeling of emissions requires further studies and analyses due their complex nature, particularly in instances where  $\text{H}_2$  enrichment is considerable or combustion regimes cannot be approximated with 1D flame structure variations, such as those observed in MILD combustion. The flame morphology can restrict the applicability of models that are commonly used for combustion and emissions predictions. Due to the high complexity of the numerical setup, which incorporates turbulence, radiation, detailed chemistry, and other factors, the precision of emissions predictions is challenging to achieve. Therefore, it is essential to carefully examine the turbulence–chemistry interaction and the impact of supporting models in accordance with experimental data within the turbulent flow field.

In the application of manifold-based reduced chemistry, such as flamelet-generated manifold (FGM) and flamelet/progress variable (FPV), identifying suitable progress variables for predicting  $\text{NO}_x$  emissions is critical to progressing with these methods for the analysis of ammonia combustion. Although different methodologies have been proposed in past decades for hydrocarbon fuels, their validity for ammonia systems mixed with different cofuels still needs to be confirmed. Furthermore, it is also desirable for the use of manifold-based reduced chemistry to be invariant with respect to the choice of progress variables, which can be achieved by using reaction–diffusion manifolds (REDIMs).

The modeling and calculation of  $\text{NO}_x$  emissions in ammonia combustion through CFD is an important requirement for fundamental and practical use due to the complex interaction between chemical kinetics and turbulent flows, which requires a high level of accuracy and precision. The accurate prediction of  $\text{NO}_x$  necessitates the utilization of comprehensive chemical mechanisms that accurately reflect the slower fuel-bound  $\text{NO}_x$  formation pathways, particularly in industrial geometries where the computational costs associated with high-fidelity models such as LES render them unreasonable. Although species transport models offer high accuracy, their computational demands render them unfeasible for large-scale applications. Pretabulated models provide a more computationally efficient alternative; however, they are unable to accurately capture the distinct  $\text{NO}_x$  formation time scales. The potential of emerging hybrid approaches, such as CRN, to achieve a balance between accuracy and efficiency is significant; however, their success is contingent on the ability of the underlying CFD simulation to replicate the essential combustion characteristics. The perspectives include the refinement of these models to enhance  $\text{NO}_x$  prediction accuracy, particularly in lean ammonia–hydrogen blends, while continuing to explore the integration of reduced kinetic mechanisms and advanced turbulence–chemistry interaction models to manage computational resources effectively.

The application of ML to NO<sub>x</sub> prediction in NH<sub>3</sub> combustion systems presents both significant opportunities and challenges. While ML has shown promise in predicting NO<sub>x</sub> emissions for various fuels and combustion systems, its application to NH<sub>3</sub> combustion remains limited, representing a critical research gap. A key challenge lies in acquiring sufficient high-quality data specific to NH<sub>3</sub> combustion, which is essential for developing accurate and robust ML models. Future research should focus on generating comprehensive data sets that capture the complex relationships between operating conditions, fuel compositions, and NO<sub>x</sub> emissions in NH<sub>3</sub>-fueled systems. Additionally, there is a need to extend ML applications beyond steady-state conditions to account for transient engine operations, as demonstrated by recent work on LSTM networks. The development of more sophisticated ML architectures that can integrate multiscale and multiphysics aspects of NH<sub>3</sub> combustion could significantly enhance predictive capabilities. Furthermore, future research directions should explore the combination of ML with traditional CFD and chemical kinetics models to create hybrid approaches that leverage the strengths of both methodologies. This could lead to more accurate and computationally efficient tools for designing and optimizing NH<sub>3</sub> combustion systems. As the field progresses, it will be crucial to develop standardized benchmarks and validation methodologies to ensure the reliability and transferability of ML models across different NH<sub>3</sub> combustion applications. Ultimately, addressing these challenges and pursuing these research directions will be vital to realizing the full potential of ML in advancing NH<sub>3</sub> as a sustainable fuel option while effectively managing NO<sub>x</sub> emissions.

## 8. CONCLUSIONS

Ammonia possesses significant potential as a zero-carbon fuel, offering advantages for hydrogen storage and renewable energy delivery. Its viability for production, preservation, and distribution makes ammonia an appealing option for meeting the requirements of future energy systems geared toward a low-carbon economy. However, widespread adoption of ammonia as a fuel is hindered by challenges such as NO<sub>x</sub> emissions and suboptimal combustion performance, including high ignition point, low combustion speed, and temperature limitations under certain conditions.

This paper provides a comprehensive review of the impacts associated with ammonia combustion. It highlights the existing knowledge gaps that necessitate further research and development to address emission reduction challenges related to NO, N<sub>2</sub>O, unburned ammonia, and carbon monoxide during cofiring. The review also examines recent studies on NO<sub>x</sub> emissions from ammonia flames under different conditions, exploring the pathways through which these emissions occur. Moreover, it emphasizes the need for improving efficiencies to enhance the economic viability of the ammonia combustion technology.

Furthermore, the review delves into the extinction limit of turbulent ammonia flames, discussing influential factors and strategies to promote flame stability. The integration of improved reaction mechanisms, computational models, and a deeper understanding of fundamental phenomena and practical implications associated with ammonia usage enriches this review, making it a valuable resource for disseminating the latest research and developments in the field of ammonia combustion.

## ■ ASSOCIATED CONTENT

### Data Availability Statement

No data is associated with this paper.

## ■ AUTHOR INFORMATION

### Corresponding Authors

**Syed Mashruk** – College of Physical Sciences and Engineering, Cardiff University, Cardiff, Wales CF24 3AA, U.K.;

orcid.org/0000-0002-3049-4932; Email: mashruks@cardiff.ac.uk

**Agustin Valera-Medina** – College of Physical Sciences and Engineering, Cardiff University, Cardiff, Wales CF24 3AA, U.K.; orcid.org/0000-0003-1580-7133;

Email: valeramedina1@cardiff.ac.uk

### Authors

**Hao Shi** – Reaktive Strömungen und Messtechnik (RSM), TU Darmstadt, 64287 Darmstadt, Germany

**Luca Mazzotta** – Department of Astronautical, Electric and Energy Engineering, Sapienza University of Rome, Rome 00184, Italy; Baker Hughes, Firenze 50127, Italy;

orcid.org/0000-0002-2416-3694

**Cihat Emre Ustun** – School of Engineering and Materials Science, Queen Mary University of London, London E1 4NS, U.K.

**B. Aravind** – College of Physical Sciences and Engineering, Cardiff University, Cardiff, Wales CF24 3AA, U.K.

**Roberto Meloni** – Baker Hughes, Firenze 50127, Italy

**Ali Alnasif** – College of Physical Sciences and Engineering, Cardiff University, Cardiff, Wales CF24 3AA, U.K.; Engineering Technical College of Al-Najaf, Al-Furat Al-Awsat Technical University, Najaf 31001, Iraq

**Elena Boulet** – College of Physical Sciences and Engineering, Cardiff University, Cardiff, Wales CF24 3AA, U.K.

**Radoslaw Jankowski** – Institute of Thermal Engineering, Poznan University of Technology, 60-965 Poznan, Poland

**Chuncan Yu** – Institute for Technical Thermodynamics, KIT—Karlsruhe Institute of Technology, 76131 Karlsruhe, Germany; orcid.org/0000-0002-0550-5003

**Mohammad Alnajideen** – College of Physical Sciences and Engineering, Cardiff University, Cardiff, Wales CF24 3AA, U.K.

**Amin Paykani** – School of Engineering and Materials Science, Queen Mary University of London, London E1 4NS, U.K.

**Ulrich Maas** – Institute for Technical Thermodynamics, KIT—Karlsruhe Institute of Technology, 76131 Karlsruhe, Germany

**Rafal Slefarski** – Institute of Thermal Engineering, Poznan University of Technology, 60-965 Poznan, Poland

**Domenico Borello** – Department of Mechanical and Aerospace Engineering, Sapienza University of Rome, Rome 00184, Italy

Complete contact information is available at:

<https://pubs.acs.org/10.1021/acs.energyfuels.4c03381>

### Notes

The authors declare no competing financial interest.

### Biographies

Syed Mashruk is currently working as a lecturer in thermofluids and combustion science at Cardiff University's School of Engineering. He received his Ph.D. from Cardiff University and his M.Sc. and B.Eng. from Cranfield University and the University of Hertfordshire,

respectively. His research is focused on the experimental and numerical characterization of alternative, low-carbon fuels for power generation, as well as in transport industries. He specializes in  $\text{NO}_x$  emissions and advanced optical and laser diagnostic systems.

Hao Shi received his Ph.D. in mechanical engineering from the King Abdullah University of Science and Technology, Saudi Arabia, in 2022. That same year, he was awarded a research fellowship by the Alexander von Humboldt Foundation. Currently, he is a postdoctoral fellow in the RSM, TU Darmstadt, Germany. His research interests include ammonia/hydrogen combustion, renewable energy, engine combustion, and optical diagnostics.

Luca Mazzotta is an energy and combustion engineer and a Ph.D. research student at the Department of Astronautical, Electrical and Energy Engineering at Sapienza University of Rome. His research focuses on hydrogen and ammonia combustion on gas turbine burners in collaboration with Baker Hughes. He specializes in computational fluid dynamics (CFD), analysing  $\text{NO}_x$  formation and combustion dynamics, to optimize thermal performance, emissions, and efficiency.

Cihat Emre Ustun is a Ph.D. researcher at the Intelligent Transport Centre of Queen Mary University of London. He holds an M.Sc. in sustainable energy engineering from the University of the Basque Country. His research focuses on using data-driven models for combustion simulations of low-carbon fuels, aiming to reduce computational requirements. He specializes in machine learning, computational fluid dynamics, combustion, ammonia, and hydrogen.

B. Aravind completed his doctoral research in combustion at the Indian Institute of Technology Bombay in 2020. He then worked as a postdoctoral fellow at CCRC, King Abdullah University of Science and Technology (KAUST), Saudi Arabia, from 2021 to 2023. Currently, he is a research associate at the College of Physical Sciences and Engineering, Cardiff University, U.K., since 2024. His research interests include ammonia swirl flames, thermoacoustic instability, microcombustion, and plasma-assisted combustion.

Roberto Meloni holds a Ph.D. from Sapienza University of Rome and is a senior engineer at Baker Hughes. He has more than 10 years of experience in computational fluid dynamics applied to the combustion sector and in particular to the design of gas turbine combustor. He supports several EU funded projects through Baker Hughes aiming to decarbonize the energy generation sector, namely, TRANSITION (101069665), FLEXnCONFU (884157), and HyPowerGT (101136656).

Ali Alnasif is currently a Ph.D. student at Cardiff University and an active member of the Centre of Excellence on Ammonia Technologies (CEAT). He focuses his research on the combustion characteristics of zero-carbon fuels, emphasizing kinetic chemistry in ammonia flames. His work is crucial for advancing ammonia as a sustainable energy source, particularly in power generation. He has made significant scholarly contributions through various publications in this field.

Elena Boulet's background in astrophysics first led her to work as a satellite test engineer on the interplanetary missions BepiColombo and Solar Orbiter. Following this, she changed her career path to study sustainable energy at Cardiff University. She carried out research on the conversion of a spark ignition engine using alternative fuels such as ammonia and hydrogen to support decarbonization efforts. She is currently a systems engineer.

Radoslaw Jankowski is an assistant professor at the Institute of Thermal Power Engineering at Poznan University of Technology. He has an M.Sc. in mechanical engineering and a Ph.D. in combustion technology from the same University. He has 15 years' experience in

industry as a technologist and designer of energy systems. He is currently working on technologies for the decarbonization of industrial processes, mainly by using alternative gaseous fuels ( $\text{H}_2$ ,  $\text{NH}_3$ ) and improving technological efficiency.

Chuncan Yu is a postdoc at the Karlsruhe Institute of Technology, Institute of Technical Thermodynamics, from which he also obtained his Ph.D. degree. His research interest includes the flame–solid interaction, modeling of reduced chemical kinetics, and PDF modeling for turbulent reacting flows.

Mohammad Alnajideen is the manager of the Centre of Excellence on Ammonia Technologies at Cardiff University and an EPSRC—UKRI Research Associate, leading innovations in alternative fuels for combustion engine systems. With 15 years of experience in renewable energy R&D&I, his expertise spans academia and industry. He has served as an assistant professor and a gas turbine and balance of plant engineer. His work focuses on ammonia–hydrogen fuel blends for net-zero-energy solutions and advancing energy systems.

Amin Paykani is a lecturer in sustainable propulsion systems and the research director at the Centre for Intelligent Transport at Queen Mary University of London (QMUL). Before his role at QMUL, he held academic positions at the University of Hertfordshire and ETH Zurich. His research is primarily focused on studying low-/zero-carbon-energy vectors for the decarbonization of transport. He has been the recipient of several funding grants from EPSRC and the Royal Society.

Ulrich Maas is professor and head of the Institute of Technical Thermodynamics at the Karlsruhe Institute of Technology. He obtained his Ph.D. degree from Heidelberg University, Germany. His research topics cover mathematical modeling of reacting flows and the ignition process and the development of reduction methods for chemical kinetics.

Rafal Slefarski is professor and head of Institute of Thermal Energy at Poznan University of Technology. He holds an M.Sc. in mechanical engineering and a Ph.D. in combustion technology from the same university. Prof. Slefarski has more than 15 years of experience in the theoretical, numerical, and experimental study of combustion processes of nonstandard fuels in industrial applications. He is currently involved in studies related to the use of decarbonized fuels (hydrogen, ammonia) in energy machines and devices.

Domenico Borello is professor of power systems at Sapienza University of Rome. He has an M.Sc. in mechanical engineering and a Ph.D. in power systems from the same university. Domenico has more than 25 years of experience in the field of numerical and experimental study of thermofluid dynamic problems in industrial flows. He is currently involved in several topics pertinent to decarbonization, with a particular interest in alternative fuels, such as ammonia, synthetic natural gas and hydrogen.

Agustin Valera-Medina is professor in combustion and thermofluids at Cardiff University. He has participated as principal investigator/co-investigator on 31 industrial projects attracting >£35M. He has supported two Royal Society Policy Briefings on the use of ammonia and authored the book *Techno-Economic Challenges of Ammonia as an Energy Vector*. He is co-director of the Institute of Net Zero Innovation (CU) and director of the Centre of Excellence on Ammonia Technologies. He is a Fellow of the Learned Society of Wales.

## ■ ACKNOWLEDGMENTS

The authors gratefully acknowledge support from the EPSRC through the program SAFE AGT (EP/T009314/1), Ocean-



REFuel (EP/W005018/1), MariNH<sub>3</sub> (EP/W016656/1), FLEXnCONFU (EU No. 884157), Optimal fuel blends for ammonia fueled thermal propulsion systems (EP/T033800/1), and AMBURN (Fuel Switching II, DESNZ).

## REFERENCES

- (1) Heubaum, H.; Biermann, F. Integrating global energy and climate governance: The changing role of the International Energy Agency. *Energy Policy* **2015**, *87*, 229–239.
- (2) Intergovernmental Panel on Climate Change. Summary for policymakers. In *Climate Change 2007—Mitigation of Climate Change*; Cambridge University Press: 2007; pp 7–22..
- (3) Tol, R. S. J. The Economic Effects of Climate Change. *Journal of Economic Perspectives* **2009**, *23* (2), 29–51.
- (4) Baetcke, L.; Kaltschmitt, M. Hydrogen storage for mobile application: Technologies and their assessment. In *Hydrogen Supply Chains*; Elsevier: 2018; pp 167–206. DOI: 10.1016/B978-0-12-811197-0.00005-1.
- (5) Chai, W. S.; Bao, Y. L.; Jin, P. F.; Tang, G.; Zhou, L. A review on ammonia, ammonia-hydrogen and ammonia-methane fuels. *Renewable & Sustainable Energy Reviews* **2021**, *147*, 111254.
- (6) Kandemir, T.; Schuster, M. E.; Senyshyn, A.; Behrens, M.; Schlögl, R. The Haber-Bosch Process Revisited: On the Real Structure and Stability of "Ammonia Iron" under Working Conditions. *Angew. Chem., Int. Ed.* **2013**, *52* (48), 12723–12726.
- (7) Tian, J.; Wang, L.; Xiong, Y.; Wang, Y. Q.; Yin, W.; Tian, G. H.; Wang, Z. Y.; Cheng, Y.; Ji, S. B. Enhancing combustion efficiency and reducing nitrogen oxide emissions from ammonia combustion: A comprehensive review. *Process Safety and Environmental Protection* **2024**, *183*, 514–543.
- (8) Elbaz, A. M.; Wang, S.; Guiberti, T. F.; Roberts, W. L. Review on the recent advances on ammonia combustion from the fundamentals to the applications. *Fuel Communications* **2022**, *10*, 100053.
- (9) Kobayashi, H.; Hayakawa, A.; Somarathne, K. D. K. A.; Okafor, E. C. Science and technology of ammonia combustion. *Proceedings of the Combustion Institute* **2019**, *37* (1), 109–133.
- (10) Valera-Medina, A.; Xiao, H.; Owen-Jones, M.; David, W. I. F.; Bowen, P. J. Ammonia for power. *Prog. Energy Combust. Sci.* **2018**, *69*, 63–102.
- (11) Jiang, Z.; Zhu, R.; Miyazaki, K.; McDonald, B. C.; Klimont, Z.; Zheng, B.; Boersma, K. F.; Zhang, Q.; Worden, H.; Worden, J. R.; et al. Decadal Variabilities in Tropospheric Nitrogen Oxides Over United States, Europe, and China. *Journal of Geophysical Research-Atmospheres* **2022**, *127* (3), No. e2021JD035872.
- (12) de Diego, L. F.; Londono, C. A.; Wang, X. S.; Gibbs, B. M. Influence of operating parameters on NO<sub>x</sub> and N<sub>2</sub>O axial profiles in a circulating fluidized bed combustor. *Fuel* **1996**, *75* (8), 971–978.
- (13) Mashruk, S.; Kovaleva, M.; Alnasif, A.; Chong, C. T.; Hayakawa, A.; Okafor, E. C.; Valera-Medina, A. Nitrogen oxide emissions analyses in ammonia/hydrogen/air premixed swirling flames. *Energy* **2022**, *260*, 125183.
- (14) Vitousek, P. M.; Aber, J. D.; Howarth, R. W.; Likens, G. E.; Matson, P. A.; Schindler, D. W.; Schlesinger, W. H.; Tilman, D. Human alteration of the global nitrogen cycle: Sources and consequences. *Ecological Applications* **1997**, *7* (3), 737–750.
- (15) Swain, W.; Colborn, T.; Bason, C.; Howarth, R.; Lamey, L.; Palmer, B.; Swackhamer, D.; U.S. EPA. Exposure and effects of airborne contamination. In *Report to Great Waters Program*; U.S. EPA: Washington DC, 1992.
- (16) Price, D.; Birnbaum, R.; Batiuk, R.; McCullough, M.; Smith, R. *Nitrogen Oxides: Impacts on Public Health and the Environment*; U.S. Environmental Protection Agency: Washington, DC, 1997.
- (17) Neubauer, S. C. Global warming potential is not an ecosystem property. *Ecosystems* **2021**, *24* (8), 2079–2089.
- (18) Zhu, X.; Khateeb, A. A.; Guiberti, T. F.; Roberts, W. L. NO and OH\* emission characteristics of very-lean to stoichiometric ammonia-hydrogen-air swirl flames. *Proceedings of the Combustion Institute* **2021**, *38* (4), 5155–5162.
- (19) Newhall, H. K.; Starkman, E. S. Theoretical Performance of Ammonia as a Gas Turbine Fuel. *SAE Transactions* **1967**, *75*, 772–784.
- (20) Pratt, D. T. *Performance of Ammonia-Fired Gas-Turbine Combustors*; University of California, Berkeley: 1967.
- (21) Verkamp, F.; Hardin, M.; Williams, J. Ammonia combustion properties and performance in gas-turbine burners. *Symposium (International) on Combustion* **1967**, *11*, 985–992.
- (22) Bull, M. *Development of an Ammonia-Burning Gas Turbine Engine*; Defense Technical Information Center: 1968.
- (23) Kailos, N. C. *Utilization of Ammonia as an Alternate Fuel in Army Aircraft Engines*; U.S. Army Aviation Materiel Laboratories: 1966.
- (24) X-15 Hypersonic Research Program. *Encyclopedia, NASA*, February 28, 2014. <https://www.nasa.gov/reference/x-15/>.
- (25) Seaman, R. W.; Huson, G. The choice of NH<sub>3</sub> to fuel the X-15 rocket plane. Presented at the 8th NH<sub>3</sub> Fuel Association Conference, 2011.
- (26) Lieuwen, T. C.; Yang, V. *Gas Turbine Emissions*; Cambridge University Press: 2013.
- (27) *Ammonia as a power generation fuel*. GE Vernova, 2021. [https://www.governova.com/content/dam/gepower-new/global/en\\_US/images/gas-new-site/future-of-energy/GEA34985-ammonia-power-gen.pdf](https://www.governova.com/content/dam/gepower-new/global/en_US/images/gas-new-site/future-of-energy/GEA34985-ammonia-power-gen.pdf).
- (28) Pochet, M.; Jeanmart, H.; Contino, F. A 22:1 Compression Ratio Ammonia-Hydrogen HCCI Engine: Combustion, Load, and Emission Performances. *Front Mech Eng-Switz* **2020**, *6*, 43.
- (29) Hayakawa, A.; Arakawa, Y.; Mimoto, R.; Somarathne, K. D. K. A.; Kudo, T.; Kobayashi, H. Experimental investigation of stabilization and emission characteristics of ammonia/air premixed flames in a swirl combustor. *Int. J. Hydrogen Energy* **2017**, *42* (19), 14010–14018.
- (30) Mashruk, S.; Shi, H.; Zitouni, S.-E.; Valera-Medina, A. Nitrogen Oxide Emissions in Ammonia Combustion. In *Ammonia and Hydrogen for Green Energy Transition*; Springer: 2024; pp 289–328.
- (31) Lindstedt, R. P.; Lockwood, F. C.; Selim, M. A. Detailed Kinetic Modeling of Chemistry and Temperature Effects on Ammonia Oxidation. *Combust. Sci. Technol.* **1994**, *99* (4–6), 253–276.
- (32) Sullivan, N.; Jensen, A.; Glarborg, P.; Day, M. S.; Grcar, J. F.; Bell, J. B.; et al. Ammonia conversion and NO formation in laminar coflowing nonpremixed methane-air flames. *Combust. Flame* **2002**, *131* (3), 285–298.
- (33) Lee, J. H.; Kim, J. H.; Park, J. H.; Kwon, O. C. Studies on properties of laminar premixed hydrogen-added ammonia/air flames for hydrogen production. *Int. J. Hydrogen Energy* **2010**, *35* (3), 1054–1064.
- (34) Hayakawa, A.; Hayashi, M.; Kovaleva, M.; Gotama, G. J.; Okafor, E. C.; Colson, S.; Mashruk, S.; Valera-Medina, A.; Kudo, T.; Kobayashi, H. Experimental and numerical study of product gas and N<sub>2</sub>O emission characteristics of ammonia/hydrogen/air premixed laminar flames stabilized in a stagnation flow. *Proceedings of the Combustion Institute* **2023**, *39* (2), 1625–1633.
- (35) Wang, S. X.; Wang, Z. H.; Elbaz, A. M.; Han, X. L.; He, Y.; Costa, M.; Konnov, A. A.; Roberts, W. L. Experimental study and kinetic analysis of the laminar burning velocity of NH<sub>3</sub>/syngas/air, NH<sub>3</sub>/CO/air and NH<sub>3</sub>/H<sub>2</sub>/air premixed flames at elevated pressures. *Combust. Flame* **2020**, *221*, 270–287.
- (36) Mei, B. W.; Zhang, J. G.; Shi, X. X.; Xi, Z. Y.; Li, Y. Y. Enhancement of ammonia combustion with partial fuel cracking strategy: Laminar flame propagation and kinetic modeling investigation of NH<sub>3</sub>/H<sub>2</sub>/N<sub>2</sub> /air mixtures up to 10 atm. *Combust. Flame* **2021**, *231*, 111472.
- (37) Zheng, S.; He, Y. Z.; Hu, B.; Zhu, J. J.; Zhou, B.; Lu, Q. Effects of radiation reabsorption on the flame speed and NO emission of NH<sub>3</sub>/H<sub>2</sub>/air flames at various hydrogen ratios. *Fuel* **2022**, *327*, 125176.
- (38) Nawaz, B.; Nasim, M. N.; Das, S. K.; Landis, J.; Sublaban, A.; Trelles, J. P.; Assanis, D.; Van Dam, N.; Mack, J. H. Combustion characteristics and emissions of nitrogen oxides (NO, NO<sub>2</sub>, NO) from

- spherically expanding laminar flames of ammonia-hydrogen blends. *Int. J. Hydrogen Energy* **2024**, *49*, 164–176.
- (39) Alnasif, A.; Jójka, J.; Mashruk, S.; Nagy, T.; Valera-Medina, A. Analysis of the performance of kinetic reaction mechanisms in estimating N<sub>2</sub>O mole fractions in 70/30 vol% NH<sub>3</sub>/H<sub>2</sub> premixed flames. *Fuel* **2024**, *371*, 131897.
- (40) Ariemma, G. B.; Sorrentino, G.; Ragucci, R.; de Joannon, M.; Sabia, P. Ammonia/Methane combustion: Stability and NO emissions. *Combust. Flame* **2022**, *241*, 112071.
- (41) Kovaleva, M.; Hayakawa, A.; Colson, S.; Okafor, E. C.; Kudo, T.; Valera-Medina, A.; Kobayashi, H. Numerical and experimental study of product gas characteristics in premixed ammonia/methane/air laminar flames stabilised in a stagnation flow. *Fuel Communications* **2022**, *10*, 100054.
- (42) Okafor, E. C.; Naito, Y.; Colson, S.; Ichikawa, A.; Kudo, T.; Hayakawa, A.; Kobayashi, H. Experimental and numerical study of the laminar burning velocity of CH-NH-air premixed flames. *Combust. Flame* **2018**, *187*, 185–198.
- (43) Wang, S.; Wang, Z.; Chen, C.; Elbaz, A. M.; Sun, Z.; Roberts, W. L. Applying heat flux method to laminar burning velocity measurements of NH<sub>3</sub>/CH<sub>4</sub>/air at elevated pressures and kinetic modeling study. *Combust. Flame* **2022**, *236*, 111788.
- (44) Woo, M.; Choi, B. C.; Ghoniem, A. F. Experimental and numerical studies on NO emission characteristics in laminar non-premixed jet flames of ammonia-containing methane fuel with oxygen/nitrogen oxidizer. *Energy* **2016**, *114*, 961–972.
- (45) Mei, B. W.; Zhang, X. Y.; Ma, S. Y.; Cui, M. L.; Guo, H. W.; Cao, Z. H.; Li, Y. Y. Experimental and kinetic modeling investigation on the laminar flame propagation of ammonia under oxygen enrichment and elevated pressure conditions. *Combust. Flame* **2019**, *210*, 236–246.
- (46) Meng, X. Y.; Zhang, M. K.; Zhao, C. H.; Tian, H.; Tian, J. P.; Long, W. Q.; Bi, M. S. Study of combustion and NO chemical reaction mechanism in ammonia blended with DME. *Fuel* **2022**, *319*, 123832.
- (47) Yu, M.; Luo, G.; Sun, R.; Qiu, W.; Chen, L.; Wang, L.; Hu, Z.; Li, X.; Yao, H. Experimental and numerical study on emission characteristics of NH<sub>3</sub>/DME/air flames in a premixed burner. *Combust. Flame* **2024**, *259*, 113098.
- (48) Alekseev, V. A.; Brackmann, C.; Liu, X.; Nilsson, E. J. K. Nitric oxide formation in flames of NH<sub>3</sub>/DME binary mixtures: Laser-induced fluorescence measurements and detailed kinetic analysis. *Fuel* **2024**, *371*, 131951.
- (49) Zhou, S.; Cui, B.; Yang, W.; Tan, H.; Wang, J.; Dai, H.; Li, L.; ur Rahman, Z.; Wang, X.; Deng, S.; Wang, X. An experimental and kinetic modeling study on NH<sub>3</sub>/air, NH<sub>3</sub>/H<sub>2</sub>/air, NH<sub>3</sub>/CO/air, and NH<sub>3</sub>/CH<sub>4</sub>/air premixed laminar flames at elevated temperature. *Combust. Flame* **2023**, *248*, 112536.
- (50) Filipe Ramos, C.; Rocha, R. C.; Oliveira, P. M. R.; Costa, M.; Bai, X. S. Experimental and kinetic modelling investigation on NO, CO and NH emissions from NH/CH/air premixed flames. *Fuel* **2019**, *254*, 115693.
- (51) Thomas, D. E.; Wadkar, C.; Goertemiller, C. F.; Northrop, W. F. Structure and nitric oxide formation in laminar diffusion flames of ammonia-hydrogen and air. *Fuel* **2024**, *362*, 130764.
- (52) Wang, S.; Wang, Z.; Roberts, W. L. Measurements and simulations on effects of elevated pressure and strain rate on NO<sub>x</sub> emissions in laminar premixed NH<sub>3</sub>/CH<sub>4</sub>/air and NH<sub>3</sub>/H<sub>2</sub>/air flames. *Fuel* **2024**, *357*, 130036.
- (53) Klippenstein, S. J.; Harding, L. B.; Glarborg, P.; Miller, J. A. The role of NNH in NO formation and control. *Combust. Flame* **2011**, *158* (4), 774–789.
- (54) Hayakawa, A.; Goto, T.; Mimoto, R.; Kudo, T.; Kobayashi, H. NO formation/reduction mechanisms of ammonia/air premixed flames at various equivalence ratios and pressures. *Mechanical Engineering Journal* **2015**, *2* (1), 14-00402.
- (55) Glarborg, P.; Miller, J. A.; Ruscic, B.; Klippenstein, S. J. Modeling nitrogen chemistry in combustion. *Prog. Energy Combust. Sci.* **2018**, *67*, 31–68.
- (56) Pugh, D.; Valera-Medina, A.; Bowen, P.; Giles, A.; Goktepe, B.; Runyon, J.; Morris, S.; Hewlett, S.; Marsh, R. Emissions Performance of Staged Premixed and Diffusion Combustor Concepts for an NH<sub>3</sub>/Air Flame With and Without Reactant Humidification. *Journal of Engineering for Gas Turbines and Power-Transactions of the Asme* **2021**, *143* (5), 051012.
- (57) Okafor, E. C.; Tsukamoto, M.; Hayakawa, A.; Somarathne, K. D. K. A.; Kudo, T.; Tsujimura, T.; Kobayashi, H. Influence of wall heat loss on the emission characteristics of premixed ammonia-air swirling flames interacting with the combustor wall. *Proceedings of the Combustion Institute* **2021**, *38* (4), 5139–5146.
- (58) Okafor, E. C.; Kurata, O.; Yamashita, H.; Inoue, T.; Tsujimura, T.; Iki, N.; Hayakawa, A.; Ito, S.; Uchida, M.; Kobayashi, H. Liquid ammonia spray combustion in two-stage micro gas turbine combustors at 0.25 MPa; Relevance of combustion enhancement to flame stability and NO<sub>x</sub> control. *Applications in Energy and Combustion Science* **2021**, *7*, 100038.
- (59) Liu, Z.; Zhang, Y.; Li, W.; Shi, X.; Li, Y. Self-promoted fuel pyrolysis under oxygen enrichment enables clean and efficient ammonia combustion. *Innovation Energy* **2024**, *1* (1), 100006.
- (60) Kim, H. K.; Ku, J. W.; Ahn, Y. J.; Kim, Y. H.; Kwon, O. C. Effects of O enrichment on NH<sub>3</sub>/air flame propagation and emissions. *Int. J. Hydrogen Energy* **2021**, *46* (46), 23916–23926.
- (61) Tian, Z. Y.; Li, Y. Y.; Zhang, L. D.; Glarborg, P.; Qi, F. An experimental and kinetic modeling study of premixed NH/CH/O/Air flames at low pressure. *Combust. Flame* **2009**, *156* (7), 1413–1426.
- (62) Mendiara, T.; Glarborg, P. Ammonia chemistry in oxy-fuel combustion of methane. *Combust. Flame* **2009**, *156* (10), 1937–1949.
- (63) Valera-Medina, A.; Marsh, R.; Runyon, J.; Pugh, D.; Beasley, P.; Hughes, T.; Bowen, P. Ammonia-methane combustion in tangential swirl burners for gas turbine power generation. *Applied Energy* **2017**, *185*, 1362–1371.
- (64) Xiao, H.; Valera-Medina, A.; Bowen, P. J. Study On premixed combustion characteristics of co-firing ammonia/methane fuels. *Energy* **2017**, *140*, 125–135.
- (65) Li, S.; Zhang, S. S.; Zhou, H.; Ren, Z. Y. Analysis of air-staged combustion of NH/CH mixture with low NO emission at gas turbine conditions in model combustors. *Fuel* **2019**, *237*, 50–59.
- (66) Okafor, E. C.; Somarathne, K. D. K. A.; Rathanan, R.; Hayakawa, A.; Kudo, T.; Kurata, O.; Iki, N.; Tsujimura, T.; Furutani, H.; Kobayashi, H. Control of NO<sub>x</sub> and other emissions in micro gas turbine combustors fuelled with mixtures of methane and ammonia. *Combust. Flame* **2020**, *211*, 406–416.
- (67) Zhang, M.; An, Z. H.; Wei, X. T.; Wang, J. H.; Huang, Z. H.; Tan, H. Z. Emission analysis of the CH<sub>4</sub>/NH<sub>3</sub>/air co-firing fuels in a model combustor. *Fuel* **2021**, *291*, 120135.
- (68) An, Z. H.; Zhang, M.; Zhang, W. J.; Mao, R. Z.; Wei, X. T.; Wang, J. H.; Huang, Z. H.; Tan, H. Z. Emission prediction and analysis on CH/NH/air swirl flames with LES-FGM method. *Fuel* **2021**, *304*, 121370.
- (69) Zhang, M.; An, Z. H.; Wang, L.; Wei, X. T.; Jianayihan, B.; Wang, J. H.; Huang, Z. H.; Tan, H. Z. The regulation effect of methane and hydrogen on the emission characteristics of ammonia/air combustion in a model combustor. *Int. J. Hydrogen Energy* **2021**, *46* (40), 21013–21025.
- (70) Otomo, J.; Koshi, M.; Mitsumori, T.; Iwasaki, H.; Yamada, K. Chemical kinetic modeling of ammonia oxidation with improved reaction mechanism for ammonia/air and ammonia/hydrogen/air combustion. *Int. J. Hydrogen Energy* **2018**, *43* (5), 3004–3014.
- (71) Kurata, O.; Iki, N.; Matsunuma, T.; Inoue, T.; Suzuki, M.; Tsujimura, T.; Furutani, H. Power generation by a micro gas turbine firing kerosene and ammonia. In *The Proceedings of the International Conference on Power Engineering (ICOPE)*, 2015.12; The Japan Society of Mechanical Engineers: 2015; paper ICOPE-15-1139.
- (72) Xiao, H.; Lai, S. N.; Valera-Medina, A.; Li, J. Y.; Liu, J. Y.; Fu, H. D. Study on counterflow premixed flames using high concentration ammonia mixed with methane. *Fuel* **2020**, *275*, 117902.
- (73) Somarathne, K. D. K. A.; Okafor, E. C.; Sugawara, D.; Hayakawa, A.; Kobayashi, H. Effects of OH concentration and

- temperature on NO emission characteristics of turbulent non-premixed CH<sub>4</sub>/NH<sub>3</sub>/air flames in a two-stage gas turbine like combustor at high pressure. *Proceedings of the Combustion Institute* **2021**, *38* (4), 5163–5170.
- (74) Mashruk, S.; Viguera-Zuniga, M. O.; Tejada-del-Cueto, M. E.; Xiao, H.; Yu, C.; Maas, U.; Valera-Medina, A. Combustion features of CH<sub>4</sub>/NH<sub>3</sub>/H<sub>2</sub> blends. *Int. J. Hydrogen Energy* **2022**, *47* (70), 30315–30327.
- (75) Yu, M.; Luo, G.; Sun, R.; Wang, L.; Li, X.; Yao, H. Experimental and numerical study on NO<sub>x</sub> reduction from NH<sub>3</sub>/DME/air flame using fuel staging method. *Fuel* **2024**, *372*, 132100.
- (76) Lian, T. Y.; Shi, X. X.; Han, S. B.; Zhang, Y.; Liu, Z. D.; Xi, Z. Y.; Li, W.; Li, Y. Y. Unraveling the impact of CO<sub>2</sub> exhaust gas recirculation on flame characteristics and NO<sub>x</sub> emissions of premixed NH<sub>3</sub>/DME swirl flames. *Applications in Energy and Combustion Science* **2024**, *17*, 100256.
- (77) Joo, J. M.; Lee, S.; Kwon, O. C. Effects of ammonia substitution on combustion stability limits and NO emissions of premixed hydrogen-air flames. *Int. J. Hydrogen Energy* **2012**, *37* (8), 6933–6941.
- (78) Li, J.; Huang, H. Y.; Kobayashi, N.; He, Z. H.; Nagai, Y. Study on using hydrogen and ammonia as fuels: Combustion characteristics and NO formation. *International Journal of Energy Research* **2014**, *38* (9), 1214–1223.
- (79) Valera-Medina, A.; Pugh, D. G.; Marsh, P.; Bulat, G.; Bowen, P. Preliminary study on lean premixed combustion of ammonia-hydrogen for swirling gas turbine combustors. *Int. J. Hydrogen Energy* **2017**, *42* (38), 24495–24503.
- (80) Xiao, H.; Valera-Medina, A. Chemical Kinetic Mechanism Study on Premixed Combustion of Ammonia/Hydrogen Fuels for Gas Turbine Use. *Journal of Engineering for Gas Turbines and Power-Transactions of the ASME* **2017**, *139* (8), 081504.
- (81) Xiao, H.; Valera-Medina, A.; Bowen, P. J. Modeling Combustion of Ammonia/Hydrogen Fuel Blends under Gas Turbine Conditions. *Energy Fuels* **2017**, *31* (8), 8631–8642.
- (82) Khateeb, A. A.; Guiberti, T. F.; Zhu, X. R.; Younes, M.; Jamal, A.; Roberts, W. L. Stability limits and NO emissions of technically-premixed ammonia-hydrogen-nitrogen-air swirl flames. *Int. J. Hydrogen Energy* **2020**, *45* (41), 22008–22018.
- (83) Mashruk, S.; Okafor, E. C.; Kovaleva, M.; Alnasif, A.; Pugh, D.; Hayakawa, A.; Valera-Medina, A. Evolution of N<sub>2</sub>O production at lean combustion condition in NH<sub>3</sub>/H<sub>2</sub>/air premixed swirling flames. *Combust. Flame* **2022**, *244*, 112299.
- (84) Pugh, D.; Bowen, P.; Valera-Medina, A.; Giles, A.; Runyon, J.; Marsh, R. Influence of steam addition and elevated ambient conditions on NO<sub>x</sub> reduction in a staged premixed swirling NH<sub>3</sub>/H<sub>2</sub> flame. *Proceedings of the Combustion Institute* **2019**, *37* (4), 5401–5409.
- (85) Mashruk, S.; Xiao, H.; Valera-Medina, A. Rich-Quench-Lean model comparison for the clean use of humidified ammonia/hydrogen combustion systems. *Int. J. Hydrogen Energy* **2021**, *46* (5), 4472–4484.
- (86) Mashruk, S.; Kovaleva, M.; Chong, C. T.; Hayakawa, A.; Okafor, E. C.; Valera-Medina, A. Nitrogen oxides as a by-product of ammonia/hydrogen combustion regimes. *Chemical Engineering Transactions* **2021**, *89*, 613–618.
- (87) Gutesa Božo, M. G.; Mashruk, S.; Zitouni, S.; Valera-Medina, A. Humidified ammonia/hydrogen RQL combustion in a trigeneration gas turbine cycle. *Energy Conversion and Management* **2021**, *227*, 113625.
- (88) Mashruk, S.; Xiao, H.; Pugh, D.; Chiong, M.-C.; Runyon, J.; Goktepe, B.; Giles, A.; Valera-Medina, A. Numerical analysis on the evolution of NH<sub>2</sub> in ammonia/hydrogen swirling flames and detailed sensitivity analysis under elevated conditions. *Combust. Sci. Technol.* **2023**, *195* (6), 1251–1278.
- (89) Shi, X. X.; Lian, T. Y.; Zhang, Y.; Liu, Z. D.; Li, W.; Xi, Z. Y.; Li, Y. Y. Enhanced ammonia combustion by partial pre-cracking strategy in a gas turbine model combustor: Flame macrostructures, lean blowout characteristics and exhaust emissions. *Applications in Energy and Combustion Science* **2024**, *17*, 100247.
- (90) Cui, M. S.; Niu, F.; Ji, R. S.; Duan, L.; Zhang, X. Experimental Study on Flame Chemical Composition of Coal and Ammonia Gas-Solid Jet in Flat Flame Burner. *ACS Omega* **2024**, *9* (10), 11769–11779.
- (91) Chen, P.; Gong, C.; Hua, C. H.; Gu, M. Y.; Jiang, B. Y.; Fan, J. R.; Wang, Y. Mechanism analysis of fuel-N oxidation during ammonia-coal co-combustion: Influence of H<sub>2</sub>O. *Fuel* **2023**, *342*, 127747.
- (92) Jeon, M.; Lee, E. S.; Kim, M.; Jegal, H.; Park, S.; Chi, J. H.; Baek, S.; Lee, J. M.; Keel, S. I. Nitric oxide (NO) and nitrous oxide (N<sub>2</sub>O) emissions during selective non-catalytic reduction and selective catalytic reduction processes in a pulverized coal/Ammonia Co-fired boiler. *Journal of Environmental Chemical Engineering* **2023**, *11* (2), 109398.
- (93) Fan, W. D.; Wu, X. F.; Guo, H.; Zhu, J. T.; Liu, P.; Chen, C.; Wang, Y. Experimental study on the impact of adding NH<sub>3</sub> on NO production in coal combustion and the effects of char, coal ash, and additives on NH<sub>3</sub> reducing NO under high temperature. *Energy* **2019**, *173*, 109–120.
- (94) Chen, P.; Jiang, B.; Wang, H.; Gu, M.; Fang, Y.; Wang, P. Experimental and theoretical calculations study on heterogeneous reduction of NO by char/NH<sub>3</sub> in the reduction zone of ammonia co-firing with pulverized coal: Influence of mineral Fe. *Fuel* **2022**, *310*, 122374.
- (95) Ishihara, S.; Zhang, J. W.; Ito, T. Numerical calculation with detailed chemistry on ammonia co-firing in a coal-fired boiler: Effect of ammonia co-firing ratio on NO emissions. *Fuel* **2020**, *274*, 117742.
- (96) Ishihara, S.; Zhang, J.; Ito, T. Numerical calculation with detailed chemistry of effect of ammonia co-firing on NO emissions in a coal-fired boiler. *Fuel* **2020**, *266*, 116924.
- (97) Jiang, B. Experimental Study on NO Formation Characteristics of Ammonia-coal Co-combustion. *Proceedings of the CSEE* **2023**, *43* (17), 6746–6755.
- (98) Niu, T.; Zhang, W.; Liu, X.; Hu, D.; Wang, T.; Xie, Y.; Wang, H. Industrial-scale experimental investigation of ammonia-coal cofiring in coal-fired boiler. *Clean Coal Technol.* **2022**, *28* (3), 193–200.
- (99) Ju, Y. G.; Sun, W. T. Plasma assisted combustion: Dynamics and chemistry. *Prog. Energy Combust. Sci.* **2015**, *48*, 21–83.
- (100) Aravind, B.; Yu, L.; Lacoste, D. Enhancement of lean blowout limits of swirl stabilized NH<sub>3</sub>-CH<sub>4</sub>-Air flames using nanosecond repetitively pulsed discharges at elevated pressures. *Applications in Energy and Combustion Science* **2023**, *16*, 100225.
- (101) Shah, Z. A.; Mehdi, G.; Congedo, P. M.; Mazzeo, D.; De Giorgi, M. G. A review of recent studies and emerging trends in plasma-assisted combustion of ammonia as an effective hydrogen carrier. *Int. J. Hydrogen Energy* **2024**, *51*, 354–374.
- (102) Radwan, A. M.; Paul, M. C. Plasma assisted NH<sub>3</sub> combustion and NO<sub>x</sub> reduction technologies: Principles, challenges and prospective. *Int. J. Hydrogen Energy* **2024**, *52*, 819–833.
- (103) Choe, J.; Sun, W. T.; Ombrello, T.; Carter, C. Plasma assisted ammonia combustion: Simultaneous NO reduction and flame enhancement. *Combust. Flame* **2021**, *228*, 430–432.
- (104) Miller, J. A.; Pilling, M. J.; Troe, E. Unravelling combustion mechanisms through a quantitative understanding of elementary reactions. *Proceedings of the Combustion Institute* **2005**, *30* (1), 43–88.
- (105) Tang, Y.; Xie, D. J.; Shi, B. L.; Wang, N. F.; Li, S. Q. Flammability enhancement of swirling ammonia/air combustion using AC powered gliding arc discharges. *Fuel* **2022**, *313*, 122674.
- (106) Kim, G. T.; Park, J.; Chung, S. H.; Yoo, C. S. Effects of non-thermal plasma on turbulent premixed flames of ammonia/air in a swirl combustor. *Fuel* **2022**, *323*, 124227.
- (107) Lin, Q. F.; Jiang, Y. M.; Liu, C. Z.; Chen, L. W.; Zhang, W. J.; Ding, J.; Li, J. G. Controllable NO emission and high flame performance of ammonia combustion assisted by non-equilibrium plasma. *Fuel* **2022**, *319*, 123818.
- (108) Mao, X.; Zhong, H.; Liu, N.; Wang, Z.; Ju, Y. Ignition enhancement and NO<sub>x</sub> formation of NH<sub>3</sub>/air mixtures by non-equilibrium plasma discharge. *Combust. Flame* **2024**, *259*, 113140.



- (109) Zhong, H. T.; Mao, X. Q.; Liu, N.; Wang, Z. Y.; Ombrello, T.; Ju, Y. G. Understanding non-equilibrium NO/NO<sub>2</sub> chemistry in plasma-assisted low-temperature NH<sub>3</sub> oxidation. *Combust. Flame* **2023**, *256*, 112948.
- (110) Kim, G. T.; Park, J.; Chung, S. H.; Yoo, C. S. Synergistic effect of non-thermal plasma and CH<sub>4</sub> addition on turbulent NH<sub>3</sub>/air premixed flames in a swirl combustor. *Int. J. Hydrogen Energy* **2024**, *49*, 521–532.
- (111) Koch, E. Ammonia-a fuel for motor buses. *J. Inst. Pet.* **1945**, *31*, 213–223.
- (112) Cornelius, W.; Huellmantel, L. W.; Mitchell, H. R. Ammonia as an engine fuel. *SAE Transactions* **1966**, *74*, 300–326.
- (113) Starkman, E. S.; Newhall, H.; Sutton, R.; Maguire, T.; Farbar, L. Ammonia as a Spark Ignition Engine Fuel - Theory and Application. *SAE Transactions* **1967**, *75*, 765–784. <https://www.jstor.org/stable/44563674>. Sawyer, R. F.; Starkman, E. S.; Muzio, L.; Schmidt, W. Oxides of nitrogen in the combustion products of an ammonia fueled reciprocating engine. *SAE Technical Paper* 1968; no. 680401..
- (114) Pearsall, T. *Ammonia Application to Reciprocating Engines*; Continental Aviation and Engineering Corp.: 1967.
- (115) Starkman, E. S.; James, G. E.; Newhall, H. K. Ammonia as a Diesel Engine Fuel - Theory and Application. *SAE Transactions* **1968**, *76*, 3193 [jstor.org/stable/44562852](https://www.jstor.org/stable/44562852).
- (116) *Get to know the Wärtsilä 25 Ammonia*. Wärtsilä, May 6, 2024. <https://www.wartsila.com/about/190/article/get-to-know-the-wartsila-25-ammonia>.
- (117) Tan, F. *MAN Energy Solutions to offer ammonia-fuelled ship engines after 2027*. Reuters, March 3, 2024. <https://www.reuters.com/business/energy/man-energy-solutions-offer-ammonia-fuelled-ship-engines-after-2027-2024-03-04/>.
- (118) Mounaïm-Rousselle, C.; Bréquigny, P.; Medina, A. V.; Boulet, E.; Emberson, D.; Lovås, T. Ammonia as fuel for transportation to mitigate zero carbon impact. *Engines and Fuels for Future Transport* **2022**, *257*–279.
- (119) Dimitriou, P.; Javid, R. A review of ammonia as a compression ignition engine fuel. *Int. J. Hydrogen Energy* **2020**, *45* (11), 7098–7118.
- (120) Chiong, M. C.; Chong, C. T.; Ng, J. H.; Mashruk, S.; Chong, W. W. F.; Samiran, N. A.; Mong, G. R.; Valera-Medina, A. Advancements of combustion technologies in the ammonia-fuelled engines. *Energy Conversion and Management* **2021**, *244*, 114460.
- (121) Grannell, S. M.; Assanis, D. N.; Bohac, S. V.; Gillespie, D. E. The fuel mix limits and efficiency of a stoichiometric, ammonia, and gasoline dual fueled spark ignition engine. *Journal of Engineering for Gas Turbines and Power* **2008**, *130* (4), 042802.
- (122) Ryu, K.; Zacharakis-Jutz, G. E.; Kong, S. C. Performance enhancement of ammonia-fueled engine by using dissociation catalyst for hydrogen generation. *Int. J. Hydrogen Energy* **2014**, *39* (5), 2390–2398.
- (123) Verhelst, S.; Turner, J. W. G.; Sileghem, L.; Vancoillie, J. Methanol as a fuel for internal combustion engines. *Prog. Energy Combust. Sci.* **2019**, *70*, 43–88.
- (124) Mounaïm-Rousselle, C.; Bréquigny, P. Ammonia as fuel for low-carbon spark-ignition engines of tomorrow's passenger cars. *Frontiers in Mechanical Engineering* **2020**, *6*, 70.
- (125) Lhuillier, C.; Bréquigny, P.; Contino, F.; Rousselle, C. Combustion characteristics of ammonia in a modern spark-ignition engine. *SAE Technical Paper* 2019; no. 2019-24-0237..
- (126) Mounaïm-Rousselle, C.; Bréquigny, P.; Dumand, C.; Houillé, S. Operating limits for ammonia fuel spark-ignition engine. *Energies* **2021**, *14* (14), 4141.
- (127) Frigo, S.; Gentili, R. Analysis of the behaviour of a 4-stroke Si engine fuelled with ammonia and hydrogen. *Int. J. Hydrogen Energy* **2013**, *38* (3), 1607–1615.
- (128) Bréquigny, P.; Pacaud, E.; Mounaïm-Rousselle, C. Combustion of a syngas from sewage sludge gasification enriched with ammonia in a spark-ignition engine. Presented at the 30th European Biomass Conference and Exhibition (EUBCE), 2022.
- (129) Lhuillier, C.; Bréquigny, P.; Contino, F.; Rousselle, C. Performance and emissions of an ammonia-fueled SI engine with hydrogen enrichment. *SAE Technical Paper* 2019; no. 2019-24-0137..
- (130) Koike, M.; Miyagawa, H.; Suzuoki, T.; Ogasawara, K. Ammonia as a hydrogen energy carrier and its application to internal combustion engines. *Sustainable Vehicle Technologies: Driving the Green Agenda* **2012**, 61–70.
- (131) Westlye, F. R.; Ivarsson, A.; Schramm, J. Experimental investigation of nitrogen based emissions from an ammonia fueled SI-engine. *Fuel* **2013**, *111*, 239–247.
- (132) Mørch, C. S.; Bjerre, A.; Gøttrup, M. P.; Sorenson, S. C.; Schramm, J. Ammonia/hydrogen mixtures in an SI-engine: Engine performance and analysis of a proposed fuel system. *Fuel* **2011**, *90* (2), 854–864.
- (133) Grannell, S. M.; Assanis, D. N.; Gillespie, D. E.; Bohac, S. V. Exhaust emissions from a stoichiometric, ammonia and gasoline dual fueled spark ignition engine. In *Internal Combustion Engine Division Spring Technical Conference*; ASME: 2009; pp 135–141. Woo, Y.; Jang, J.; Lee, Y.; Kim, J. Recent progress on the ammonia-gasoline and the ammonia-diesel dual fueled internal combustion engines in Korea. In *Proceedings of the 11th NH3 Fuel Conference*; NH3 Fuel Association: 2014; pp 21–24.
- (134) Oh, S.; Park, C.; Kim, S.; Kim, Y.; Choi, Y.; Kim, C. Natural gas-ammonia dual-fuel combustion in spark-ignited engine with various air-fuel ratios and split ratios of ammonia under part load condition. *Fuel* **2021**, *290*, 120095.
- (135) Pearsall, T. J.; Garabedian, C. G. Combustion of anhydrous ammonia in diesel engines. *SAE Transactions* **1968**, *76*, 3213–3221.
- (136) Niki, Y. Experimental investigation of effects of split diesel-pilot injection on emissions from ammonia-diesel dual fuel engine. In *Internal Combustion Engine Division Fall Technical Conference*; ASME: 2021; no. V001T001A002.
- (137) Nadimi, E.; Przybyła, G.; Lewandowski, M. T.; Adamczyk, W. Effects of ammonia on combustion, emissions, and performance of the ammonia/diesel dual-fuel compression ignition engine. *Journal of the Energy Institute* **2023**, *107*, 101158.
- (138) Niki, Y. Reductions in Unburned Ammonia and Nitrous Oxide Emissions From an Ammonia-Assisted Diesel Engine With Early Timing Diesel Pilot Injection. *Journal of Engineering for Gas Turbines and Power-Transactions of the Asme* **2021**, *143* (9), 091014.
- (139) Mounaïm-Rousselle, C.; Mercier, A.; Bréquigny, P.; Dumand, C.; Bourriot, J.; Houillé, S. Performance of ammonia fuel in a spark assisted compression Ignition engine. *International Journal of Engine Research* **2022**, *23* (5), 781–792.
- (140) Pochet, M.; Truedsson, I.; Foucher, F.; Jeanmart, H.; Contino, F. Ammonia-hydrogen blends in homogeneous-charge compression-ignition engine; *SAE Technical Paper* 2017; no. 2017-24-0087..
- (141) Lhuillier, C.; Bréquigny, P.; Contino, F.; Mounaïm-Rousselle, C. Experimental investigation on ammonia combustion behavior in a spark-ignition engine by means of laminar and turbulent expanding flames. *Proceedings of the Combustion Institute* **2021**, *38* (4), 5859–5868.
- (142) Mercier, A.; Mounaïm-Rousselle, C.; Bréquigny, P.; Bourriot, J.; Dumand, C. Improvement of SI engine combustion with ammonia as fuel: Effect of ammonia dissociation prior to combustion. *Fuel Communications* **2022**, *11*, 100058.
- (143) Cavaliere, A.; de Joannon, M. Mild combustion. *Prog. Energy Combust. Sci.* **2004**, *30* (4), 329–366.
- (144) Sabia, P.; Sorrentino, G.; Ariemma, G. B.; Manna, M. V.; Ragucci, R.; de Joannon, M. MILD Combustion and Biofuels: A Minireview. *Energy Fuels* **2021**, *35* (24), 19901–19919.
- (145) Sorrentino, G.; Sabia, P.; Bozza, P.; Ragucci, R.; de Joannon, M. Low-NO conversion of pure ammonia in a cyclonic burner under locally diluted and preheated conditions. *Applied Energy* **2019**, *254*, 113676.
- (146) Sorrentino, G.; Sabia, P.; Ariemma, G. B.; Ragucci, R.; de Joannon, M. Reactive Structures of Ammonia MILD Combustion in Diffusion Ignition Processes. *Frontiers in Energy Research* **2021**, *9*, 649141.

- (147) Ariemma, G. B.; Sabia, P.; Sorrentino, G.; Bozza, P.; de Joannon, M.; Ragucci, R. Influence of water addition on MILD ammonia combustion performances and emissions. *Proceedings of the Combustion Institute* **2021**, *38* (4), 5147–5154.
- (148) Rocha, R. C.; Costa, M.; Bai, X.-S. Combustion and emission characteristics of ammonia under conditions relevant to modern gas turbines. *Combust. Sci. Technol.* **2021**, *193* (14), 2514–2533.
- (149) Liu, X.; Wang, G.; Wang, F.; Li, P.; Si, J.; Hanif, F.; Mi, J. Classification and characteristics of ammonia combustion in well stirred reactor. *Int. J. Hydrogen Energy* **2024**, *55*, 1–13.
- (150) Mohammadpour, A.; Mazaheri, K.; Alipoor, A. Reaction zone characteristics, thermal performance and NO<sub>x</sub>/NO emissions analyses of ammonia MILD combustion. *Int. J. Hydrogen Energy* **2022**, *47* (48), 21013–21031.
- (151) Shi, H.; Liu, S.; Zou, C.; Dai, L.; Li, J.; Xia, W.; Yang, J.; Luo, J.; Li, W. Experimental study and mechanism analysis of the NO<sub>x</sub> emissions in the NH<sub>3</sub>MILD combustion by a novel burner. *Fuel* **2022**, *310*, 122417.
- (152) Giuntini, L.; Frascino, L.; Ariemma, G. B.; Sorrentino, G.; Galletti, C.; Ragucci, R. Modeling of Ammonia MILD Combustion in Systems with Internal Recirculation. *Combust. Sci. Technol.* **2023**, *195* (14), 3513–3528.
- (153) Nakamura, H.; Hasegawa, S.; Tezuka, T. Kinetic modeling of ammonia/air weak flames in a micro flow reactor with a controlled temperature profile. *Combust. Flame* **2017**, *185*, 16–27.
- (154) Li, Q. B. An Improved Gas-Kinetic Scheme for Multimaterial Flows. *Commun. Comput. Phys.* **2019**, *27* (1), 145–166.
- (155) Wang, G.; Liu, X.; Li, P.; Shi, G.; Cai, X.; Liu, Z.; Mi, J. MILD combustion of a premixed NH<sub>3</sub>/air jet flame in hot coflow versus its CH<sub>4</sub>/air counterpart. *Fuel* **2024**, *355*, 129523.
- (156) Üstün, C. E.; Herfatmanesh, M. R.; Valera-Medina, A.; Paykani, A. Applying machine learning techniques to predict laminar burning velocity for ammonia/hydrogen/air mixtures. *Energy and AI* **2023**, *13*, 100270.
- (157) Üstün, C. E.; Eckart, S.; Valera-Medina, A.; Paykani, A. Data-driven prediction of laminar burning velocity for ternary ammonia/hydrogen/methane/air premixed flames. *Fuel* **2024**, *368*, 131581.
- (158) Lewandowski, M. T.; Pedersen, K. A.; Lovas, T. Evaluation of classical MILD combustion criteria for binary blends of ammonia, methane and hydrogen. *Int. J. Hydrogen Energy* **2024**, *60*, 566–580.
- (159) Czyzewski, P.; Slefarski, R.; Golebiewski, M.; Alnajideen, M.; Valera-Medina, A. Experimental study of CO<sub>2</sub>/H<sub>2</sub>/NH<sub>3</sub> influence on CH<sub>4</sub> flameless combustion process in semi-industrial furnace. *Energy* **2024**, *296*, 131014.
- (160) Slefarski, R.; Czyzewski, P.; Golebiewski, M. Experimental Study on Combustion of CH/NH Fuel Blends in an Industrial Furnace Operated in Flameless Conditions. *Thermal Science* **2020**, *24* (6), 3625–3635.
- (161) Mousavi, S. M.; Sotoudeh, F.; Jun, D.; Lee, B. J.; Esfahani, J. A.; Karimi, N. On the effects of NH addition to a reacting mixture of H/CH under MILD combustion regime: Numerical modeling with a modified EDC combustion model. *Fuel* **2022**, *326*, 125096.
- (162) Kuang, Y.; Han, D.; Xu, Z.; Wang, Y.; Wang, C. Numerical study on combustion characteristics of ammonia mixture under different combustion modes. *Int. J. Hydrogen Energy* **2024**, *54*, 1403–1409.
- (163) Mousavi, S. M.; Lee, B. J.; Kim, J.; Sotoudeh, F.; Chun, B.; Jun, D.; Karimi, N.; Esfahani, J. A. On the effects of adding syngas to an ammonia-MILD combustion regime—A computational study of the reaction zone structure. *Int. J. Hydrogen Energy* **2024**, *52*, 226–240.
- (164) Kiani, M.; Kohansal, M.; Masoumi, S.; Ashjaee, M.; Houshfar, E. An experimental investigation on non-preheated MILD combustion of syngas/ammonia/air. *J. Therm. Anal. Calorim.* **2023**, *148* (21), 11783–11797.
- (165) Jiang, T.; Dai, L. F.; Zou, C.; Li, W. Y.; Shi, H. Y.; Yu, Y. Ammonia/syngas MILD combustion by a novel burner. *Combust. Flame* **2023**, *256*, 112943.
- (166) Ariemma, G. B.; Sorrentino, G.; Sabia, P.; Ragucci, R.; de Joannon, M. MILD Combustion of Methanol, Ethanol and 1-Butanol binary blends with Ammonia. *Proceedings of the Combustion Institute* **2023**, *39* (4), 4509–4517.
- (167) Miller, J. A.; Smooke, M. D.; Green, R. M.; Kee, R. J. Kinetic Modeling of the Oxidation of Ammonia in Flames. *Combust. Sci. Technol.* **1983**, *34* (1–6), 149–176.
- (168) Alzueta, M. U.; Mercader, V.; Cuoci, A.; Gersen, S.; Hashemi, H.; Glarborg, P. Flow Reactor Oxidation of Ammonia-Hydrogen Fuel Mixtures. *Energy Fuels* **2024**, *38* (4), 3369–3381.
- (169) Shrestha, K. P.; Seidel, L.; Zeuch, T.; Mauss, F. Detailed Kinetic Mechanism for the Oxidation of Ammonia Including the Formation and Reduction of Nitrogen Oxides. *Energy Fuels* **2018**, *32* (10), 10202–10217.
- (170) Girhe, S.; Snackers, A.; Lehmann, T.; Langer, R.; Loffredo, F.; Glaznev, R.; Beeckmann, J.; Pitsch, H. Ammonia and ammonia/hydrogen combustion: Comprehensive quantitative assessment of kinetic models and examination of critical parameters. *Combust. Flame* **2024**, *267*, 113560.
- (171) Alzueta, M. U.; Abián, M.; Elvira, I.; Mercader, V. D.; Sieso, L. Unraveling the NO reduction mechanisms occurring during the combustion of NH/CH mixtures. *Combust. Flame* **2023**, *257*, 112531.
- (172) Shawnam; Berwal, P.; Singh, M.; Kumar, S. Laminar burning velocity measurements of NH<sub>3</sub>/H<sub>2</sub>+Air 3 /H 2+Air mixtures at elevated temperatures. *Int. J. Hydrogen Energy* **2024**, *71*, 143–154.
- (173) Cornell, R. E.; Barbet, M. C.; Burke, M. P. Toward a More Comprehensive Understanding of the Kinetics of a Common Biomass-Derived Impurity: NH<sub>3</sub> Oxidation by N<sub>2</sub>O in a Jet-Stirred Reactor. *Energy Fuels* **2021**, *35* (16), 13338–13348.
- (174) Wang, Q.; Wang, H.; Chen, H.; Liao, W.; Liu, Z.; Hu, Z.; Sui, R.; Wang, Z.; Yang, B. New insights into the NH<sub>3</sub>/N<sub>2</sub>O/Ar system: Key steps in N<sub>2</sub>O evolution. *Proceedings of the Combustion Institute* **2024**, *40* (1–4), 105236.
- (175) Alnasif, A.; Mashruk, S.; Hayashi, M.; Jojka, J.; Shi, H.; Hayakawa, A.; Valera-Medina, A. Performance Investigation of Currently Available Reaction Mechanisms in the Estimation of NO Measurements: A Comparative Study. *Energies* **2023**, *16* (9), 3847.
- (176) Singh, A. S.; Dash, S. K.; Reddy, V. M. Chemical kinetic analysis on influence of hydrogen enrichment on the combustion characteristics of ammonia air using newly proposed reaction model. *International Journal of Energy Research* **2022**, *46* (5), 6144–6163.
- (177) Alnasif, A.; Mashruk, S.; Kovaleva, M.; Wang, P.; Valera-Medina, A. Experimental and numerical analyses of nitrogen oxides formation in a high ammonia-low hydrogen blend using a tangential swirl burner. *Carbon Neutrality* **2022**, *1* (1), 24.
- (178) Nakamura, H.; Hasegawa, S. Combustion and ignition characteristics of ammonia/air mixtures in a micro flow reactor with a controlled temperature profile. *Proceedings of the Combustion Institute* **2017**, *36* (3), 4217–4226.
- (179) Zhang, X. Y.; Moosakutty, S. P.; Rajan, R. P.; Younes, M.; Sarathy, S. M. Combustion chemistry of ammonia/hydrogen mixtures: Jet-stirred reactor measurements and comprehensive kinetic modeling. *Combust. Flame* **2021**, *234*, 111653.
- (180) Miller, J. A.; Bowman, C. T. Mechanism and Modeling of Nitrogen Chemistry in Combustion. *Prog. Energy Combust. Sci.* **1989**, *15* (4), 287–338.
- (181) Ding, X.; Li, W. F.; Liu, P. Y.; Kang, Z. Z. Numerical calculation on combustion process and NO transformation behavior in a coal-fired boiler blended ammonia: Effects of the injection position and blending ratio. *Int. J. Hydrogen Energy* **2023**, *48* (76), 29771–29785.
- (182) Glarborg, P.; Jensen, A. D.; Johnsson, J. E. Fuel nitrogen conversion in solid fuel fired systems. *Prog. Energy Combust. Sci.* **2003**, *29* (2), 89–113.
- (183) Wang, X.; Fan, W. D.; Chen, J.; Feng, G. Y.; Zhang, X. Experimental study and kinetic analysis of the impact of ammonia co-firing ratio on products formation characteristics in ammonia/coal co-firing process. *Fuel* **2022**, *329*, 125496.

- (184) Hashemi, H.; Christensen, J. M.; Gersen, S.; Levinsky, H.; Klippenstein, S. J.; Glarborg, P. High-pressure oxidation of methane. *Combust. Flame* **2016**, *172*, 349–364.
- (185) Glarborg, P.; Damjohansen, K.; Miller, J. A.; Kee, R. J.; Coltrin, M. E. Modeling the Thermal Denox Process in Flow Reactors - Surface Effects and Nitrous-Oxide Formation. *International Journal of Chemical Kinetics* **1994**, *26* (4), 421–436.
- (186) Miller, J. A.; Glarborg, P. Modelling the Formation of N<sub>2</sub>O and NO<sub>2</sub> in the Thermal De-NO<sub>x</sub> process. In *Gas Phase Chemical Reaction Systems: Experiments and Models 100 Years After Max Bodenstein Proceedings of an International Symposium, held at the "Internationales Wissenschaftsforum Heidelberg", Heidelberg, Germany, July 25–28, 1995*; Springer: 1996; pp 318–333.
- (187) Miller, J. A.; Glarborg, P. Modeling the Thermal De-NO Process:: Closing in on a final solution. *International Journal of Chemical Kinetics* **1999**, *31* (11), 757–765.
- (188) Mulvihill, C. R.; Mathieu, O.; Petersen, E. L. The unimportance of the reaction  $H + NO \rightleftharpoons HO + N$ : A shock-tube study using H<sub>2</sub>O time histories and ignition delay times. *Combust. Flame* **2018**, *196*, 478–486.
- (189) Zhang, Y. J.; Mathieu, O.; Petersen, E. L.; Bourque, G.; Curran, H. J. Assessing the predictions of a NO kinetic mechanism on recent hydrogen and syngas experimental data. *Combust. Flame* **2017**, *182*, 122–141.
- (190) Klippenstein, S. J.; Pfeifle, M.; Jasper, A. W.; Glarborg, P. Theory and modeling of relevance to prompt-NO formation at high pressure. *Combust. Flame* **2018**, *195*, 3–17.
- (191) Glarborg, P.; Miller, J.; Ruscic, B.; Klippenstein, S. Modeling nitrogen chemistry in combustion. *Prog. Energy Combust. Sci.* **2018**, *67*, 31–68.
- (192) Dean, A. M.; Bozzelli, J. W. Combustion chemistry of nitrogen. In *Gas-Phase Combustion Chemistry*; Springer: 2000; pp 125–341.
- (193) Mulvihill, C. R.; Alturaifi, S. A.; Petersen, E. L. A shock-tube study of the  $N_2O + M \rightleftharpoons N_2 + O + M$  ( $M = Ar$ ) rate constant using N<sub>2</sub>O laser absorption near 4.6  $\mu m$ . *Combust. Flame* **2021**, *224*, 6–13.
- (194) Sun, J. H.; Yang, Q.; Zhao, N. B.; Chen, M. M.; Zheng, H. T. Numerically study of CH/NH combustion characteristics in an industrial gas turbine combustor based on a reduced mechanism. *Fuel* **2022**, *327*, 124897.
- (195) Bowman, C. T. Kinetics of pollutant formation and destruction in combustion. *Progress in energy and combustion science* **1975**, *1* (1), 33–45.
- (196) Javoy, S.; Mevel, R.; Paillard, C. E. A Study of NO Decomposition Rate Constant at High Temperature: Application to the Reduction of Nitrous Oxide by Hydrogen. *International Journal of Chemical Kinetics* **2009**, *41* (5), 357–375.
- (197) Gimenez-Lopez, J.; Rasmussen, C. T.; Hashemi, H.; Alzueta, M. U.; Gao, Y.; Marshall, P.; Goldsmith, C. F.; Glarborg, P. Experimental and kinetic modeling study of C<sub>2</sub>H<sub>2</sub> oxidation at high pressure. *International Journal of Chemical Kinetics* **2016**, *48* (11), 724–738. Glarborg, P.; Miller, J. A.; Kee, R. J. Kinetic Modeling and Sensitivity Analysis of Nitrogen-Oxide Formation in Well-Stirred Reactors. *Combust. Flame* **1986**, *65* (2), 177–202.
- (198) Glarborg, P. The NH/NO/O system: Constraining key steps in ammonia ignition and NO formation. *Combust. Flame* **2023**, *257*, 112311.
- (199) Klippenstein, S. J.; Harding, L. B.; Glarborg, P.; Gao, Y.; Hu, H.; Marshall, P. Rate constant and branching fraction for the NH<sub>2</sub> + NO<sub>2</sub> reaction. *J. Phys. Chem. A* **2013**, *117* (37), 9011–9022.
- (200) Lindholm, N.; Hershberger, J. F. Product branching ratios of the NH<sub>2</sub> (X<sup>2</sup>B<sub>1</sub>) + NO<sub>2</sub> reaction. *J. Phys. Chem. A* **1997**, *101* (27), 4991–4995.
- (201) Sun, F.; DeSain, J. D.; Scott, G.; Hung, P. Y.; Thompson, R. I.; Glass, G. P.; Curl, R. F. Reactions of NH<sub>2</sub> with NO<sub>2</sub> and of OH with NH<sub>2</sub>O. *J. Phys. Chem. A* **2001**, *105* (25), 6121–6128.
- (202) Hashemi, H.; Christensen, J. M.; Gersen, S.; Glarborg, P. Hydrogen oxidation at high pressure and intermediate temperatures: Experiments and kinetic modeling. *Proceedings of the Combustion Institute* **2015**, *35* (1), 553–560.
- (203) Meng, Q. H.; Lei, L.; Lee, J.; Burke, M. P. On the role of HNNO in NO<sub>x</sub> formation. *Proceedings of the Combustion Institute* **2023**, *39* (1), 551–560.
- (204) Lee, J.; Barbet, M. C.; Meng, Q. H.; Cornell, R. E.; Burke, M. P. Experimental support for a new NO<sub>x</sub> formation route via an HNNO intermediate. *Combust. Flame* **2023**, *257*, 112632.
- (205) Han, X. L.; Lavadera, M. L.; Konnov, A. A. An experimental and kinetic modeling study on the laminar burning velocity of NH + NO + air flames. *Combust. Flame* **2021**, *228*, 13–28. Shrestha, K. P.; Lhuillier, C.; Barbosa, A. A.; Brequigny, P.; Contino, F.; Mounaïm-Rousselle, C.; Seidel, L.; Mauss, F. An experimental and modeling study of ammonia with enriched oxygen content and ammonia/hydrogen laminar flame speed at elevated pressure and temperature. *Proceedings of the Combustion Institute* **2021**, *38* (2), 2163–2174. Stagni, A.; Cavallotti, C.; Arunthanayothin, S.; Song, Y.; Herbinet, O.; Battin-Leclerc, F.; Faravelli, T. An experimental, theoretical and kinetic-modeling study of the gas-phase oxidation of ammonia. *Reaction Chemistry & Engineering* **2020**, *5* (4), 696–711. Lamoureux, N.; El Merhubi, H.; Pillier, L.; de Persis, S.; Desgroux, P. Modeling of NO formation in low pressure premixed flames. *Combust. Flame* **2016**, *163*, 557–575.
- (206) Goussis, D. A.; Maas, U. Model reduction for combustion chemistry. In *Turbulent Combustion Modeling: Advances, New Trends and Perspectives*; Springer: 2011; pp 193–220.
- (207) Maas, U.; Pope, S. B. Implementation of simplified chemical kinetics based on intrinsic low-dimensional manifolds. *Symposium (International) on Combustion* **1992**, *24*, 103–112.
- (208) Lam, S.-H.; Goussis, D. A. Understanding complex chemical kinetics with computational singular perturbation. *Symposium (International) on Combustion* **1989**, *22*, 931–941.
- (209) Bykov, V.; Gol'dshtein, V.; Maas, U. Simple global reduction technique based on decomposition approach. *Combustion Theory and Modelling* **2008**, *12* (2), 389–405.
- (210) Bykov, V.; Maas, U. The extension of the ILDM concept to reaction-diffusion manifolds. *Combustion Theory and Modelling* **2007**, *11* (6), 839–862.
- (211) Van Oijen, J.; De Goey, L. Modelling of premixed laminar flames using flamelet-generated manifolds. *Combustion Science and Technology* **2000**, *161* (1), 113–137.
- (212) Peters, N. Laminar flamelet concepts in turbulent combustion. *Symposium (International) on combustion* **1988**, *21*, 1231–1250.
- (213) Rabbani, S.; Manias, D. M.; Kyritsis, D. C.; Goussis, D. A. Comparative review of the chemical dynamics underlying five models of ammonia fuel oxidation. *Fuel* **2023**, *352*, 129063.
- (214) Fratallocchi, V.; Kok, J. B. W. The CSP/PSR approach in reduced chemistry of premixed ammonia combustion. *Proceedings of the 9th International Conference on Applied Energy* **2017**, *142*, 4145–4150.
- (215) Bykov, V.; Stein, M.; Maas, U. Study of mechanism of ammonia decomposition and oxidation: From NO<sub>x</sub> reduction to ammonia auto-ignition problem. *Proceedings of the Combustion Institute* **2023**, *39* (4), 4267–4275.
- (216) Füzesi, D.; Wang, S.; Józsa, V.; Chong, C. T. Ammonia-methane combustion in a swirl burner: experimental analysis and numerical modeling with Flamelet Generated Manifold model. *Fuel* **2023**, *341*, 127403.
- (217) Yadav, S.; Yu, P.; Tanno, K.; Watanabe, H. Evaluation of coal ammonia flames using a non-adiabatic three mixture fraction flamelet progress variable approach. *Energy* **2024**, *288*, 129833.
- (218) Akaotsu, S.; Matsushita, Y.; Aoki, H.; Malalasekera, W. Analysis of flame structure using detailed chemistry and applicability of flamelet/progress variable model in the laminar counter-flow diffusion flames of pulverized coals. *Advanced Powder Technology* **2020**, *31* (3), 1302–1322.
- (219) Kai, R.; Ayukawa, S.; Kinuta, K.; Kurose, R. Effects of preferential diffusion and flame stretch on FGM method for



numerical simulations of ammonia/air premixed combustion. *Applications in Energy and Combustion Science* **2024**, *17*, 100253.

(220) An, Z. H.; Zhang, W. J.; Zhang, M.; Xing, J. K.; Kai, R.; Lin, W. J.; Wang, R. X.; Wang, J. H.; Huang, Z. H.; Kurose, R. Experimental and Numerical Investigation on Combustion Characteristics of Cracked Ammonia Flames. *Energy Fuels* **2024**, *38* (8), 7412–7430.

(221) da Rocha, R. C.; Costa, M.; Bai, X.-S. Chemical kinetic modelling of ammonia/hydrogen/air ignition, premixed flame propagation and NO emission. *Fuel* **2019**, *246*, 24–33.

(222) Magnussen, B. On the structure of turbulence and a generalized eddy dissipation concept for chemical reaction in turbulent flow. *19th Aerospace Sciences Meeting*; AIAA: 1981; paper AIAA 1981-42. DOI: 10.2514/6.1981-42

(223) Chomiak, J. *Combustion: A Study in Theory, Fact and Application*; Abacus Press: 1990.

(224) *Turbulent Combustion Modeling: Advances, New Trends and Perspectives*; Echehki, T., Mastorakos, E., Eds.; Springer: 2011.

(225) Chaturvedi, S.; Santhosh, R.; Mashruk, S.; Yadav, R.; Valera-Medina, A. Prediction of NO<sub>x</sub> emissions and pathways in premixed ammonia-hydrogen-air combustion using CFD-CRN methodology. *Journal of the Energy Institute* **2023**, *111*, 101406.

(226) Ehrhardt, K.; Toqan, M.; Jansohn, P.; Teare, J. D.; Beer, J. M.; Sybon, G.; Leuckel, W. Modeling of NO reburning in a pilot scale furnace using detailed reaction kinetics. *Combust. Sci. Technol.* **1998**, *131* (1–6), 131–146.

(227) Cerutti, M.; Meloni, R.; Pucci, E.; Zucca, A. Numerical Investigation of Gas Turbine Burners Operating with Hydrogen and Hydrogen-Ammonia Blends. Presented at the 10th International Gas Turbine Conference, 2021.

(228) Wang, C. M.; Wang, H. O.; Luo, K.; Fan, J. R. The Effects of Cracking Ratio on Ammonia/Air Non-Premixed Flames under High-Pressure Conditions Using Large Eddy Simulations. *Energies* **2023**, *16* (19), 6985.

(229) Honzawa, T.; Kai, R.; Okada, A.; Valera-Medina, A.; Bowen, P. J.; Kurose, R. Predictions of NO and CO emissions in ammonia/methane/air combustion by LES using a non-adiabatic flamelet generated manifold. *Energy* **2019**, *186*, 115771.

(230) Mathieu, O.; Petersen, E. L. Experimental and modeling study on the high-temperature oxidation of Ammonia and related NO<sub>x</sub> chemistry. *Combust. Flame* **2015**, *162* (3), 554–570.

(231) Jiang, Y.; Gruber, A.; Seshadri, K.; Williams, F. An updated short chemical-kinetic nitrogen mechanism for carbon-free combustion applications. *International Journal of Energy Research* **2020**, *44* (2), 795–810.

(232) Tang, H.; Yang, C. B.; Wang, G. Q.; Krishna, Y.; Guiberti, T. F.; Roberts, W. L.; Magnotti, G. Scalar structure in turbulent non-premixed NH<sub>3</sub>/H<sub>2</sub>/N<sub>2</sub> jet flames at elevated pressure using Raman spectroscopy. *Combust. Flame* **2022**, *244*, 112292.

(233) Bellotti, D.; Meloni, R.; Pucci, E. Ammonia as fuel for Gas Turbine. *E3S Web of Conferences* **2023**, *414*, 02007.

(234) Bioche, K.; Bricteux, L.; Bertolino, A.; Parente, A.; Blondeau, J. Large Eddy Simulation of rich ammonia/hydrogen/air combustion in a gas turbine burner. *Int. J. Hydrogen Energy* **2021**, *46* (79), 39548–39562.

(235) Shen, Y. Z.; Zhang, K.; Duwig, C. Investigation of wet ammonia combustion characteristics using LES with finite-rate chemistry. *Fuel* **2022**, *311*, 122422.

(236) Indlekofer, T.; Wiseman, S.; Nogenmyr, K. J.; Larfeldt, J.; Gruber, A. Numerical Investigation of Rich-Lean Staging in a SGT-750 Scaled Dry Low Emission Burner With Partially Decomposed Ammonia. *Journal of Engineering for Gas Turbines and Power-Transactions of the Asme* **2023**, *145* (4), 041018.

(237) Fűzesi, D.; Józsa, V. The importance of unsteady phenomena of ammonia/methane combustion in an experimental swirl burner: Comparison of steady-state and transient simulation results. *Combust. Flame* **2024**, *260*, 113207.

(238) Mikulčić, H.; Baleta, J.; Wang, X.; Wang, J.; Qi, F.; Wang, F. Numerical simulation of ammonia/methane/air combustion using

reduced chemical kinetics models. *International journal of hydrogen energy* **2021**, *46* (45), 23548–23563.

(239) Mazzotta, L.; Lamioni, R.; D'Alessio, F.; Meloni, R.; Morris, S.; Goktepe, B.; Cerutti, M.; Romano, C.; Creta, F.; Galletti, C.; et al. Modeling Ammonia-Hydrogen-Air Combustion and Emission Characteristics of a Generic Swirl Burner. *Journal of Engineering for Gas Turbines and Power-Transactions of the Asme* **2024**, *146* (9), 091022.

(240) Viguera-Zuniga, M. O.; Tejada-del-Cueto, M. E.; Vasquez-Santacruz, J. A.; Herrera-May, A. L.; Valera-Medina, A. Numerical Predictions of a Swirl Combustor Using Complex Chemistry Fueled with Ammonia/Hydrogen Blends. *Energies* **2020**, *13* (2), 288.

(241) Somaratne, K. D. K. A.; Hatakeyama, S.; Hayakawa, A.; Kobayashi, H. Numerical study of a low emission gas turbine like combustor for turbulent ammonia/air premixed swirl flames with a secondary air injection at high pressure. *Int. J. Hydrogen Energy* **2017**, *42* (44), 27388–27399.

(242) Sun, Y.; Cai, T.; Zhao, D.; Shahsavari, M.; Sun, D.; Sun, X.; Wang, B. RANS simulations on combustion and emission characteristics of a premixed NH<sub>3</sub>/H<sub>2</sub> swirling flame with reduced chemical kinetic model. *Chin. J. Aeronaut.* **2021**, *34*, 17.

(243) Cai, X.; Fan, Q. S.; Bai, X. S.; Wang, J. H.; Zhang, M.; Huang, Z. H.; Alden, M.; Li, Z. S. Turbulent burning velocity and its related statistics of ammonia-hydrogen-air jet flames at high Karlovitz number: Effect of differential diffusion. *Proceedings of the Combustion Institute* **2023**, *39* (4), 4215–4226.

(244) Tian, T.; Song, C.; Wang, H.; Xu, C.; Luo, K.; Fan, J. The effects of turbulence on the flame structure and NO formation of ammonia turbulent premixed combustion at various equivalence ratios. *Fuel* **2023**, *332*, 126127.

(245) Chi, C.; Han, W.; Thévenin, D. Effects of molecular diffusion modeling on turbulent premixed NH<sub>3</sub>/H<sub>2</sub>/air flames. *Proceedings of the Combustion Institute* **2023**, *39* (2), 2259–2268.

(246) Osipova, K. N.; Sarathy, S. M.; Korobeinichev, O. P.; Shmakov, A. G. Chemical structure of premixed ammonia/hydrogen flames at elevated pressures. *Combust. Flame* **2022**, *246*, 112419.

(247) Lv, Y.; Liu, J. Z.; Yang, T. T.; Zeng, D. L. A novel least squares support vector machine ensemble model for NO emission prediction of a coal-fired boiler. *Energy* **2013**, *55*, 319–329.

(248) Yuan, Z. W.; Meng, L.; Gu, X. B.; Bai, Y. Y.; Cui, H. M.; Jiang, C. Y. Prediction of NO<sub>x</sub> emissions for coal-fired power plants with stacked-generalization ensemble method. *Fuel* **2021**, *289*, 119748.

(249) Dirik, M. Prediction of NO<sub>x</sub> emissions from gas turbines of a combined cycle power plant using an ANFIS model optimized by GA. *Fuel* **2022**, *321*, 124037.

(250) Le Cornec, C. M. A.; Molden, N.; van Reeuwijk, M.; Stettler, M. E. J. Modelling of instantaneous emissions from diesel vehicles with a special focus on NO(x): Insights from machine learning techniques. *Sci. Total Environ.* **2020**, *737*, 139625.

(251) Li, N.; Lu, G.; Li, X. L.; Yan, Y. Prediction of NO<sub>x</sub> Emissions from a Biomass Fired Combustion Process Based on Flame Radical Imaging and Deep Learning Techniques. *Combust. Sci. Technol.* **2016**, *188* (2), 233–246.

(252) Ye, T.; Dong, M.; Liang, Y.; Long, J.; Li, W.; Lu, J. Modeling and optimization of the NO<sub>x</sub> generation characteristics of the coal-fired boiler based on interpretable machine learning algorithm. *International Journal of Green Energy* **2022**, *19* (5), 529–543.

(253) Yan, P. L.; Fan, W. J.; Zhang, R. C. Predicting the NO<sub>x</sub> emissions of low heat value gas rich-quench-lean combustor via three integrated learning algorithms with Bayesian optimization. *Energy* **2023**, *273*, 127227.

(254) Zhang, L. W.; Zhu, G. H.; Chao, Y. P.; Chen, L. B.; Ghanbari, A. Simultaneous prediction of CO<sub>2</sub>, CO, and NO<sub>x</sub> emissions of biodiesel-hydrogen blend combustion in compression ignition engines by supervised machine learning tools. *Energy* **2023**, *282*, 128972.

(255) Saleem, A.; Karimi, I. A.; Farooq, S. Estimating NO<sub>x</sub> emissions of useful two-fuel blends from literature data. *Fuel* **2022**, *316*, 123213.

(256) Mao, G.; Shi, T.; Mao, C.; Wang, P. Prediction of NO<sub>x</sub> emission from two-stage combustion of NH<sub>3</sub>-H<sub>2</sub> mixtures under

various conditions using artificial neural networks. *Int. J. Hydrogen Energy* **2024**, *49*, 1414–1424.

(257) Xing, Z. H.; Jiang, X. Neural network potential-based molecular investigation of pollutant formation of ammonia and ammonia-hydrogen combustion. *Chemical Engineering Journal* **2024**, *489*, 151492.

(258) Elumalai, R.; Ravi, K.; Elumalai, P. V.; Sreenivasa Reddy, M.; Prakash, E.; Sekar, P. Development of an ammonia-biodiesel dual fuel combustion engine's injection strategy map using response surface optimization and artificial neural network prediction. *Sci. Rep* **2024**, *14* (1), 543.

(259) Mi, S. J.; Wu, H. Q.; Pei, X. Z.; Liu, C. Y.; Zheng, L.; Zhao, W. B.; Qian, Y.; Lu, X. C. Potential of ammonia energy fraction and diesel pilot-injection strategy on improving combustion and emission performance in an ammonia-diesel dual fuel engine. *Fuel* **2023**, *343*, 127889.

(260) Arivalagan, P.; Kamarudin, S. K.; Ali Alharbi, S.; Arul Gnana Dhas, A.; Manigandan, S. Assessment of ammonia-diesel fuel blends on compression ignition engine performance and emissions using machine learning techniques. *Fuel* **2024**, *373*, 132135.